ONE DIMENSIONAL TRANSPORT OF ULTRACOLD FERMIONS

by

RORY WHELAN

A thesis submitted to
The University of Birmingham
for the degree of
DOCTOR OF PHILOSOPHY

Theoretical Physics Research Group
School of Physics and Astronomy
College of Engineering & Physical Sciences
University of Birmingham
August 2021

Abstract

This thesis concerns the transport of fermions through a one-dimensional channel. I consider two three-dimensional reservoirs that contain BCS superconductors, that are connected via weak tunnelling junctions to a one-dimensional channel in which the fermions have attractive interactions. The current through the channel is entirely driven by the phase difference in the superconducting order parameters of the two reservoirs. I theoretically investigate the current as a function of phase difference and show that the flow has characteristics that are completely distinct from an equivalent system without attractive interactions between fermions. As a perturbative solution fails for attractive fermions, I develop a non-pertubative mean field description of the fermionic current. With the inclusion of fluctuations in this mean field solution, I show that the system of fermions with attractive interactions can identically map onto a system of bosons in the same geometry, with Bose-Einstein condensate reservoirs. I show that the novel features of the bosonic flow are retained in the attractive fermionic system, namely the two seperate branches of the mean field solution. I show that these branches are degenerate at an applied phase difference of π, and that the degeneracy is robust against fluctuations. I compare this degeneracy in the attractive fermionic and bosonic systems to the topologically protected degeneracy in nanowires that host Majorana zero modes.

Acknowledgements

This work would not have been possible without the help and guidance of my supervisors, Dima Gangardt and Igor Lerner. Thank you for the support when my research hit dead-ends, as well as the countless conversations about interesting physics.

I would also like to thank the rest of the academic staff of the Theory Group, for making every seminar and journal club interesting with your constant questions.

Thank you to all Theory PhD students, past and present, for creating the most friendly and welcoming office environment I could have asked for. I will miss our afternoons comparing the ways we write the different Greek letters! In particular I would like to thank a few groups of colleagues; Jack Gartlan, Manjinder Kainth and Jordan Moodie for being the wise elders of the group and encouraging me on sporting endeavours; Rose Davies, Enrico Martello and Ewan McCulloch for being brilliant officemates and putting up with any random questions that I had; and finally Chris Oliver and James Pallister for diligently proof-reading various chapters of this thesis.

I would like to thank my housemates, Will Barker, Mike Clark, Tom Loveland and Ben McCanna for the non-stop jokes and memorable game nights that we spent together.

I thank Hayley Whelan with whom I have shared many of my happiest moments with. Our adventures across Birmingham and Gloucestershire have been the best distraction from work.

Finally, a special thanks goes to my parents and sister for their immense support during the last four years and throughout my life. I would not be able to achieve what I have without their encouragement and belief in me.

Contents

List of Figures

"Such a life, with all vision limited to a Point, and all motion to a Straight Line, seemed to me inexpressibly dreary; and I was surprised to note the vivacity and cheerfulness of the King"

- A. Square, commenting on life in One Dimension in 'Flatland' by Edwin Abbot.

Chapter 0

Introduction

Ever since the first experimental observation of a Bose-Einstein condensate over 25 years ago, the study of cold atoms has been a hot topic in condensed matter research. In the lab, these cold atom systems offer much greater flexibility and control over parameters than in the solid state. Recent experiments have been able to cool many different species of atom (both bosonic and fermionic), and also engineer a myriad of different interactions between them [1, 2, 3, 4, 5]. This has allowed for various theoretical models to be simulated and explored in the lab.

This thesis is concerned with the transport of ultracold fermionic atoms in a one-dimensional geometry. I consider a system that consists of two three-dimensional reservoirs that contain BCS superconductors, connected to a one-dimensional channel through weak tunnelling links. I consider a the current that flows through the channel, as a function of the phase difference between the two reservoirs. This geometry has been considered for fermions with repulsive interactions [6, 7] and bosons with repulsive interactions [8] and these systems behave significantly different. In this thesis I investigate the current when the fermions have attractive interactions in the channel. I show that the behaviour can be exactly mapped onto the bosonic system previously considered, and I draw some links from these systems to those that are predicted to host Majorana fermions as edge modes [9, 10].

This thesis is made of three parts, first of which is an introduction to the topics in physics that are relevant to understand the results. In chapter 1 I introduce the concepts of Bose-Einstein condensation and superconductivity. I also introduce the phenomenon of the Josephson effect, which is critical for

describing currents between quantum-coherent systems. Chapter 2 focuses on one-dimensional physics and the oddities of describing systems of bosons and fermions in one spatial dimension. I introduce the concept of a Luttinger liquid, and explain the concept of bosonisation which is used to describe the low energy behaviour of one-dimensional systems. In chapter 3 I provide an introduction to Majorana fermions in condensed matter systems. I start with the intuitive model of the Kitaev chain, before moving onto describing the solid state systems predicted to host the Majorana fermions as edge modes.

In the second part of this thesis I cover the mathematical techniques I require to attain the results in part III. The first technique, covered in chapter 4, is functional integration. I calculate correlation functions of BCS superconductors and Luttinger liquids. In chapter 5 I explain the technique of the renormalisation group, which I illustrate with two examples of impurities in Luttinger liquids.

In the third part I present the main results of the thesis. In chapter 6 I show the results obtained by Simpson et. al. [8] for the bosonic system, and I highlight the links that this system has to the Majorana systems described in chapter 3. Chapter 7 is my own work, and is to be published as a pre-print. I introduce the model of interest and then show that it can be identically mapped onto the bosonic system. Some pieces of mathematics required for the results in chapter 7 are included in the appendix.

Part I

Concepts Background: Physics

Chapter 1

Quantum Matter

The physics of quantum matter can be dated back to prehistory, with the discovery of lodestone and other itinerant ferromagnets. Little did our ancient ancestors know that to describe the emergence of this state of matter, you would need a many particle quantum theory. Quantum matter can be broadly defined as any material, which has properties that are described by quantum mechanics. The study of quantum matter is a broad subset of condensed matter physics, coming into prominence in the 20th century with various experimental discoveries and the development of quantum theories to describe them. First of these discoveries came in 1911, with the discovery of superconductivity in mercury by Kamerlingh Onnes. When cooled to cryogenic temperatures, Onnes found the electrical resistance of mercury to drop abruptly to almost zero. Further metals were found to superconduct, and various theories were proposed to explain the origin of superconductivity [11]. The theories that are relevant to my work are the Ginzburg-Landau theory, a phenomenological theory based on Landau's theory of phase transitions, and BCS theory, a microscopic theory that explains the mechanism that underlies many superconductors. In section 1.2 I shall give a qualitative overview of BCS and Ginzburg-Landau theory, and some relevant phenomena related to superconductivity.

Concurrent to these discoveries was investigation into a different phenomena, that of Bose-Einstein condensates. A Bose-Einstein condensate (BEC) is a state of matter first predicted by Albert Einstein and Satyendra Nath Bose in 1924 [12]. It arises from Bose-Einstein statistics, that allow for any number of quantum particles to occupy the same energy level, and is where a macroscopic fraction of particles are

in the ground state energy. The initial prediction was based on a model of a non-interacting Bose gas, and the decades that followed more detailed models were developed to describe BECs with interacting particles. The experimental realisation of a BEC came in 1995, with Eric Cornell and Carl Wieman's group as well as Wolfgang Ketterle's group creating BECs out of laser cooled groups of alkali earth atoms. Since then more species of bosonic atoms have been condensed and techniques have been developed to control the inter-atomic interactions. The level of control you can have over a system of cold atoms has made them an ideal platform to investigate the behaviour of various theoretical models, which are unsolvable or unscalable through classical computational means. In section 1.1 I shall give a theoretical overview of Bose-Einstein condensation, including how to find the dynamics and dispersion relation of a weakly interacting Bose gas.

1.1 Bose-Einstein Condensation

1.1.1 Quantum Statistics

When describing more than one particle in quantum mechanics, the nature of the joint wavefunction, $|\psi_1, \psi_2\rangle$, under swapping of particles needs to be considered. There are two possibilities[1], either the wavefunction is symmetric or antisymmetric under exchange of particles, $|\psi_1, \psi_2\rangle = |\psi_1\rangle\,|\psi_2\rangle \pm |\psi_2\rangle\,|\psi_1\rangle = \pm\,|\psi_2, \psi_1\rangle$. The exchange symmetry has a profound effect on the counting statistics of the particles, with symmetric exchange particles being described by Bose-Einstein statistics and similarly antisymmetric exchange having Fermi-Dirac statistics. These particles are called bosons and fermions. For a non-interacting gas of bosons, the average occupation number of an energy level ε_i is given by the Bose distribution,

$$n_{\mathrm{B}}(\varepsilon_i) = \frac{1}{e^{\beta(\varepsilon_i - \mu)} - 1}, \tag{1.1.1}$$

[1] In three dimensions. In two dimensions fractional statistics are possible, where an arbitrary phase is accumulated through particle exchange. In one dimension things are slightly different, as discussed in chapter 2

where $\beta = 1/k_{\rm B}T$ and $\mu(T, N)$ is the chemical potential which is set by the total number of particles,

$$N_{\rm B} = \sum_i n_{\rm B}(\varepsilon_i) = \int {\rm d}\varepsilon\, g(\varepsilon) n_{\rm B}(\varepsilon), \tag{1.1.2}$$

where $g(\varepsilon) = \sum_i \delta(\varepsilon - \varepsilon_i)$ is the density of states. Similarly, non-interacting fermions obey the Fermi distribution,

$$n_{\rm F}(\varepsilon_i) = \frac{1}{e^{\beta(\varepsilon_i - \mu)} + 1}. \tag{1.1.3}$$

At high temperatures, both of these distributions are approximated by the classical Maxwell-Boltzmann distribution, $n_{\rm B,F} \sim e^{-\beta(\varepsilon_i - \mu)}$, where the probability of finding a particle in any one state is exponentially small. The implications of these statistics are two inherently quantum ena. For fermions this is the Pauli exclusion principle, where no two fermions can be in the same state. The occupation number of any one state cannot exceed one, which at $T = 0$ leads to fermions occupying all of the lowest energy levels up to the Fermi energy, $\varepsilon_i = \mu(T = 0, N) \equiv \varepsilon_{\rm F}$.

For bosons, their statistics leads to Bose-Einstein condensation. Below a critical temperature, T_c, the ground state becomes macroscopically occupied (N_0/N is of order 1). To see how this occurs we shall look at calculating the number of particles at this critical temperature. For the bose distribution Eq. 1.1.1 the chemical potential is always smaller than the lowest energy level, ε_0, which can be set to zero without loss of generality. As temperature decreases, μ reaches its maximum value of 0 at T_c. For a Bose gas of mass m, in a box of volume V, the density of states is, $g(\varepsilon) = V\sqrt{2m^3\varepsilon}/2\pi^2\hbar^3$. The critical temperature is then calculated from Eq. 1.1.2 with the dimensionless energy $x = \beta\varepsilon$,

$$\frac{N(T_c)}{V} = \frac{\sqrt{2m^3}}{2\pi^2\hbar^3}(k_{\rm B}T_c)^{3/2}\int_0^\infty {\rm d}x\, \frac{x^{1/2}}{e^x - 1} = \frac{g_{3/2}(1)}{\Lambda^3(T_c)}. \tag{1.1.4}$$

Here, $\Lambda(T) = \sqrt{2\pi\hbar^3/mk_{\rm B}T}$ is the thermal de-Broglie wavelength and $g_p(z) = \frac{1}{\Gamma(p)}\int_0^\infty {\rm d}x \frac{x^{p-1}}{z^{-1}e^x - 1}$ is the Bose function which takes the value, $g_{3/2}(1) = \zeta(3/2) = 2.612$. As the temperature decreases beyond T_c, the chemical potential remains at 0 but and so it seems that the total number of particles is decreasing as $N(T) \propto T^{3/2}$. This is remedied by remembering that the ground state isn't counted by

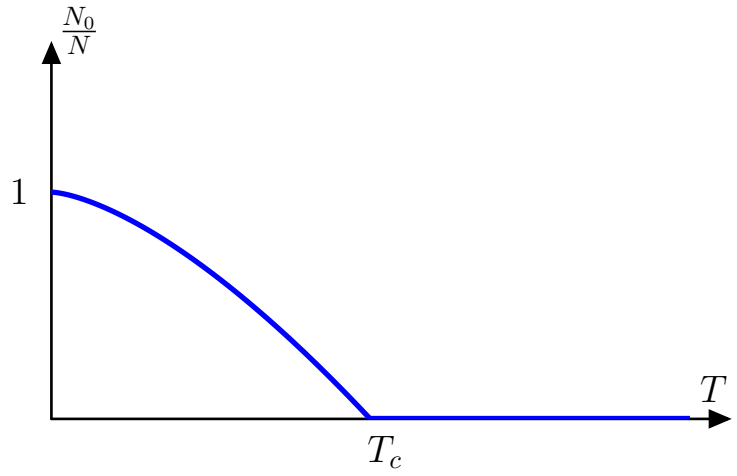

Figure 1.1: Graph showing the condensate fraction as a function of temperature. Above the critical temperature, T_c, there is no condensate. Below T_c, the ground state is macroscopically occupied.

the integral Eq. 1.1.2, and therefore the remaining particles must be populating the ground state. The ground state occupancy, defined as the difference between total particles and number of excited particles $N_0 = N - N_{\rm ex}(T)$, has the temperature dependence (plotted in figure 1.1),

$$N_0 = N\left[1 - \left(\frac{T}{T_c}\right)^{\frac{3}{2}}\right] \tag{1.1.5}$$

At zero temperature all of the particles are in the ground state, however many of the interesting properties that arise from the quantum coherence of the condensate will be present for fractions that don't necessarily seem large. If $N_0/N \sim 1/100$ in an experiment with $10^5 - 10^6$ atoms, then you will still have a condensate consisting of $\sim 10^4$ particles.

1.1.2 Interacting Bosons

A non-interacting Bose gas is a pathological problem, as it has divergent compressibility. In reality if you were to compress a Bose gas, the particles will interact through some two body scattering. This interaction between particles will always be present and for all cases that we consider will be repulsive. In terms of the field operator; $\hat{\Psi}(\boldsymbol{r}) = \sum_\alpha \psi_\alpha(\boldsymbol{r})\hat{a}_\alpha$, the macroscopic occupation of the ground state can be expressed as, $\langle \hat{a}_0^\dagger \hat{a}_0 \rangle = N_0 \gg 1$. Since the condensate has such a large particle number in it, creating or annihilating a particle doesn't change the state noticeably. That means we can take the creation and

annihilation operators to just be a number, $a_0 = a_0^\dagger = \sqrt{N_0}$. All other number operators are much smaller which means that the bosonic field operator can be expressed as the ground state plus fluctuations:

$$\hat{\Psi}(\boldsymbol{r}) = \Psi_0(\boldsymbol{r}) + \delta\hat{\Psi}(\boldsymbol{r}) = \sqrt{N_0}\psi_0(\boldsymbol{r}) + \sum_{\alpha\neq 0}\psi_\alpha(\boldsymbol{r})\hat{a}_\alpha. \tag{1.1.6}$$

In this description, $\Psi_0(\boldsymbol{r})$ is given by the mean value of the quantum mechanical operator $\Psi_0(\boldsymbol{r}) = \langle\hat{\Psi}_0(\boldsymbol{r})\rangle$, which for the condensate is a complex number with a defined modulus and phase. It plays the role of a macroscopic wavefunction for the condensate, also known as an order parameter in the context of phase transitions. We can use the order parameter to describe a condensate made up of bosons in a potential that have repulsive interactions. For bosons in a potential $U(\boldsymbol{r}, t)$ and contact interactions parameterised with interaction strength g, the Hamiltonian is,

$$\hat{H} = \int \mathrm{d}\boldsymbol{r}\left[\frac{\hbar^2}{2m}\nabla\hat{\Psi}^\dagger\cdot\nabla\hat{\Psi} + (U(\boldsymbol{r},t)-\mu)\left|\hat{\Psi}(\boldsymbol{x})\right|^2 + g\left|\hat{\Psi}(\boldsymbol{x})\right|^4\right]. \tag{1.1.7}$$

The interaction strength g can be related back to the s-wave scattering length by $g = 4\pi\hbar^2 a_s/m$. Through the Heisenberg equation of motion for $\hat{\Psi}$, $i\hbar\frac{\partial}{\partial t}\hat{\Psi} = [\hat{\Psi}, \hat{H}]$, the equation of motion that governs Ψ can be deduced to be:

$$i\hbar\frac{\partial}{\partial t}\hat{\Psi}(\boldsymbol{r},t) = \left[-\frac{\hbar^2}{2m}\nabla^2 + U(\boldsymbol{r},t) - \mu + g\left|\hat{\Psi}(\boldsymbol{x})\right|^2\right]\hat{\Psi}(\boldsymbol{r},t). \tag{1.1.8}$$

This is known as the Gross-Pitaevskii equation and is commonly used to describe weakly interacting BECs. For a spatially homogeneous gas held at a constant potential, the gas is in a steady state for, $U = \mu + gn$, where $n = \left|\hat{\Psi}(\boldsymbol{x})\right|^2$ is the density of the condensate.

We can now investigate it the behaviour of the ground state by replacing $\hat{\Psi}(\boldsymbol{r}) = \Psi_0(\boldsymbol{r})$, and then expressing the order parameter in terms of its modulus and phase:

$$\Psi_0(\boldsymbol{r},t) = \sqrt{n(\boldsymbol{r},t)}\, e^{i\phi(\boldsymbol{r},t)}, \tag{1.1.9}$$

where $n(\boldsymbol{r}, t)$ is the density of the condensate and $\phi(\boldsymbol{r}, t)$ is the phase. Substituting this form of the order

parameter into the Gross-Pitaevskii equation (GPE) eq.1.1.8 gives us:

$$-n\hbar\dot{\phi}+\frac{i\hbar}{2}\dot{n}=-i\frac{\hbar^2 n}{2m}\nabla^2\phi+\frac{\hbar^2 n}{2m}(\nabla\phi)^2-i\frac{\hbar^2}{2m}\nabla n\cdot\nabla\phi-\frac{\hbar^2}{4m}\nabla^2 n+\frac{\hbar^2}{8mn}(\nabla n)^2+(U-\mu)n+gn^2. \quad (1.1.10)$$

The imaginary part of this equation yields a continuity equation,

$$\dot{n}=-\frac{\hbar}{m}\Big(n(\nabla^2\phi)++\nabla n\cdot\nabla\phi\Big)=-\frac{\hbar}{m}\nabla\left(n\nabla\phi\right), \quad (1.1.11)$$

which allows us to define a superfluid velocity,

$$v=\frac{\hbar}{m}\nabla\phi, \quad (1.1.12)$$

and a current density, $j = nv$. From this we can see that a gradient in phase will produce a current of particles, even without a difference in densities. The real part of Eq. 1.1.10 yields,

$$-\hbar\dot{\phi}=\frac{mv^2}{2}+U-\mu+gn-\frac{\hbar^2}{2m\sqrt{n}}\nabla^2\sqrt{n}. \quad (1.1.13)$$

These two equations (1.1.12, 1.1.13) are known as the hydrodynamic description of BECs because of the links to classical fluid dynamics.

Another notion to take from the GPE is one of a "healing length", which is the length scale at which the density of the condensate can vary. De-dimensionalising the time independent GPE will give the healing length to be $\xi = \hbar/\sqrt{mgn}$. Changes that occur on lengths shorter than the healing length are unable to be accounted for by the condensate.

From the GPE we can investigate the low energy excitations that exist in a weakly repulsive BEC. To do this we account for the leading order fluctuations in Eq. 1.1.6 and then find their dispersion. To leading order, the α-th term gives,

$$i\hbar\frac{\partial\psi_\alpha}{\partial t}\hat{a}_\alpha=\left(\frac{-\hbar^2}{2m}\nabla^2+U-\mu+2g|\Psi_0|^2\right)\psi_\alpha\hat{a}_\alpha+g\Psi_0^2\psi_\alpha^*\hat{a}_\alpha^\dagger. \quad (1.1.14)$$

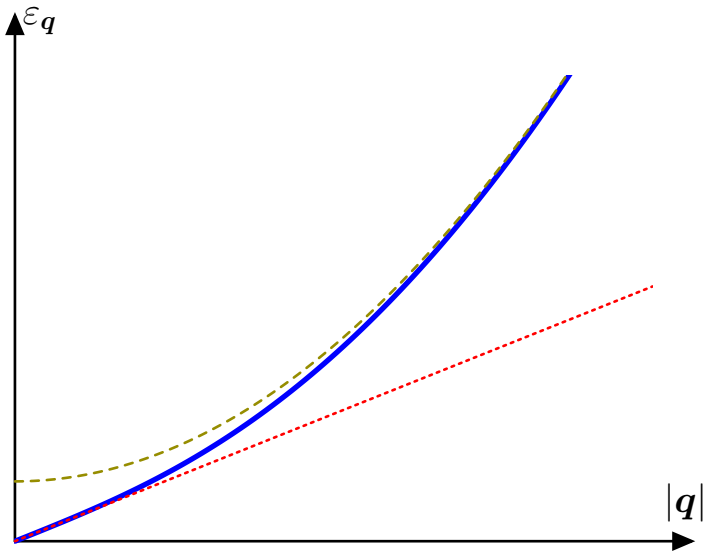

Figure 1.2: Graph showing the Bogoliubov dispersion (solid line), with the two limits of linear dispersion for small $|\boldsymbol{q}|$ (dotted), and quadratic for large $|\boldsymbol{q}|$ (dashed).

The same can be done for the Hermitian conjugate to give the equation,

$$-i\hbar\frac{\partial\psi_\alpha^*}{\partial t}\hat{a}_\alpha^\dagger = \left(\frac{-\hbar^2}{2m}\nabla^2 + U - \mu + 2g|\Psi_0|^2\right)\psi_\alpha^*\hat{a}_\alpha^\dagger + g(\Psi_0^*)^2\psi_\alpha\hat{a}_\alpha. \tag{1.1.15}$$

For plane wave solutions, $\psi_\alpha = e^{-i\omega_\alpha t + i\boldsymbol{q}_\alpha\cdot\boldsymbol{r}}$, and substituting the 0th order form of $U - \mu = gn$, the equation for fluctuations becomes,

$$\hbar\omega_\alpha\begin{pmatrix}\hat{a}_\alpha\\ -\hat{a}_\alpha^\dagger\end{pmatrix} = \begin{pmatrix}\frac{\hbar^2|\boldsymbol{q}_\alpha|^2}{2m} + gn & -g\psi_0^2\\ g(\psi_0^*)^2 & -\frac{\hbar^2|\boldsymbol{q}_\alpha|^2}{2m} - gn\end{pmatrix}\begin{pmatrix}\hat{a}_\alpha\\ -\hat{a}_\alpha^\dagger.\end{pmatrix} \tag{1.1.16}$$

In the continuum (ω and $\boldsymbol{q}$ become continuous and not quantised with index α), the spectrum of fluctuations becomes,

$$\hbar\omega = \epsilon_q = \sqrt{\frac{\hbar^2|\boldsymbol{q}|^2}{2m}\left(\frac{\hbar^2|\boldsymbol{q}|^2}{2m} + 2gn\right)}. \tag{1.1.17}$$

This dispersion is known as the Bogolioubov dispersion, and is plotted in figure 1.2. For large $|\boldsymbol{q}|$ it appears to be quadratic, as expected for free particles. For $|\boldsymbol{q}| \ll \sqrt{gnm}/\hbar = \xi^{-1}$, the dispersion is linear, $\epsilon_q = \hbar c|\boldsymbol{q}|$, where $c = \sqrt{gn/m} = \hbar/m\xi$ is the sounds velocity of excitations. This tells us that the low

energy excitations of the system are sound waves, which have a wavelength much larger than that of the coherence length.

1.2 Superconductivity

Superconductivity is the phase transition that happens in many metals where below a critical temperature, T_c, the metal loses all electrical resistance. This allows for currents to flow unimpeded, which sees many uses in technology. Many places that require large magnetic fields, such as medical imaging (MRI) and beam deflection in particle accelerators, use superconducting electromagnets to induce them with giant electric currents that don't lose energy to resistance. Since their discovery physicists have sought to describe superconductors and the emergence of superconductivity with a microscopic model, a description of why certain collections of atoms and electrons behave this way. The first theory to achieve this was BCS theory in 1957, titled after its creators John Bardeen, Leon Cooper and John Robert Schrieffer in 1957. In the next section we shall discuss BCS theory qualitatively, saving a mathematical description for section 4.2 once we have the tools of functional integration to help us.

1.2.1 Introduction to BCS Theory

It was shown in the Little-Parks effect that the charge carriers in a superconductor are not single electrons, but pairs of electrons. These pairs are most commonly known as Cooper pairs, after Leon Cooper's calculation that a net attractive interaction between electrons at the Fermi surface would create a bound state of electron pairs, which would then be the carriers of the supercurrent. In the solid state, the origin of this attractive interaction is due to electrons coupling to phonons, the quantum of lattice vibrations.

A sketch for how the net attraction arises is illustrated in figure 1.3 in real space. The negatively charged electron travels through a lattice of positively charged ions and the electrostatic forces cause the lattice to contract around the electron. The relaxation timescales of the lattice is much longer ($\mathcal{O}(\omega_{\mathrm{D}}^{-1})$) than the timescale the electron spends near the atoms ($\mathcal{O}(\epsilon_{\mathrm{F}}^{-1})$). This means that for some period of time after the electron has travelled far away but before the lattice has relaxed, there is a local positive charge density. This charge density can then attract an electron towards it. This illustrates how an effective attraction, mediated by the lattice, can arise between two electrons. In cold atom systems of fermionic atoms, similar attractive interactions can be engineered despite the lack of a physical lattice.

A more physically accurate picture can be explained in momentum space. Around the Fermi surface there is a shell of width $\sim \omega_{\mathrm{D}}/v_{\mathrm{F}}$ in which electrons can couple. This is due to the energy the phonons

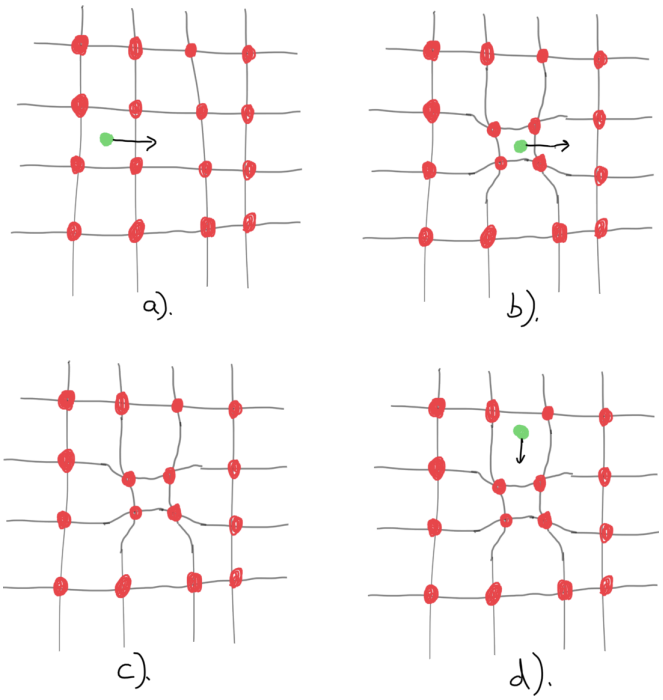

Figure 1.3: Cartoon illustrating phonon-mediated attraction between two electrons

being of $\mathcal{O}(\omega_{\mathrm{D}})$. For many superconductors the Cooper pair is formed out of a singlet of electrons that have opposite momentum states, $|\boldsymbol{k}\uparrow, -\boldsymbol{k}\downarrow\rangle$. This maximises the amount of accessible states the pair can scatter into through interaction. This type of pairing is known as s-wave superconductivity, due to the symmetry of the pairing potential being the same as s-orbitals in atomic physics. There are more exotic materials that exhibit p-wave (with spin triplets as Cooper pairs), and d-wave superconductivity however only s-wave pairing shall be considered in my work.

Since the a Cooper pair is made of two spin-1/2 fermions (forming a singlet in s-wave superconductors) it can be treated as a boson, and thus superconductivity can be thought of as the condensation of Cooper pairs. It is important to note that Cooper pairs are not point-like bosons as you might imagine cold atomic gases. The 'size' of the Cooper pair is of the order $\sim 10^{-7}$m, which compared to the average distance between electrons ($\sim 10^{-10}m$) is massive. There will be billions of Cooper pairs overlapping the volume that a single one takes up.

1.2.2 Ginzburg-Landau Theory

Building upon Lev Landau's theory of second order phase transitions, Ginzburg-Landau theory is a enalogical theory of superconductors that describes their behaviour through the use of an order parameter. This order parameter, $\psi_{\mathrm{GL}}(\boldsymbol{r}, t)$, is a complex field which is zero for $T > T_c$ and takes a non-zero value for $T < T_c$. It can be thought of as the wavefunction of condensed Cooper pairs, much like we have seen in section 1.1.2 with the wavefunction for the Bose-Einstein condensate.

The core of Ginzburg-Landau theory is the free energy as a functional of ψ_{GL}, of the form:

$$F - F_n = \alpha|\psi_{\mathrm{GL}}|^2 + \frac{\beta}{2}|\psi_{\mathrm{GL}}|^4 + \frac{1}{2m}|(-i\hbar\boldsymbol{\nabla} - 2e\boldsymbol{A})\,\psi_{\mathrm{GL}}|^2 + \frac{|\boldsymbol{B}|^2}{2\mu_0}. \tag{1.2.1}$$

Here α and β are enalogical parameters who's values will be found either through experiment or a microscopic theory. This is minimised with respect to the order parameter and vector potential to give the Ginzburg-Landau equations,

$$\left[\alpha + \beta|\psi_{\mathrm{GL}}|^2 + \frac{1}{2m}(-i\hbar\boldsymbol{\nabla} - 2e\boldsymbol{A})^2\right]\psi_{\mathrm{GL}} = 0, \tag{1.2.2}$$

$$\boldsymbol{\nabla}\times\boldsymbol{B} = \mu_0\boldsymbol{j}, \qquad \boldsymbol{j} = \frac{2e}{m}\mathrm{Re}\left\{\psi^*_{\mathrm{GL}}(-i\hbar\boldsymbol{\nabla} - 2e\boldsymbol{A})\psi_{\mathrm{GL}}\right\}. \tag{1.2.3}$$

Equation 1.2.2 looks very similar to the Gross-Pitaevskii equation (Eq. 1.1.8), with the addition of a magnetic field included with minimal coupling. For a spatially homogeneous superconductor with no currents, Eq. 1.2.2 omits two solutions. Either $\psi_{\mathrm{GL}} = 0$ which corresponds to the absence of superconductivity, or $|\psi_{\mathrm{GL}}|^2 = -\alpha/\beta$ for the superconducting phase. As amplitudes must be positive, this implies that $\alpha < 0$ for the superconductor to exist[1]. The way of encoding the transition in these parameters is to define, $\alpha = \alpha_0(T - T_c)$. For $T < T_c$, $\alpha < 0$ and the order parameter will take a non-zero value. This value is, $\psi_{\mathrm{GL}} = \sqrt{\frac{\alpha_0(T_c - T)}{\beta}}e^{i\phi}$, where the phase ϕ can take any value. This is an example of spontaneous symmetry breaking, where the order parameter spontaneously picks a phase upon the phase transition.

[1] If $\beta < 0$ then the energy would be unbounded from below for $|\psi_{\mathrm{GL}}| \to \infty$.

1.2.3 The Josephson Effect

The Josephson effect is an important concept in this thesis, it is the first step in investigating phenomena of currents between reservoirs of quantum coherent matter. The formulation of the Josephson effect that we shall look at now is relevant both for BECs as well as superconductors, as they can both be described by a complex valued order parameter with a definite phase. If two of these systems, described by order parameters $\Psi_{1,2} = \sqrt{N_{1,2}}e^{i\phi_{1,2}}$, are in close proximity then there could be some overlap of their wavefunctions. This will lead to quantum tunnelling from one system to the other with some amplitude, t. Experimentally systems like this can be created with solid state superconductors that are separated by a thin layer of an insulator, or in cold atomic BECs that are confined to a double-well trap. The tunnelling Hamiltonian for such a setup is, $H_{\text{tun}} = -t(\Psi_1^\dagger\Psi_2 + \Psi_2^\dagger\Psi_1)$. Including this tunnelling term into the Hamiltonian for the two systems will give:

$$H = E_1N_1 + E_2N_2 - 2t\sqrt{N_1N_2}\cos(\phi_1 - \phi_2). \tag{1.2.4}$$

This can be re-written in terms of total phase difference between the two condensates/superconductors, $\Phi = \phi_1 - \phi_2$, total particle number, $N_T = N_1 + N_2$, and difference in particle number between the two reservoirs, $\Delta N = N_1 - N_2$,

$$H = \frac{E_1 + E_2}{2}N_T + \frac{E_1 - E_2}{2}\Delta N - tN_T\sqrt{1 - \left(\frac{\Delta N}{N_T}\right)^2}\cos\Phi. \tag{1.2.5}$$

Hamilton's equations for ΔN and Φ lead to the Josephson relations. The DC Josephon relation describes current that passes through a Josephson junction as a function of the phase,

$$I_{\text{J}} = I_{\text{c}}\sin\Phi(t). \tag{1.2.6}$$

Here the critical current is defined as, $I_{\text{c}} = tN_T$. For systems where the particle imbalance is small compared to the total number ($\Delta N/N_T \ll 1$), the AC Josephson relations can be expressed as:

$$\dot{\Phi} = -\frac{E_1 - E_2}{2}. \tag{1.2.7}$$

For superconductors, $E_1 - E_2$ is the voltage across the Josephson junction whereas in neutrally charged cold atomic systems it will be the difference in chemical potentials.

For my work, the DC Josephson effect is incredibly relevant as I have investigated phase driven transport between reservoirs.

1.2.4 Cold Atoms

The systems described theoretically in this thesis will be able to be examined experimentally using ultracold atoms. Techniques of cooling and trapping atomic gases have been developed since the creation of an atomic BEC of Rubidium atoms in 1995 [13], and since then many more species of atoms have been trapped and cooled [12]. Bosonic atoms, such as ^{87}Rb and ^{6}Na have been trapped as well as fermionic atoms such as ^{6}Li. These fermionic atoms form a degenerate Fermi gas, instead of a condensate, due to their exchange statistics. Through utilising a phenomenon known as Feshbach resonance, s-wave scattering lengths between atoms can be changed. This means that inter-particle interactions can be tuned to a remarkable degree. Magneto-optical traps that trap these atoms can have their geometry engineered as well, with the creation of coupled reservoirs being achievable.

One limitation of cold atoms is the difficulty in making measurements of the system, particularly for transport properties. Unlike in the solid state where currents can be detected as the flow of charged particles, detecting currents of neutral particles is a harder task. A common method is time-of-flight measurements. This is where the cold atom system is initialised in a trap and allowed to evolve for an interval of time. Then the trap is removed and the particles are allowed to fly out to be imaged. From imaging the density of particles can be measured. When combined with time-of-flight, the spatial density and the momentum distribution can be calculated. The obvious drawback is that this procedure is destructive, meaning that the system needs to be re-initialised for repeat measurements to be made.

Several transport phenomena have been observed in cold atom systems that are relevant to the theoretical results in this thesis. First is the creation of a bosonic Josephson junction by Albiez et. al. in 2005 [14]. The system consisted of ^{87}Rb atoms in a double well potential, initialised with a population imbalance. Inside the double well, the condensates were observed to be weakly coupled and seen to obey the Josephson relations 1.2.6 and 1.2.7.

Second is the measurement of resistance in a defect free system of ultracold fermions by Esslinger's group in 2012 [3]. With ultracold ^{6}Li atoms, they created a geometry of two reservoirs connected to a mesoscopic channel. They were able to measure ohmic conduction, despite the lack of defects in the channel.

Third, and most recently, is the observation of dc Josephson currents in a strongly correlated fermionic superfluid consisting of ultracold ^{6}Li atoms. This was achieved by Kwon et. al. in 2020 [15]. The system they created consisted of two reservoirs that were intialised to have an equal number of particles and then the current between the two reservoirs was measured as a function of the phase difference between the two reservoirs. Through utilising the Feshbach resonance they were also able to investigate the behaviour of the Josephson current through the BEC-BCS crossover. This experimental system would be the ideal platform to investigate the main results of this thesis, as detailed in chapter 7.

Chapter 2

One Dimensional Physics

One dimensional systems are of incredible importance in this thesis. It is their properties that results in the novel behaviour detailed in part (III). Contrary to what one might think initially, the behaviour of interacting quantum systems in one dimension (1D) is markedly different to those of higher dimensions, and thus the techniques needed will be different. This section will give justification for why a different approach is needed for 1D systems and then introduce the technique of Bosonisation and Luttinger liquids.

2.1 Why is 1D Weird?

When solving quantum mechanical problems, including the effects of interaction and scattering is a big step and one which can render problems insoluble. For many cases of interacting Fermions, Landau's Fermi-Liquid theory is a great approximation. This is a perturbative approach that can simplify the effects of interactions in a many-body system into a non-interacting Fermi-gas with a modified effective mass. Fermi-liquid theory does fail sometimes, and the most important failure for us is 1D.

One justification of the failure of Fermi-Liquid theory comes from thinking of quasiparticle excitations. The excitations of a Fermi-liquid are electrons with a renormalised effective mass. These are single particle excitations which correspond to an actual particle (the electron) with interactions (i.e. with an underlying lattice). This is in contrast to collective excitations, such as phonons, where the quasiparticles involve the collective motion of many discrete particles. In figure 2.1 is an illustration of how excitations

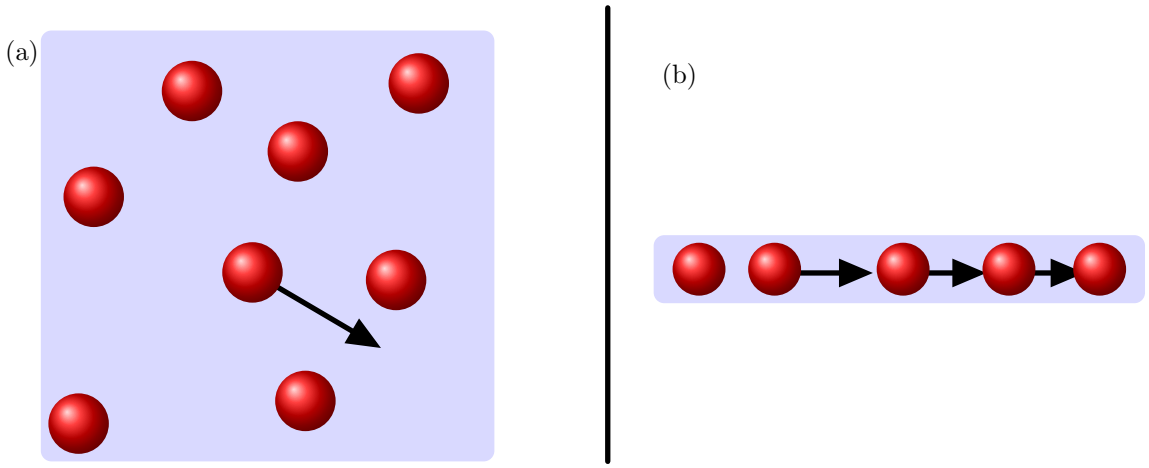

Figure 2.1: Cartoon of particle excitations. a). In 2D single particle excitations are possible. b). In 1D single particle excitations are not possible as they will be converted into collective excitations.

behave differently in 1D. In 2 or 3 dimensions an single excited particle can have a mean free path that is considerably large when compared to inter-particle spacing or even the size of the system. In 1D however, any excitations are confined to travel longitudinally. Any excited particle in 1D will have to collide with its neighbours, imparting energy and momentum, who then in turn collide with their neighbours etc. It is no longer sensible to talk about single particle excitations in 1D since any single particle excitation will be converted to collective excitations of particles. This is further justified by considering how excitations look in momentum space. The low energy excitations in a Fermi gas will come from exciting a particle from below the Fermi surface to above, with some momentum change q. The energies of such excitations form the particle-hole spectrum, as a hole is left in the Fermi sea while the particle is excited. In two and three dimensions, we are able to create excitations of arbitrarily low energy for any $q < 2k_F$ as we can always find two points on the Fermi surface that are connected by the vector $\boldsymbol{q}$. In 1D the Fermi surface consists of two disconnected points, which means the particle hole spectrum only goes to zero for $q = 0, 2k_{\mathrm{F}}$. This makes the quasiparticle from the electron and hole have a low uncertainty in energy, and from the uncertainty principle, a longer lifetime. These long-lived quasiparticles are bosonic in nature as they are comprised of two half-integer spin fermions.

2.2 Luttinger Liquids

This section will introduce the concept of a Luttinger liquid as well as the method of bosonisation. There are several "brands" of bosonisation, but they all produce the same low energy Hamiltonian at the end of the day. The particular approach to bosonisation we shall focus on is what is known as 'Phenomenological Bosonisation', as it is motivated by the phenomenology of 1D systems instead of a rigorous procedure of bosonising operators and keeping a consistent Fock space. Phenomenological bosonisation is easily applied to the systems of ultracold bosons and fermions that I model later in this thesis. This closely follows chapter 3 in Giamarchi's Quantum Physics in One Dimension [16] and is rigorously justified in Cazalilla's paper [17].

We start by considering a general one-dimensional system of bosons or fermions. A general form of the density in such a system can be written as:

$$\rho(x) = \sum_i \delta(x - x_i), \tag{2.2.1}$$

where the positions, x_i, is the position operator of the ith particle. Due to these particles existing in 1D, we can uniquely label them with $x_i < x_j$ when $i < j$. We can then introduce a labelling field $\Theta(x)$, which has the job of expressing the density and fluctuations as a continuous function of x. To do this it is prescribed the property $\Theta(x_i) = 2\pi i$, at the particle positions x_i. This means that $\Theta(x)$ is monotonic-increasing function, an example of which is shown in Fig. (2.2).

Using the properties of delta functions we can rewrite the density in terms of the labelling function:

$$\rho(x) = \partial_x \Theta(x) \sum_n \delta(\Theta(x) - 2\pi n), \tag{2.2.2}$$

and then rewritten again through Poisson's summation formula for the delta function:

$$\rho(x) = \frac{\partial_x \Theta(x)}{2\pi} \sum_m e^{im\Theta(x)}. \tag{2.2.3}$$

It is convenient to introduce a new field, $\theta(x)$, which is the deviation $\Theta(x)$ takes from the perfect crystalline

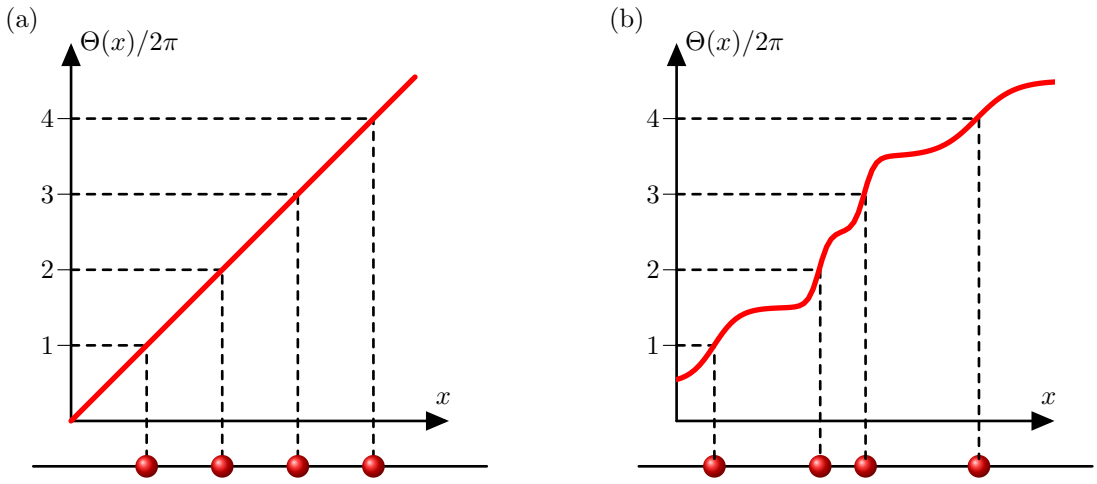

Figure 2.2: Examples of labelling functions $\Theta(x)$. (a) is the perfect crystalline solution where particles are evenly spaced, $\Theta(x) = 2\pi\rho_0 x$. (b) shows an example of a non-uniform particle distribution.

solution where particles are evenly spaced:

$$\Theta(x) = 2\pi\rho_0 x - 2\theta(x), \tag{2.2.4}$$

where ρ_0 is the average density. The density then becomes:

$$\rho(x) = \left(\rho_0 - \frac{1}{\pi}\partial_x\theta(x)\right)\sum_m e^{i2m(\pi\rho_0 x - \theta(x))}. \tag{2.2.5}$$

Up to this point we have not been concerned with the nature of the particles that make up our 1D system, as we have only been expressing density in a uniquely 1D way. We can now use this form of density to express a bosonic creation operator $\psi_B^\dagger$ as:

$$\begin{aligned}\psi_B^\dagger(x) &= \sqrt{\rho(x)}e^{-i\varphi(x)} \\ &= \sqrt{\rho_0 - \tfrac{1}{\pi}\partial_x\theta(x)}\sum_m e^{i2m(\pi\rho_0 x - \theta(x))}e^{-i\varphi(x)}.\end{aligned} \tag{2.2.6}$$

The $m = 0$ term of the density can be thought of as a "smeared" density, which is the dominant term in the long range ($x \gg 1/\rho_0$) dynamics. From the commutation relations that the bosonic operators $\psi_B^\dagger$

and ψ_B have,

$$\left[\frac{1}{\pi}\partial_x\theta(x), \varphi(x')\right] = -i\delta(x-x'). \tag{2.2.7}$$

If our system was made of fermionic particles we would want there to be anticommutation between operators instead. This can be achieved by modifying Eq. (2.2.6) to include a relative factor of -1 when the fermionic operators are commuted. This is done by adding a factor of $e^{i\frac{1}{2}\Theta(x)}$, which oscillates from ± 1 between consecutive particles. Thus the fermionic fields can be expressed as,

$$\begin{aligned}\psi_F^\dagger(x) &= e^{i\frac{1}{2}\Theta(x)}\psi_B^\dagger \\ &= \sqrt{\rho_0 - \tfrac{1}{\pi}\partial_x\theta(x)}\sum_m e^{i(2m+1)(\pi\rho_0 x - \theta(x))}e^{-i\varphi(x)}.\end{aligned} \tag{2.2.8}$$

With the bosonic fields expressed in terms of the low energy bosonic degrees of freedom, Eq. (2.2.6), we can substitute it into a generic Hamiltonian that describes bosons with repulsive contact interactions,

$$H = \frac{\hbar^2}{2m}\int \mathrm{d}x\, \partial_x\psi^\dagger(x)\partial_x\psi(x) + \frac{1}{2}\int \mathrm{d}x\mathrm{d}x'\, g\delta\left(x-x'\right)\psi^\dagger(x)\psi^\dagger(x')\psi(x')\psi(x). \tag{2.2.9}$$

This substitution leads to a Hamiltonian in terms of the phase and density fields,

$$H = \frac{\hbar^2}{2m}\int \mathrm{d}x\, \left\{\rho_0\left(\partial_x\varphi(x)\right)^2 + \frac{gm}{\hbar^2\pi^2}\left(\partial_x\theta(x) - \pi\rho_0\right)^2\right\}. \tag{2.2.10}$$

In the expansion of the second term, only term that is quadratic in $\partial_x\theta$ will play a part in the dynamics. This then gives the Luttinger liquid Hamiltonian,

$$H = \frac{\hbar}{2\pi}\int \mathrm{d}x\left(cK\left(\partial_x\varphi(x)\right)^2 + \frac{c}{K}\left(\partial_x\theta(x)\right)^2\right). \tag{2.2.11}$$

The speed of sound, c, and Luttinger parameter, K, have been defined as:

$$cK = \frac{\pi\hbar\rho_0}{m}, \quad \frac{c}{K} = \frac{g}{\hbar\pi}. \tag{2.2.12}$$

The two parameters introduced have fairly intuitive meanings. The sound velocity, c, is the speed that the bosonic (phononic) excitations travel at. For both systems of 1D bosons and fermions this sound velocity is related to the gradient of the dispersions at low energy, the linear part of the Bogoliubov dispersion for bosons or the Fermi velocity for fermions. The Luttinger parameter K is a dimensionless phenomenological parameter that characterises the interactions present in the Luttinger liquid. The value of K will be determined by the microscopic Hamiltonian, which in our case gives $K = \pi\rho_0\xi$. For condensed bosons, we expect there to be many particles within a healing length ξ, which means $K \geq 1$. For bosons with repulsive interactions (or fermions with attractive ones), $K \geq 1$, with $K = 1$ being reached for infinitely repulsive (Tonks-Girardeau) bosons. This corresponds to non-interacting fermions, as the bosons are effectively "hard core" particles. Values of K ranging between 0 and 1 classify fermionic Luttinger liquids that have repulsive interactions. It can be seen that for large K, the θ term in the Hamiltonian Eq. (2.2.11) shrinks whereas the φ term grows. This illustrates the phase coherence of the condensate, as density fluctuations ($\partial_x\theta$) are "cheap" and fluctuations in the phase are energetically more costly. The opposite argument can be made for $K < 1$, with density fluctuations being more energetically "expensive" for fermionic systems. The fact that we can classify both fermionic and bosonic systems with one parameter illustrates that particle statistics are blurred in 1D. If we were to check the statistics of a pair of particles by exchanging them, we would have to pass them through each other, thus causing them to interact. The statistical phase that is accumulated through the exchange cannot be separated from the scattering phase that occurs when they interact.

2.3 Spinful Luttinger Liquids

So far we have seen the bosonisation of spinless particles, when in reality the spin degrees of freedom in a system can produce a wide gamut of behaviour. In this section we shall investigate what happens when you include spin into a fermionic Luttinger liquid and what behaviour arises from it. We start from considering chiral fermions and then use their bosonisation identities to see what happens to generic scattering processes in terms of the bosonic fields. We will then add an additional spin index to the fields, which will alter some of these scattering terms but leave much of the base level behaviour the same.

2.3.1 Functional Bosonisation of Chiral Fermions

An alternative approach to bosonisation comes from bosonising within the functional integral (see chapter 4 for details on defining and using functional integrals). Here we shall only focus on definitions and results, and details of how the procedure works will be omitted and can be found in [18]. We start with the Hamiltonian density for a system of non-interacting fermions in 1D and linearise around the Fermi points ($p \approx \pm p_{\mathrm{F}}$):

$$\mathcal{H}_0 - \varepsilon_{\mathrm{F}} = \frac{p^2 - p_{\mathrm{F}}^2}{2m} = \frac{(p + p_{\mathrm{F}})(p - p_{\mathrm{F}})}{2m} \approx v_{\mathrm{F}}(|p| - p_{\mathrm{F}}) \to \eta v_{\mathrm{F}} q. \tag{2.3.1}$$

We can see that there are two *almost* independent branches, labelled by their chirality $\eta = \pm 1 \equiv R/L$, and the momentum $q = \eta p - p_{\mathrm{F}}$ measured from the appropriate Fermi point. These two branches correspond to right movers and left movers, which is all that is possible in 1D. The action with this linearised Hamiltonian (with $\xi \equiv x, t$) is;

$$\begin{aligned} \mathcal{S}_0 &= \int \mathrm{d}\xi\, \overline{\psi}(\xi) \left[i\partial_t - (\mathcal{H}_0 - \varepsilon_{\mathrm{F}}) \right] \psi(\xi) \\ &= \sum_{\eta=\pm} \int \mathrm{d}\xi\, \overline{\psi}_\eta(\xi) i \left(\partial_t - \eta v_{\mathrm{F}} \partial_x \right) \psi(\xi), \end{aligned} \tag{2.3.2}$$

where the fields $\overline{\psi}$ and ψ are the the row and column vectors, with $\overline{\psi} = (\overline{\psi}_+, \overline{\psi}_-)$. The fields are now bosonised, similarly to Eq. (2.2.6), with all the dynamics being consolidated into chiral bosonic fields $\theta_\eta(\xi)$,

$$\psi_\eta(\xi) = \chi_\eta e^{i\theta_\eta(\xi)}. \tag{2.3.3}$$

The field χ_η is a global (co-ordinate independent) Majorana field, which exists to preserve the anti-commutation relations between the fields ψ_η. To this end, they obey the anticommutation relation, $\{\chi_\eta, \chi_{\eta'}\} = 0$. They are the equivalent to the Klein factors seen in operator bosonisation (chapter 2 in Giamarchi [16]). It is at this point where the non-trivial details of this transformation arise, which we will skip over in this section. Namely, this transformation appears to lead to a vanishing action due to $\chi_\eta^2 = 0$. This is a well known anomaly, and is carefully considered in [18, 19]. The gist of how to deal

with this anomaly is from the Jacobian of the transformation, leading to a non-zero Hamiltonian for the fields $\theta_\eta(\xi)$:

$$\begin{aligned}\mathcal{H}_0 &= \frac{v_\mathrm{F}}{4\pi}\int \left[(\partial_x\theta_\mathrm{L})^2 + (\partial_x\theta_\mathrm{R})^2\right]\mathrm{d}x \\ &= \frac{v_\mathrm{F}}{2\pi}\int \left[(\partial_x\theta)^2 + (\partial_x\varphi)^2\right]\mathrm{d}x. \end{aligned} \tag{2.3.4}$$

The second line comes from the transformation from the chiral bosonic fields to the more familiar density-phase fields,

$$\theta = \frac{1}{2}(\theta_\mathrm{L} - \theta_\mathrm{R}), \quad \varphi = \frac{1}{2}(\theta_\mathrm{L} + \theta_\mathrm{R}). \tag{2.3.5}$$

The densities of left and right movers (obtained through the use of source fields [18]), is expressed as:

$$\rho_\eta = \frac{\eta}{2\pi}\partial_x\theta_\eta = \frac{1}{2\pi}(\eta\partial_x\varphi - \partial_x\theta). \tag{2.3.6}$$

Knowledge of what the chiral density operators look like when bosonised it critical for the next subsection, where scattering processes depend of terms quadratic in density.

2.3.2 Scattering Processes & Spin-Charge Separation

The beauty of bosonisation is that once we know the identity that takes us from our original fields to the bosonised ones, we can add a multitude of terms to our Hamiltonian and still keep the low energy behaviour categorically unchanged. The lowest energy interaction terms we could add have to act around the Fermi surface, which in 1D is close to $-k_\mathrm{F}$ or $+k_\mathrm{F}$. The extra terms we can add are labelled by their co-efficient g_i, and is commonly known as "g-ology" because of this. A g_4 term couples fermions that live near the same Fermi point, a g_2 term couples fermions that live on opposite Fermi points. Both of these processes are forward scattering, the particles stay on the same side of the fermi surface after scattering. The last term, g_1, couples fermions on opposite sides and has them exchange sides (backscattering)[1]. For spinless fermions, g_1 and g_2 terms are identical due to both particles involved in both processes being

[1] There are also g_3 processes that represent Umklapp scattering, but they are irrelevant in systems we investigate in this thesis

indistinguishable. When a spin index is added they become distinct, but also all g terms are separated into parallel, $g_{\parallel}$, for processes involving the same spin species, and perpendicular, $g_{\perp}$, where the spin species are mixed. For spinless fermions, the g_2 and g_4 terms are bosonised as:

$$\begin{aligned}\frac{g_4}{2}\left(\overline{\psi}_R\psi_R\overline{\psi}_R\psi_R+\overline{\psi}_L\psi_L\overline{\psi}_L\psi_L\right) &= \frac{g_4}{2}\left(\rho_R\rho_R+\rho_L\rho_L\right)\\ &= \frac{g_4}{4\pi^2}\left[(\partial_x\varphi)^2+(\partial_x\theta)^2\right],\end{aligned} \tag{2.3.7}$$

$$\begin{aligned}g_2\overline{\psi}_R\psi_R\overline{\psi}_L\psi_L &= g_2\rho_R\rho_L\\ &= \frac{g_2}{4\pi^2}(\partial_x\varphi-\partial_x\theta)(-\partial_x\varphi-\partial_x\theta)\\ &= \frac{g_2}{4\pi^2}\left[(\partial_x\theta)^2-(\partial_x\varphi)^2\right]\end{aligned} \tag{2.3.8}$$

The bosonised form of these interaction terms fits perfectly into the Hamiltonian Eq. (2.3.4),

$$H=\frac{1}{2\pi}\int \mathrm{d}x\left(cK\left(\partial_x\varphi(x)\right)^2+\frac{c}{K}\left(\partial_x\theta(x)\right)^2\right). \tag{2.3.9}$$

allowing us to define the Luttinger parameter and speed of sound in a similar way to (2.2.11):

$$c=v_{\mathrm{F}}\left[(1+y_4/2)^2-(y_2/2)^2\right]^{1/2} \tag{2.3.10}$$

$$K=\left[\frac{1+y_4/2-y_2/2}{1+y_4/2+y_2/2}\right]^{1/2}. \tag{2.3.11}$$

Here the dimensionless coupling constants are defined as, $y_i=g_i/(\pi v_{\mathrm{F}})$. At this point we can introduce spin degrees of freedom into the Luttinger liquid. This is done by bosonising the two spin species separately and introducing a new index, $\nu=\uparrow,\downarrow$, to denote the spin species. The bosonisation identity Eq. (2.3.3) remains the same, except for the addition of the spin index being included with the chirality index. The two spin species, with the two chirality indices gives us 4 independent, anticommuting χ's. The non-interacting Hamiltonian Eq. (2.3.4) retains its structure, $\mathcal{H}_0=\mathcal{H}_{0,\uparrow}+\mathcal{H}_{0\downarrow}$, and the interaction

terms will be treated much the same as before,

$$\mathcal{H}_4 = \sum_{\eta,\nu} \int \mathrm{d}x \left[\frac{g_{4\parallel}}{2} \rho_{\eta,\nu}(x)\rho_{\eta,\nu}(x) + \frac{g_{4\perp}}{2} \rho_{\eta,\nu}(x)\rho_{\eta,\overline{\nu}}(x) \right]. \tag{2.3.12}$$

$$\mathcal{H}_2 = \sum_{\nu} \int \mathrm{d}x \left[g_{2\parallel} \rho_{R,\nu}(x)\rho_{L,\nu}(x) + g_{2\perp} \rho_{R,\nu}(x)\rho_{L,\overline{\nu}}(x) \right]. \tag{2.3.13}$$

These terms will mix different spin species, but is easily diagonalised with the transformation:

$$\begin{aligned} \varphi_\rho(x) &= \frac{1}{2}\left[\varphi_\uparrow(x) + \varphi_\downarrow(x)\right] \\ \varphi_\sigma(x) &= \frac{1}{2}\left[\varphi_\uparrow(x) - \varphi_\downarrow(x)\right], \end{aligned} \tag{2.3.14}$$

and similarly for $\theta_\nu(x)$. This splits excitations and terms into ones that are of charge (ρ) and those of spin (σ) degrees of freedom. This turns the $g_{2,4}$ interactions into,

$$\begin{aligned} \mathcal{H}_4 = \frac{1}{2\pi^2} \int \mathrm{d}x [g_{4\parallel} + g_{4\perp}] \Big((\partial_x \varphi_\rho)^2 + (\partial_x \theta_\rho)^2 \Big) \\ + [g_{4\parallel} - g_{4\perp}] \Big((\partial_x \varphi_\sigma)^2 + (\partial_x \theta_\sigma)^2 \Big). \end{aligned} \tag{2.3.15}$$

$$\begin{aligned} \mathcal{H}_2 = \frac{1}{2\pi^2} \int \mathrm{d}x [g_{2\parallel} + g_{2\perp}] \Big((\partial_x \theta_\rho)^2 - (\partial_x \varphi_\rho)^2 \Big) \\ + [g_{2\parallel} - g_{2\perp}] \Big((\partial_x \theta_\sigma)^2 - (\partial_x \varphi_\sigma)^2 \Big). \end{aligned} \tag{2.3.16}$$

We can see that the inclusion of these types of scattering doesn't stop the spin and charge Hamiltonians from being completely decouple. They can be nicely incorporated into the Luttinger Hamiltonians for the charge and spin sectors easily. We shall now turn our attention to the g_1 terms. Without spin this term was identical to g_2 and thus not considered, however when including spin things become more interesting.

The g_1 Hamiltonian in full is:

$$\mathcal{H}_1 = \sum_\nu \int \mathrm{d}x \left[g_{1\parallel} \overline{\psi}_{L,\nu} \overline{\psi}_{R,\nu} \psi_{L,\nu} \psi_{R,\nu} + g_{1\perp} \overline{\psi}_{L,\nu} \overline{\psi}_{R,\bar{\nu}} \psi_{L,\bar{\nu}} \psi_{R,\nu} \right] \tag{2.3.17}$$

$$= \sum_\nu \int \mathrm{d}x \left[(-g_{1\parallel}) \overline{\psi}_{L,\nu} \psi_{L,\nu} \overline{\psi}_{R,\nu} \psi_{R,\nu} + g_{1\perp} \overline{\psi}_{L,\nu} \psi_{R,\nu} \overline{\psi}_{R,\bar{\nu}} \psi_{L,\bar{\nu}} \right] \tag{2.3.18}$$

$$= \sum_\nu \int \mathrm{d}x \left[(-g_{1\parallel}) \rho_{L,\nu} \rho_{R,\nu} + g_{1\perp} e^{-i(2\theta_\nu)} e^{i(2\theta_{\bar{\nu}})} \right] \tag{2.3.19}$$

The parallel term is identical to $g_{2\parallel}$, so in Eq. (2.3.16) we can replace $g_{2\parallel} \to g_{2\parallel} - g_{1\parallel}$. The $g_{1\perp}$ term is bosonised with the identity Eq. (2.3.14) to become:

$$\mathcal{H}_{1\perp} = g_{1\perp} \int \mathrm{d}x \sum_{\nu=\uparrow,\downarrow} e^{-i(2\theta_\nu)} e^{i(2\theta_{\bar{\nu}})} \tag{2.3.20}$$

$$= 2g_{1\perp} \int \mathrm{d}x \cos(4\theta_\sigma(x)). \tag{2.3.21}$$

Combining all of these scattering processes results in the total Hamiltonian, $\mathcal{H} = \mathcal{H}_\rho + \mathcal{H}_\sigma$ with sectors for spin and charge degrees of freedom. These two sectors are decoupled, they have no cross-terms arising from $g_{1,2,4}$ interactions. This phenomena is known as "spin-charge separation" and is unique to 1D. In higher dimensions, electrons that move around the lattice carry both spin and charge but in 1D the spin and charge degrees of freedom are free to travel independently. This is another example of collective excitations in 1D, as any single particle excitation will have to carry both charge and spin.

The total Hamiltonian can be expressed with Luttinger parameters K_s and speeds of sound v_s, where $s = \rho, \sigma$ denotes the sector:

$$\mathcal{H} = \frac{1}{\pi} \sum_{s=\rho,\sigma} \int \mathrm{d}x \left(v_s K_s \left(\partial_x \varphi_s(x) \right)^2 + \frac{v_s}{K_s} \left(\partial_x \theta_s(x) \right)^2 \right) + \mathcal{H}_{1\perp}. \tag{2.3.22}$$

The constants are defined as,

$$\begin{aligned} v_s &= v_{\mathrm{F}} \left[(1 + y_{4s}/2)^2 - (y_s/2)^2 \right]^{1/2} \\ K_s &= \left[\frac{1 + y_{4s}/2 - y_s/2}{1 + y_{4s}/2 + y_s/2} \right]^{1/2} \\ g_s &= g_{2\parallel} \pm g_{2\perp} - g_{1\parallel} \\ g_{4s} &= g_{4\parallel} \pm g_{4\perp} \\ y_s &= \frac{g_s}{\pi v_{\mathrm{F}}}. \end{aligned} \tag{2.3.23}$$

The non-quadratic part of the spin Hamiltonian ($g_{1\perp}$) can potentially cause problems and we shall investigate the effect of this term in section 5.3.

Chapter 3

Majorana Zero Modes

In nature we are used to having particles and anti-particles, such as electrons and positrons in particle physics or similarly electrons and holes in the solid state. For each of these examples, the particles and anti-particles are distinct from each other and in second quantisation they have distinct creation (annihilation) operators. The $\hat{c}^\dagger$ operator creates and electron and the $\hat{c}$ operator creates a hole. Mathematically speaking these operators are Hermitian conjugates of one another and, for the example of electrons and holes, are distinct. This doesn't have to be true though, and we could consider a particle who's creation and annihilation operators are self conjugates. With a pair of such operators we express fermionic creation and annihilation operators, $c, c^\dagger$, in Hermitian & anti-Hermitian parts with the Hermitian operators; $\gamma_j = \gamma_j^\dagger$;

$$\begin{aligned} c_j &= \frac{1}{2}(\gamma_{j,1} + i\gamma_{j,2}), \\ c_j^\dagger &= \frac{1}{2}(\gamma_{j,1} - i\gamma_{j,2}). \end{aligned} \tag{3.0.1}$$

One question would now be, "what commutation rules do these γ operators obey?" As the standard fermionic operators obey the anticommutation relation:

$$\{c_i^\dagger, c_j\} = c_i^\dagger c_j + c_j c_i^\dagger = \delta_{i,j}, \tag{3.0.2}$$

the Hermitian γ operators obey the anticommutation relations:

$$\{\gamma_i, \gamma_j\} = 2\delta_{i,j}. \tag{3.0.3}$$

These Hermitian operators are known as Majorana fermions[1] [21] and have been an increasingly popular topic of research in condensed matter physics. This process of writing a fermion as the superposition of two Majorana fermions is normally a purely mathematical procedure, they cannot be probed individually since they are spatially localised together and have a big overlap. Things become more interesting if the Majorana pair is spatially delocalised, for example one Majorana at each end of a 1D wire. This could equally thought of as a single Dirac fermion that delocalises over the entire system. Such a highly delocalised state has protection from local fluctuations, which is a highly desirable quality for qubits to be used in quantum computation.

From inverting the definition Eq. (3.0.1) we can conclude that each species of Majorana is an equal superposition of particle and hole (antiparticle) creation operators. For systems that have particle-hole symmetry, this forces these Majorana fermions to exist at zero energy. For this reason (and to highlight that these excitations aren't particles in a traditional sense) they are often referred to as "Majorana Zero Modes" (MZM).

In this chapter we shall investigate some proposals of condensed matter systems that are predicted to host MZMs, and discuss potential signatures for detecting them in experiments.

3.1 The Kitaev Chain

One of the simplest models that has excitations that can be described by Majorana fermions was described in 2001 by Alexei Kitaev [22]. The model describes spinless fermions hopping on a 1D chain of N sites, with p-wave superconducting pairing and has a Hamiltonian of:

$$\mathcal{H} = -\mu \sum_{j=1}^{N} c_j^\dagger c_j + \sum_{j=1}^{N-1} \left(-t c_j^\dagger c_{j+1} + \Delta c_j c_{j+1} + \text{h.c.} \right). \tag{3.1.1}$$

[1] In contrast to Dirac fermions such as electrons. It is not known if any fundamental particle such as neutrinos are Majorana fermions [20]

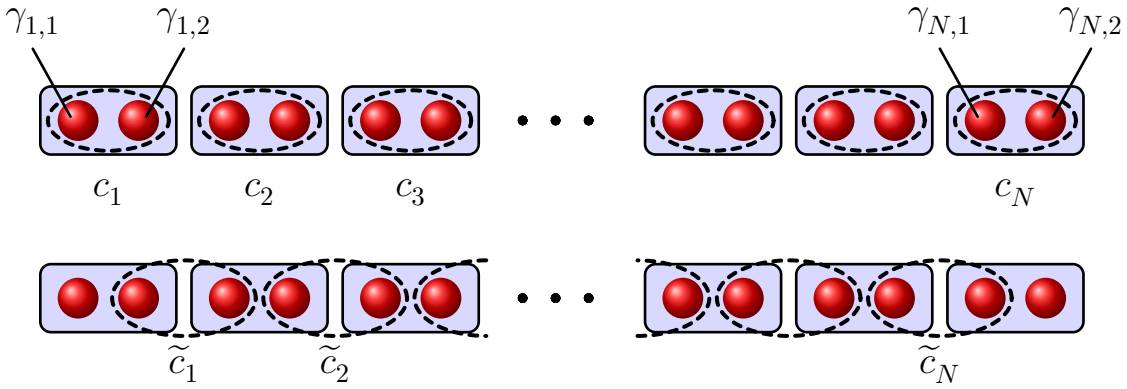

Figure 3.1: Illustration of pairings of Majorana fermions in the Kitaev chain. The top row illustrates the pairings of Majoranas that exist on the same site. The bottom row shows the half-site shift, with unpaired Majoranas at either end.

Here the parameters μ, t and Δ are the chemical potential, hopping strength and superconducting pairing respectively. Without loss of generality we can set the phase of the superconducting pairing to zero, $\Delta = |\Delta|$. This model can be simply diagonalised, however Kitaev's insight was in the details of this diagonalisation. His approach started with writing the fermionic operators on each site c_j and $c_j^\dagger$ in the form of Eq. (3.0.1). This decomposed each fermionic site j, into two species of Majorana fermions that live on that site. Under this transformation, the Hamiltonian becomes,

$$\mathcal{H} = \frac{i}{2}\sum_{j=1}\left[-\mu\gamma_{j,1}\gamma_{j,2} + (t+\Delta)\gamma_{j,2}\gamma_{j+1,1} + (-t+\Delta)\gamma_{j,1}\gamma_{j+1,2}\right]. \tag{3.1.2}$$

For the tuning of $t = \Delta = 0$ and $\mu < 0$, we can see that the model is in the "trivial" phase. The Hamiltonian reads $\mathcal{H} = \frac{i}{2}(-\mu)\sum_j \gamma_{j,1}\gamma_{j,2} = -\mu\sum_j(c_j^\dagger c_j - \frac{1}{2})$. The Majoranas from the same site form pairs that give a ground state of occupation number 0. The opposite case is true for, $\mu = 0$, $t = \Delta > 0$, where the model is in a "topological" phase:

$$\mathcal{H} = it\sum_{j=1}^{N-1}\gamma_{j,2}\gamma_{j+1,1}. \tag{3.1.3}$$

Here the Majoranas from neighbouring sites are paired together, as illustrated in fig. 3.1. So far this is only an alternative way to write the diagonalised Hamiltonian. We can see this more clearly by re-writing

eq. (3.1.3) in terms of shifted fermionic operators,

$$\widetilde{c}_j = \frac{1}{2}\left(\gamma_{j,2} + i\gamma_{j+1,1}\right), \qquad \widetilde{c}_j^\dagger = \frac{1}{2}\left(\gamma_{j,2} - i\gamma_{j+1,1}\right). \tag{3.1.4}$$

This then gives us the diagonal Hamiltonian;

$$\mathcal{H} = 2t\sum_{j=1}^{N-1}(\widetilde{c}_j^\dagger\widetilde{c}_j - 1/2). \tag{3.1.5}$$

This is nothing more than finding a diagonal basis for the model, with the new fermions $\widetilde{c}_j^\dagger$ being shifted 1/2 a site with respect to the original fermions. A key thing we can see is that the Majorana modes $\gamma_{1,1}$ and $\gamma_{N,2}$ aren't present in the Hamiltonian eq. (3.1.3). This means that the ground state is degenerate, we can choose to populate or depopulate the state described by $\widetilde{c}_0 = (\gamma_{N,2} + i\gamma_{1,1})/2$ at no energy cost. It is this fermion that is delocalised across the system, because it is formed from Majoranas that live on opposite edges. Any process that alters the occupation of this state will have to act on the length scales of the whole system, meaning that it is protected against any local fluctuations that may occur.

One way of distinguishing the ground states is fermionic parity, one ground state has an even number of fermions in the wire and the other must have an even number due to adding/removing the $\widetilde{c}_0$ fermion.

3.1.1 Bulk-Edge Correspondence in the Kitaev Chain

The identification of Majorana edge modes in the Kitaev chain might seem like an artefact from tuning the parameters in the model so precisely, and one can wonder if this novel physics would disappear if we were to deviate from this special point in parameter space, ($\Delta = t > 0$, $\mu = 0$). Fortunately this is not the case due to the protection that symmetry provides to the Majoranas. To investigate this (and models later in this chapter) it is useful to look at the Hamiltonian in its Bogoliubov-de Gennes form. This form is particularly useful when dealing with models that have particle-hole symmetry such as these superconducting models. The Hamiltonian (such as Eq. (3.1.1)) is transformed as:

$$\mathcal{H} = \frac{1}{2}C^\dagger\mathcal{H}_{\mathrm{BdG}}C, \tag{3.1.6}$$

where the column vector C contains all the creation and annihilation operators, $C = (c_1, \ldots, c_N, c_1^\dagger, \ldots, c_N^\dagger)^{\mathrm{T}}$. The first N entries in C are creation operators for particles, and the last N are the equivalent creation operators for holes. The Bogoliubov-de Gennes Hamiltonian is then a $2N \times 2N$ matrix which can be written in a compact form using Pauli matrices $\tau_{x,y,z}$ acting on particle-hole space, and row vectors $|n\rangle$ that act on the sites n. In this form, the Kitaev chain Hamiltonian Eq. (3.1.1) becomes:

$$\mathcal{H}_{\mathrm{BdG}} = -\sum_n \mu\tau_z |n\rangle\langle n| - \sum_n (t\tau_z + i\Delta\tau_y) |n\rangle\langle n+1| + \mathrm{H.c.} \tag{3.1.7}$$

This Hamiltonian acts on states $|n\rangle|\tau\rangle$, with $\tau = \pm 1$ denoting the particle/hole states respectively. The particle-hole symmetry can be expressed by the operator: $\mathcal{P} = \tau_x\mathcal{K}$, where the operator $\mathcal{K}$ performs complex conjugation. This operator acting on column vector C, swaps particles and holes. It can also be seen that the Hamiltonian Eq. (3.1.7) will anti-commute with the symmetry operator $\mathcal{P}$:

$$\mathcal{P}^{-1}\mathcal{H}_{\mathrm{BdG}}\mathcal{P} = -\mathcal{H}_{\mathrm{BdG}}. \tag{3.1.8}$$

This can clearly be seen from the structure that $\mathcal{H}_{\mathrm{BdG}}$ takes with Pauli matrices $\tau_{y,z}$. Since the Pauli matrices anti-commute among themselves, any Hamiltonian that has only $i\tau_y$ or τ_z structure in particle-hole space will have this particle-hole symmetry. This is important, because any eigenvector of $\mathcal{H}_{\mathrm{BdG}}$, $\psi = (u, v)^{\mathrm{T}}$ with energy ε will have a corresponding particle-hole symmmetric eigenvector, $\mathcal{P}\psi = (v^*, u^*)^{\mathrm{T}}$ with energy $-\varepsilon$. It is in this Bogoliubov-de Gennes form that the Hamiltonian Eq. (3.1.7) can be inspected again. For the special point of $\mu = 0$, there exists a pair of zero energy states that are spatially localised at the edges. These can be found through fixing N to be some value and then numerically finding the eigenvalues and eigenvectors of the corresponding $2N \times 2N$ matrix. The rest of the eigenvalues are separated from 0 by a gap of $2t$. It is this gap between the edge states and bulk states, along with the particle-hole symmetry that forbids the degenerate ground state from splitting. As μ is increased, the gap between the bulk states and edge states remains finite, until $\mu = 2t$ when the gap closes and the edge states disappear. It is the gaps in the band structure closing and re-opening that are important to classifying these topologically protected edge states, as we shall see in the next section.

Another way to quantify the topology of the Kitaev chain is to define an integer topological invariant,

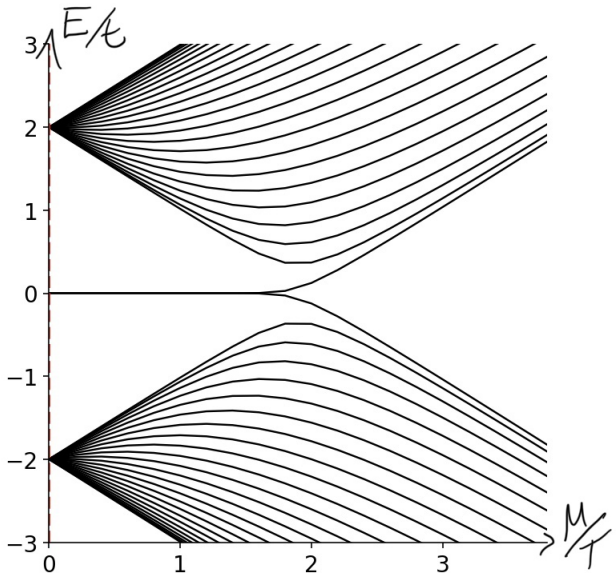

Figure 3.2: Spectrum of Kitaev model (N=25) vs μ. The edge modes exist at zero energy for $\mu < 2t$, when there is a finite bulk gap in the spectrum. From [23]

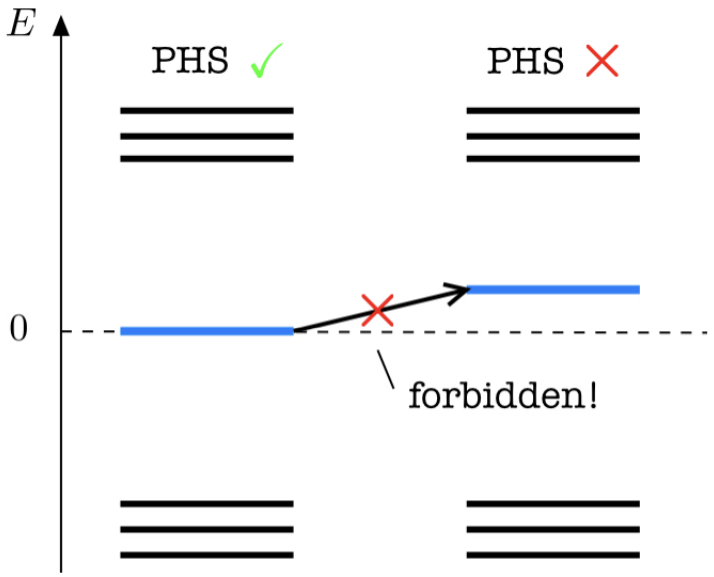

Figure 3.3: Cartoon illustrating the symmetry protection of the MZM in the Kitaev chain. From [23].

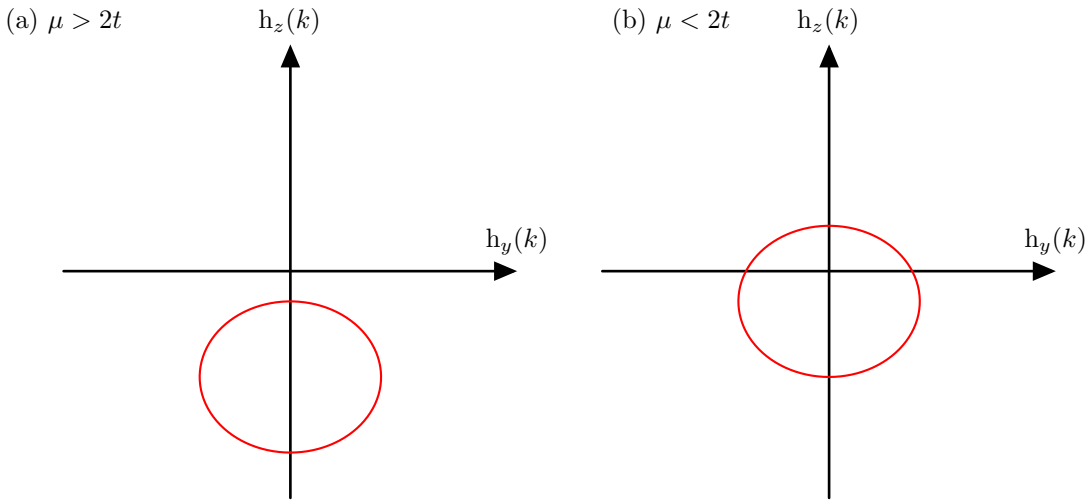

Figure 3.4: Plots of $\mathbf{h}(k)$ for different values of μ. (a) shows the topologically trivial case where the origin is not enclosed by $\mathbf{h}(k)$. (b) shows the topological phase where the origin is enclosed by $\mathbf{h}(k)$.

which changes upon the transition. To do so, we first put the model Eq. (3.1.7) into momentum space:

$$\mathcal{H} = (-2t\cos k - \mu)\tau_z + 2\Delta\tau_y \sin k. \tag{3.1.9}$$

This Hamiltonian can be written as the product,

$$\mathcal{H} = \mathbf{h}(k) \cdot \boldsymbol{\sigma}, \tag{3.1.10}$$

where the vector $\mathbf{h}(k)$ is a parameterisation of the Hamiltonian and $\boldsymbol{\sigma}$ is the vector of Pauli matrices. For the Hamiltonian (3.1.9), there is no σ_x component so the path traced by $\mathbf{h}(k)$ lies in the y, z plane. The topological invariant is the "polarisation" of the fermions, and is defined to be the winding number of $\mathbf{h}(k)$ about the origin. For $t = \Delta$, it can be seen in figure 3.4 that for $\mu < 2t$ the origin is enclosed by $\mathbf{h}(k)$, corresponding to the topologically edge modes. For $\mu > 2t$ the origin is not enclosed and the system is topologically trivial. The role particle-hole symmetry plays is to ensure that $h_x(k) = 0$ for any fluctuations. If this were non-zero then a winding number would not be able to be well defined, and thus would be fragile to fluctuations.

3.2 Majorana Fermions in "Real" Systems

The Kitaev chain is an interesting model in describing topological excitations as MZMs, but it is a fairly contrived model. Firstly is the fact that the fermions contained in the chain are spinless, contrary to all fermions that are present in the lab/nature. Secondly is the p-wave superconductivity, which is considerably rarer in materials compared to the standard s-wave superconductivity. These conditions make the hunt for Majorana fermions as edge modes in solid state systems a challenging one. A breakthrough occurred in 2008 when Fu and Kane proposed experiments to probe potential MZMs in a system of a superconductor connected to a magnet on the surface of a topological insulator [24]. Another breakthrough happened in 2010, where two groups simultaneously proposed solid state systems that would theoretically produce MZMs as edge modes [9, 10]. These systems garnered acclaim and interest as they seemed a fruitful platform for the elusive Majorana fermions to be observed however, to date, MZMs have not been observed in a condensed matter system. These systems suggested by Lutchyn et. al. [9] and Oreg et. al. [10] are of particular interest in this thesis, because of their similarities to a seemingly unrelated system of Bose-Einstein condensates flowing through a 1D channel (described in chapter 6). In this section we shall look briefly at the models which these groups proposed, and see what signatures MZMs would present in these systems. For full details, the reviews by Alicea [25], Beenakker [26] and the lecture course on Topological Condensed Matter Physics from TU Delft [23].

3.2.1 What features are needed?

Recreating the physics of the Kitaev model in a realistic system requires a few steps. First is to take the continuum Hamiltonian, (3.1.9) and linearise for small k:

$$\mathcal{H}_{\text{Kitaev}} = \left(\frac{k^2}{2m^*} - \mu\right)\tau_z + 2\Delta k\tau_y. \tag{3.2.1}$$

Here the effective mass is defined as $m^* = 1/2t$ and the chemical potential has been shift to measure from the bottom of the band: $\mu \to \mu + 2t$. The first piece of building a system to get close to this model is picking the material that will give a controllable dispersion, like the first term in Eq. (3.2.1). A semiconductor nanowire would be an ideal candidate, as it can be doped to adjust the chemical potential

with ease.

With this base, we can introduce terms that will get us closer to something that will host MZMs. Unlike the Kitaev chain model the electrons in a semiconductor will have a spin, which increases the degrees of freedom to include a spin index, $\uparrow\downarrow$, described by Pauli matrices σ_i, that act on spin space. This will double the number of bands in the spectrum, and if there are no spin dependent terms in the Hamiltonian these bands will be degenerate. If we had a zero energy mode hosting a Majorana fermion and then added spin, we would add another Majorana fermion to the edge mode. This would then just be a normal fermion tuned to zero energy and not the exciting unpaired Majoranas that the Kitaev chain describes. To lift this degeneracy a spin dependent term is needed. The type that is chosen is one of a Zeeman field, a magnetic field that acts in the z direction. This favours one spin species to another, lifting the degenerate spin bands. This is the equivalent to changing the chemical potential for the spin species. The shift between topologically trivial and non-trivial bands in the Kitaev chain comes from changing the chemical potential μ, so the Zeeman field can shift one spin species into the topological phase while shifting the other spin species to be topologically trivial.

The superconductivity now needs to be added to this semiconductor nanowire with a Zeeman field. This is important because it imposes the particle-hole symmetry that is important for hosting Majoranas. In experiment, this will come from embedding the wire on top of a superconductor and having a superconducting pairing induced through the proximity effect. For feasibility reasons, the pairing modelled will be s-wave, as opposed to the p-wave exhibited in the Kitaev chain model. This is due to the dearth of p-wave superconductors when compared to the abundance of materials that exhibit s-wave superconductivity. As with the other features added, control over the superconductivity is of upmost importance. In the papers [9, 10], spatial variation of the pairing potential is essential in creating the "edges" where the MZMs will live.

The final piece of the model is a spin-orbit coupling term. This is a momentum dependent term of the form, $H_{\mathrm{SO}} = \alpha\sigma_y k$. Without this term the total spin is conserved (σ_z commutes with the Hamiltonian), meaning that any excitations have a definite spin. As exhibited from the Kitaev chain, MZMs have no spin. This means that this conservation must be broken, and the easiest term to implement this change will be a Spin-Orbit coupling. One candidate material is Indium Arsenide, which has a strong spin orbit

coupling with a Landé g factor of ~ 35.

In total, the four terms needed are: chemical potential, magnetic field, superconducting pairing and spin orbit coupling.

3.2.2 Semiconductor-Superconductor Nanowires

In Lutchyn et. al, and Oreg et. al.'s models, all the pieces are present but in slightly different combinations. The Hamiltonian used by Oreg et. al [10] describes a nanowire, lying in the y direction, with spin-orbit coupling (u) along the z axis and a magnetic field (B) along the x axis. It can be expressed in Bogoliubov-de Gennes form with Nambu spinors, $\Psi^\dagger = (\psi_\uparrow^\dagger, \psi_\downarrow^\dagger, \psi_\downarrow, -\psi_\uparrow)$:

$$\begin{aligned} H &= \int \mathrm{d}y\, \Psi^\dagger(y) \mathcal{H}_{\mathrm{BdG}} \Psi(y), \\ \mathcal{H}_{\mathrm{BdG}} &= \left(-\frac{\partial_x^2}{2m^*} - \mu(y) \right) \tau_z + u \partial_x \sigma_z \tau_z + B(y)\sigma_x + \Delta(y)\tau_x. \end{aligned} \tag{3.2.2}$$

As before, the τ Pauli matrices act on particle-hole space and the additional σ Pauli matrices act on spin space. The spectrum for this model is easily found by going to momentum space and then squaring the Hamiltonian twice. The energy for constant μ, B, Δ and u is:

$$E_\pm^2 = B^2 + \Delta^2 + \xi_k^2 + (uk)^2 \pm 2\sqrt{B^2\Delta^2 + B^2\xi_k^2 + (uk)^2\xi_k^2}, \tag{3.2.3}$$

where $\xi_k = k^2/2m^* - \mu$. The $\pm$ denotes the different bands coming from opposite spin species, while the other two bands are the reflection about $E = 0$ from the particle-hole symmetry. As the parameters Δ, μ and B change from 0, band gaps at $k = 0$ and $k = \pm 2um^*$ open and close linearly with the parameters. This is a signature of topological phase transitions occurring. It is at the $k = 0$ point where Oreg et. al. investigated what was going on. The energy at $k = 0$ is,

$$E(k = 0) = \left| B - \sqrt{\Delta^2 + \mu^2} \right|, \tag{3.2.4}$$

which changes from being pairing dominated and topologically trivial when $B^2 < \Delta^2 + \mu^2$, to B-dominated and topologically non-trivial when $B^2 > \Delta^2 + \mu^2$. The classification can be reasoned by considering

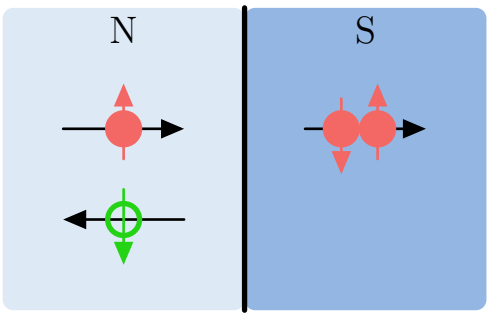

Figure 3.5: Cartoon illustrating Andreev Reflection. A particle in a normal metal, incident on a superconductor can tunnel as a Cooper pair by reflecting a hole back into the normal metal.

$B = 0, \Delta^2 + \mu^2 \neq 0$. The system must be in the topologically trivial phase because there is nothing that lifts the spin degeneracy. As B is increased, the band gap at $k = 0$ decreases until $B = \sqrt{\Delta^2 + \mu^2}$ when it closes. As the band gap closes, and then re-opens for $B > \sqrt{\Delta^2 + \mu^2}$, there must be a transition to a phase with a different topology. This is further justified by Oreg et. al. who took a spatially varying B field, that crosses the critical value at $y = 0$. They linearised the Hamiltonian Eq. (3.2.2) about $k = 0$, squared it and then diagonalised it. They were then able to explicitly write a zero energy eigenstate as a Majorana operator consisting of particle and hole operators of both spin species (see Eq. (6) in [10]).

Lutchyn et. al. have a similar model in their paper [9], but investigated some slightly different properties of the nanowire. In their model, the superconductive pairing term has the spatial dependence of: $\Delta(x) = \Delta_0\Theta(x - L) + \Delta_0 e^{i\varphi}\Theta(-x - L)$, where φ is the phase difference between the left and right sides of the wire. They were interested in solving the BdG equation (3.2.2) for zero energy. They also probed the spectrum of Andreev reflection. This is a process of tunnelling from a normal metal to a superconductor. Due to the gap in the superconductor a single particle is unable to tunnel with an energy below the gap, however Cooper pairs are allowed to. Andreev reflection is the process where a single particle, incident on a superconductor with an energy within the gap, tunnels into the superconductor as a Cooper pair by reflecting a hole back into the normal metal. By numerically solving their BdG equations, subject to the boundary conditions of Andreev reflection, Lutchyn et. al. were able to see that the spectrum of Andreev excitations has some non-trivial dependence on the phase difference across the wire. This is shown in figure 3.6, where the Andreev spectra for finite sized systems are plotted as a function of phase difference. In the topological case, there are an odd number of crossings that the bands make at zero energy. This contrasts with the topologically trivial case where there an even number of

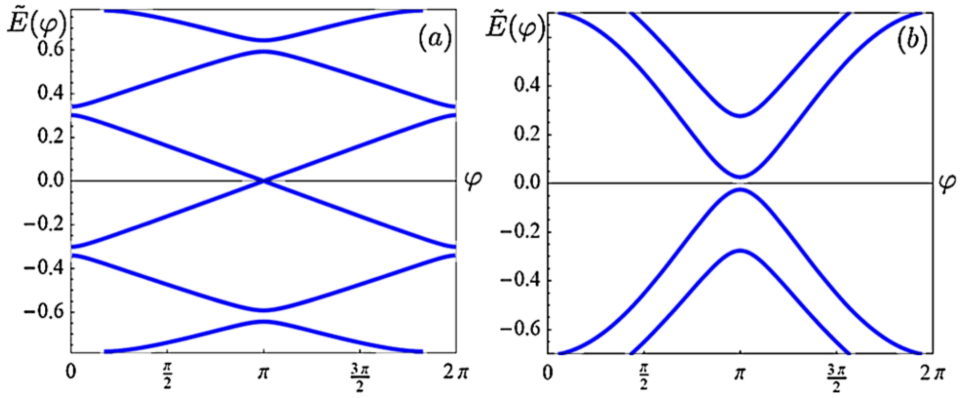

Figure 3.6: Andreev spectra for semiconctor-superconductor nanowire, from [9]. (a) The topologically non-trivial case where there is an odd number of crossings in the spectrum, occurring at a phase difference of π. (b) The topologically trivial case, where there is an even number of crossings.

crossings. This odd number of crossings for the topological case (which harbours Majorana edge modes) means that the energy (and current) is a 4π periodic function of phase. If measured in experiments, this would be a clear indicator of non-trivial physics occurring and potentially a "smoking gun" signature of Majorana zero modes. It is also a key feature of the main system covered in this thesis, namely phase driven transport of superfluids through 1D channels. In chapters 6 and 7 we shall see how these systems have similarities to these solid state systems that claim to host Majorana fermions.

3.2.3 The Bosonised Nanowire

As the system investigated by Lutchyn et. al. is one dimensional, it can be investigated by using the technique of bosonisation, as done in [27]. Through bosonising the system of the nanowire, we are able to make some statements about the nature of the degeneracy that is present when the edges host MZMs.

In the paper [27], they start with the nanowire lying on the x axis, with spin-orbit coupling, a Zeeman field and superconductive pairing:

$$\begin{aligned}\mathcal{H}_{\mathrm{NW}} &= \int_{-L/2}^{L/2} \mathrm{d}x \psi_\sigma^\dagger(x) \left(-\frac{\partial_x^2}{2m^*} - \mu + i\alpha\sigma_y\partial_x + V_x\sigma_x\right)_{\sigma,\sigma'} \psi_{\sigma'}(x) \\ \mathcal{H}_{\mathrm{P}} &= \int \mathrm{d}x \left[\Delta_0\psi_\uparrow\psi_\downarrow + \mathrm{H.c.}\right].\end{aligned} \tag{3.2.5}$$

The nanowire is projected onto the lowest band, and linearised with field operator, $\Psi(x) \equiv (\psi_\uparrow(x), \psi_\downarrow(x))$

$$\Psi(x) \approx \Phi_-(p_\mathrm{F})e^{ip_\mathrm{F}x}c_R(x) + \Phi_-(-p_\mathrm{F})e^{-ip_\mathrm{F}x}c_L(x) \tag{3.2.6}$$

where the spinors are defined as, $\Phi_-(p_\mathrm{F}) = \frac{1}{\sqrt{2}}(-e^{i\kappa(p_\mathrm{F})}, 1)$, with $\kappa(p_\mathrm{F}) = \tan^{-1}(\alpha p_\mathrm{F}/V_x)$. These diagonalise the Hamiltonian, meaning that it can be described by the spinless chiral fermions, $c_{L/R}$. These chiral fermions are bosonised in the standard way, as seen in chapter 2; $c_{R/L} = \frac{1}{\sqrt{2\pi\alpha}}e^{-i(\pm\theta-\phi)}$. The bosonised nanowire Hamiltonian then looks like:

$$\mathcal{H}_\mathrm{NW} \approx v\int_{-L/2}^{L/2}\mathrm{d}x\left[ic_L^\dagger(x)\partial_x c_L(x) - ic_R^\dagger(x)\partial_x c_R(x)\right] \tag{3.2.7}$$

$$\approx \frac{v}{2\pi}\int_{-L/2}^{L/2}\mathrm{d}x\left[K(\partial_x\phi)^2 + K^{-1}(\partial_x\theta)^2\right] \tag{3.2.8}$$

$$\mathcal{H}_\mathrm{P} = \frac{\Delta_P}{2\pi a}\int_{-L/2}^{L/2}\mathrm{d}x\sin(2\phi). \tag{3.2.9}$$

The phase field, ϕ and density field θ also obey the standard commutation relations:

$$[\partial_x\theta(x), \phi(x')] = i\pi\delta(x-x'). \tag{3.2.10}$$

The superconducting pairing is bosonised in a similar way, to give rise to a global Sine-Gordon type impurity for the phase field ϕ. In total the Hamiltonian is,

$$\mathcal{H}_\mathrm{T} = \int_{-L/2}^{L/2}\mathrm{d}x\left(\frac{v}{2\pi}\left[K(\partial\phi)^2 + K^{-1}(\partial_x\theta)^2\right] + \frac{\Delta_P}{2\pi a}\sin(2\phi)\right). \tag{3.2.11}$$

As will be shown in section 5.3, the Sine-Gordon impurity is important to consider for values of $K > 1/2$, which can be made with repulsive interactions within the nanowire (so long as they are not too repulsive). When the Sine-Gordon impurity is relevant, the ground state can be found by minimising the sine and having the field ϕ pinned to one of the minima. For $\Delta_P > 0$, this gives two different solutions for $\phi \in [-\pi, \pi]$. These are, $\phi = -\pi/4$ & $3\pi/4$, which are related by the transformation $\phi \to \phi + \pi$. This transformation between the degenerate ground states can be understood by considering the fermionic

parity operator, $(-1)^{N_F}$:

$$(-1)^{N_F} = e^{i[\theta(L/2)-\theta(-L/2)]}. \tag{3.2.12}$$

Combined with the commutation relationship Eq. (3.2.10), it can be seen that what connects these two ground states is fermionic parity, i.e. moving between them equates to adding or removing a single fermion. In Majorana language, this is the same as the degeneracy in the Kitaev chain, where the edge modes could either have the non-local fermion occupied or unoccupied at zero energy cost.

Part II

Concepts Background: Mathematics

Chapter 4

Functional Integration

Functional integrals are a powerful technique in quantum field theory, allowing for the easy computation of expectation values and ability to investigate the effects of perturbations to a system. Here we shall sketch an overview of how this method works, further details are present in Altland and Simons, chapters 3 & 4 [28] as well as Nagaosa chapter 2 [29]. The main focus of this chapter will be the calculation of correlation functions, both of Luttinger Liquids and of BCS superconductors.

4.1 Introduction to Functional Integration

We start with the definition of the partition function in imaginary time:

$$\mathcal{Z} = \det\left(i\omega - \hat{H}\right)^{-1}, \tag{4.1.1}$$

where ω is the energy and $\hat{H}$ is a single particle Hamiltonian with eigenvalues and eigenvectors labeled by α: $\hat{H}\left|\alpha\right\rangle = \varepsilon_\alpha \left|\alpha\right\rangle$. The determinant is independent of basis, so the partition function can be written as the product over eigenvalues:

$$\mathcal{Z} = \prod_\alpha \frac{1}{i\omega - \varepsilon_\alpha}. \tag{4.1.2}$$

Using the result of the Gaussian integral,

$$\int_{-\infty}^{\infty} \mathrm{d}x\, e^{-bx^2} = \sqrt{\frac{\pi}{b}} \tag{4.1.3}$$

we can express the fraction within the product as a Gaussian integral over two real variables:

$$\frac{1}{i\omega - \varepsilon_\alpha} = \frac{1}{\pi} \int_{-\infty}^{\infty} \mathrm{d}x\, \mathrm{d}y\, e^{-(i\omega - \varepsilon_\alpha)(x^2+y^2)}. \tag{4.1.4}$$

Making the transformation to complex numbers, $c = x + iy$ and $c^* = x - iy$ gives:

$$\frac{1}{i\omega - \varepsilon_\alpha} = \frac{1}{2\pi i} \int_{-\infty}^{\infty} \mathrm{d}c^*\, \mathrm{d}c\, e^{-c^*(i\omega - \varepsilon_\alpha)c}. \tag{4.1.5}$$

With this the partition function can be written as the product of these integrals, giving a functional integral:

$$\begin{aligned} \mathcal{Z} &= \prod_\alpha \left[\int \frac{\mathrm{d}c_\alpha^*\, \mathrm{d}c_\alpha}{2\pi i}\, e^{-c_\alpha^*(i\omega - \varepsilon_\alpha)c_\alpha} \right] \\ &= \int \mathrm{D}c^*\, \mathrm{D}c\, e^{-c^*(i\omega - \varepsilon_\alpha)c}. \end{aligned} \tag{4.1.6}$$

The notation of $\mathrm{D}c^*\, \mathrm{D}c$ denotes the integration over all possible complex numbers as well as absorbing the factors of $1/2\pi i$ present in the product. The complex numbers c are also denote the coefficients of the basis states of the Hilbert space as such:

$$\Psi(r) = \langle r|\Psi\rangle = \sum_\alpha \langle r|\, c_\alpha\, |\alpha\rangle = \sum_\alpha c_\alpha \psi_\alpha(r), \tag{4.1.7}$$

thus meaning that the functional integral integrates over all possible states in the Hilbert space. In real time the partition function is:

$$\mathcal{Z} = \det\left(\omega - \hat{H}\right)^{-1} = \int \mathrm{D}c^*\, \mathrm{D}c\, e^{i\sum_\alpha c_\alpha^*(\omega - \varepsilon_\alpha)c_\alpha}. \tag{4.1.8}$$

The sum in the exponent can be rewritten in terms of the real space wavefunctions as:

$$\begin{aligned}\sum_\alpha c_\alpha^*(\omega-\varepsilon_\alpha)c_\alpha &= \sum_{\alpha\beta} c_\alpha^*(\omega-\varepsilon_\alpha)c_\beta\delta_{\alpha\beta}\\ &= \sum_{\alpha\beta} c_\alpha^*(\omega-\varepsilon_\alpha)c_\beta\int \mathrm{d}r\psi_\alpha^*(r)\psi_\beta(r)\\ &= \int \mathrm{d}r\left(\sum_\alpha c_\alpha^*\psi_\alpha^*(r)\right)(\omega-\varepsilon_\alpha)\left(\sum_\beta c_\alpha\psi_\beta(r)\right)\\ &= \int \mathrm{d}r\Psi^*(r)(\omega-\varepsilon_\alpha)\Psi(r).\end{aligned} \tag{4.1.9}$$

This then Fourier transforms into:

$$\int \mathrm{d}r\Psi^*(r)(\omega-\varepsilon_\alpha)\Psi(r) \to \int \mathrm{d}r\Psi^*(r)(\partial_t-\varepsilon_\alpha)\Psi(r) = S[\Psi^*(r),\Psi(r)], \tag{4.1.10}$$

where S is the action. The partition function is now simply:

$$Z = \int \mathrm{D}\Psi^*\mathrm{D}\Psi\, e^{\frac{i}{\hbar}S[\Psi^*,\Psi]}, \tag{4.1.11}$$

where $\hbar$ has been restored for dimensionality. Assuming the action has up to quadratic terms in the fields the functional integral is over, the partition function and correlation functions can be calculated fairly simply using Gaussian integrals. For complex numbers ϕ_i & h_i and matrix M, the result is:

$$\prod_n \int \frac{\mathrm{d}\phi_n^*\mathrm{d}\phi_n}{2\pi i}\, e^{-\sum_{ij}\phi_i^*M_{ij}\phi_j+\sum_i h_i^*\phi_i+\phi_i^*h_i} = \frac{e^{\sum_{ij}h_i^*(M^{-1})_{ij}h_j}}{\det(M)} \tag{4.1.12}$$

This can be used as a generating function for correlation functions, defined as:

$$\begin{aligned}\langle\phi_p^*\phi_q\rangle &= \frac{1}{Z}\prod_n\int \frac{\mathrm{d}\phi_n^*\mathrm{d}\phi_n}{2\pi i}\,\phi_p^*\phi_q\, e^{-\sum_{ij}\phi_i^*M_{ij}\phi_j}\\ &= \lim_{h\to 0}\frac{1}{Z}\frac{\partial}{\partial h_p^*}\frac{\partial}{\partial h_q}Z\\ &= M_{pq}^{-1}.\end{aligned} \tag{4.1.13}$$

One important result is that for a real field, where $\phi^*(q) = \phi(-q)$, the correlations go as:

$$\langle \phi^*(q_1)\phi(q_2)\rangle = \frac{\int \mathrm{D}\phi^*[q]\mathrm{D}\phi[q]\phi^*(q_1)\phi(q_2)\, e^{-1/2\sum_q \phi^*(q)M(q)\phi(q)}}{\int \mathrm{D}\phi^*[q]\mathrm{D}\phi[q]\, e^{-1/2\sum_q \phi^*(q)M(q)\phi(q)}} = \frac{1}{M(q_1)}\delta_{q_1,q_2}. \tag{4.1.14}$$

The techniques of functional integration and the ways to calculate averages will be very important in the rest of the thesis, as we shall see in the next two sections.

4.2 BCS Field Theory

The main result of this thesis involves superconductors, which are introduced in section 1.2.1. In this section we shall describe the BCS action and treat it with a Hubbard-Stratonovich transformation and then calculate the singlet correlation functions. This procedure will be roughly following chapter 5 of Nagaosa [29].

4.2.1 BCS Path Integrals

BCS theory involves an attractive term in the Hamiltonian that causes the formation of singlets. For solid state realisations of BCS theory this attractive potential arises from interactions of electrons with the lattice, wheras these interactions can be generated in cold atom systems through Feshbach resonances. For fermions with creation (annihilation) operators $c^\dagger_\sigma$ and attractive s-wave, pointlike interactions with strength g, the Hamiltonian is,

$$H_{\mathrm{BCS}} = \int \mathrm{d}\boldsymbol{r}\, c^\dagger_\sigma(\boldsymbol{r})\left[-\frac{1}{2m}\nabla^2 - \mu\right] c_\sigma(\boldsymbol{r}) - g\int \mathrm{d}\boldsymbol{r}\, c^\dagger_\uparrow(\boldsymbol{r})c^\dagger_\downarrow(\boldsymbol{r})c_\downarrow(\boldsymbol{r})c_\uparrow(\boldsymbol{r}), \tag{4.2.1}$$

where summation over the repeated spin (σ) indices is implicit. The partition function is $\mathcal{Z}_{\mathrm{BCS}} = \int \mathrm{D}(\bar\psi,\psi)e^{-S_{\mathrm{BCS}}[\bar\psi,\psi]}$ with,

$$S_{\mathrm{BCS}}[\bar\psi,\psi] = \int_0^\beta d\tau \int d^3r \left[\bar\psi_\sigma\left(\partial_\tau - \frac{1}{2m}\nabla^2 - \mu\right)\psi_\sigma - g\bar\psi_\uparrow\bar\psi_\downarrow\psi_\downarrow\psi_\uparrow\right], \tag{4.2.2}$$

with $\psi(\boldsymbol{r},\tau)$ being Grassmann fields. The problem with this action is the quartic interaction term which

stops us from performing the standard Gaussian integrals. One way of dealing with this term and reduce the action down to one which is, at most, quadratic in fields is through a Hubbard-Stratonovich transformation. This exact transformation accomplishes this with the compromise of introducing new fields to decouple the interaction. The interaction term transforms as:

$$\exp\left\{g\int \mathrm{d}\tau \int \mathrm{d}\boldsymbol{r}\, \bar{\psi}_\uparrow \bar{\psi}_\downarrow \psi_\downarrow \psi_\uparrow \right\} = \int \mathrm{D}(\bar{\Delta},\Delta)\exp\left\{-\int \mathrm{d}\tau \int \mathrm{d}\boldsymbol{r}\, \left[\frac{1}{g}|\Delta|^2 - (\bar{\Delta}\psi_\downarrow\psi_\uparrow + \Delta\bar{\psi}_\uparrow\bar{\psi}_\downarrow)\right]\right\} \quad (4.2.3)$$

Now the once quartic interaction has been replaced by terms that are quadratic in the new fields Δ. It can be shown that this field Δ will take a mean field value, $\Delta_0(\boldsymbol{r})$, which is the Ginzburg-Landau order parameter. This tells us that when Δ is non-zero we have a superconducting state of matter. Taking Eq. 4.2.3 into the full action we have:

$$\begin{aligned}\mathcal{S}_{\mathrm{BCS}} = \int_0^\beta \mathrm{d}\tau \int \mathrm{d}^3 r \Bigg\{ &\frac{1}{g}|\Delta(\boldsymbol{r},\tau)|^2 - \bar{\psi}_\sigma \left(\partial_\tau - \frac{1}{2m}\nabla^2 - \mu\right)\psi_\sigma \\ &- \bar{\Delta}(\boldsymbol{r},\tau)\psi_\downarrow(\boldsymbol{r},\tau)\psi_\uparrow(\boldsymbol{r},\tau) - \bar{\psi}_\uparrow(\boldsymbol{r},\tau)\bar{\psi}_\downarrow(\boldsymbol{r},\tau)\Delta(\boldsymbol{r},\tau)\Bigg\}. \end{aligned} \quad (4.2.4)$$

This action can be rewritten in a matrix form with the identification of the Nambu spinors:

$$\Psi(\boldsymbol{r},\tau) = \begin{pmatrix} \psi_\uparrow(\boldsymbol{r},\tau) \\ \bar{\psi}_\downarrow(\boldsymbol{r},\tau)\end{pmatrix}, \qquad \bar{\Psi}(\boldsymbol{r},\tau) = \begin{pmatrix} \bar{\psi}_\uparrow(\boldsymbol{r},\tau) & \psi_\downarrow(\boldsymbol{r},\tau)\end{pmatrix} \quad (4.2.5)$$

These spinors combine particle and hole degrees of freedom into a single object, allowing for the action Eq. 4.2.4 to be written in the form:

$$\mathcal{S}_{\mathrm{BCS}} = \int_0^\beta \mathrm{d}\tau \int \mathrm{d}^3 r \left\{ \frac{1}{g}|\Delta(\boldsymbol{r},\tau)|^2 - \bar{\Psi}(\boldsymbol{r},\tau)\begin{pmatrix} -\partial_\tau + \frac{1}{2m}\nabla^2 + \mu & \Delta \\ \bar{\Delta} & -\partial_\tau - \frac{1}{2m}\nabla^2 - \mu\end{pmatrix}\Psi(\boldsymbol{r},\tau)\right\} \quad (4.2.6)$$

With this action we want to calculate correlation functions of the superconductor, specifically the anomalous correlation functions like $\langle\psi_\uparrow(\boldsymbol{r},\tau)\psi_\downarrow(\boldsymbol{r},\tau')\rangle$. To do so we will introduce source fields coupled to Ψ

and $\overline{\Psi}$ which should have the same form as the Nambu spinors:

$$\mathrm{h}(\boldsymbol{r},\tau)=\begin{pmatrix}h_{\uparrow}(\boldsymbol{r},\tau)\\ \bar{h}_{\downarrow}(\boldsymbol{r},\tau)\end{pmatrix},\qquad\qquad \bar{\mathrm{h}}(\boldsymbol{r},\tau)=\begin{pmatrix}\bar{h}_{\uparrow}(\boldsymbol{r},\tau) & h_{\downarrow}(\boldsymbol{r},\tau)\end{pmatrix} \tag{4.2.7}$$

With the source fields our action is now:

$$\mathcal{S}_{\mathrm{BCS}}=\int_0^{\beta}\mathrm{d}\tau\int\mathrm{d}^3r\left\{\frac{1}{g}|\Delta(\boldsymbol{r},\tau)|^2-\bar{\Psi}(\boldsymbol{r},\tau)\mathcal{G}^{-1}\Psi(\boldsymbol{r},\tau)+\bar{\mathrm{h}}(\boldsymbol{r},\tau)\Psi(\boldsymbol{r},\tau)+\bar{\Psi}(\boldsymbol{r},\tau)\mathrm{h}(\boldsymbol{r},\tau)\right\} \tag{4.2.8}$$

where the matrix,

$$\mathcal{G}^{-1}=\begin{pmatrix}-\partial_\tau+\frac{1}{2m}\nabla^2+\mu & \Delta\\ \bar{\Delta} & -\partial_\tau-\frac{1}{2m}\nabla^2-\mu\end{pmatrix}$$

is known as the Gor'kov Green's function. With this action we desire to calculate the anomalous correlation functions, which can be evaluated by taking the partial derivatives:

$$\langle\psi_{\uparrow}(\boldsymbol{r},\tau)\psi_{\downarrow}(\boldsymbol{r},\tau')\rangle_{\mathrm{BCS}}=\lim_{h\to0}\frac{1}{\mathcal{Z}}\frac{\partial}{\partial\bar{h}_{\uparrow}(\boldsymbol{r},\tau)}\frac{\partial}{\partial\bar{h}_{\downarrow}(\boldsymbol{r},\tau')}\mathcal{Z}. \tag{4.2.9}$$

Evaluating these partial derivatives is accomplished by making a shift in the Ψ fields of: $\Psi\mapsto\Psi+\mathcal{G}\mathrm{h}$ & $\bar{\Psi}\mapsto\bar{\Psi}+\bar{\mathrm{h}}\mathcal{G}$. This shift then makes the action quadratic in h:

$$\mathcal{S}_{\mathrm{BCS}}=\int_0^{\beta}\mathrm{d}\tau\int\mathrm{d}^3r\left\{\frac{1}{g}|\Delta(\boldsymbol{r},\tau)|^2-\bar{\Psi}(\boldsymbol{r},\tau)\mathcal{G}^{-1}\Psi(\boldsymbol{r},\tau)-\bar{\mathrm{h}}(\boldsymbol{r},\tau)\mathcal{G}\mathrm{h}(\boldsymbol{r},\tau)\right\}. \tag{4.2.10}$$

Evaluating the matrix $\mathcal{G}$ is a simple procedure in reciprocal space, as the derivative operators turn into ω and k elements. We define the Fourier transform of the fields as:

$$\psi_{\sigma}(\boldsymbol{r},\tau)=\iint\frac{\mathrm{d}\omega}{2\pi}\frac{\mathrm{d}^3\boldsymbol{k}}{(2\pi)^3}e^{i(\boldsymbol{r}\cdot\boldsymbol{k}-\omega\tau)}\psi_{\sigma}(\boldsymbol{k},\omega), \tag{4.2.11}$$

which then in turn makes the spinors transform like:

$$\Psi(\boldsymbol{k},\omega) = \begin{pmatrix} \psi_\uparrow(\boldsymbol{k},\omega) \\ \bar{\psi}_\downarrow(-\boldsymbol{k},-\omega) \end{pmatrix}. \tag{4.2.12}$$

In reciprocal space, the Green's function can be evaluated to be matrix elements,

$$\mathcal{G}^{-1} = \begin{pmatrix} i\omega - \frac{k^2}{2m} + \mu & \Delta \\ \bar{\Delta} & i\omega + \frac{k^2}{2m} - \mu \end{pmatrix}, \tag{4.2.13}$$

and then inverted:

$$\mathcal{G} = \frac{1}{\omega^2 + \xi_k^2 + |\Delta|^2} \begin{pmatrix} -i\omega - \xi_k & \Delta \\ \bar{\Delta} & -i\omega + \xi_k \end{pmatrix}. \tag{4.2.14}$$

Here we have defined the energy relative to the Fermi surface, $\xi_k \equiv k^2/2m - \mu$. For us to calculate the correlator in eq. 4.2.9 it will also need to be Fourier transformed,

$$\langle \psi_\uparrow(\boldsymbol{r},\tau)\psi_\downarrow(\boldsymbol{r},\tau')\rangle_{\mathrm{BCS}} = \int \frac{\mathrm{d}\omega}{2\pi}\frac{\mathrm{d}\omega'}{2\pi}\frac{\mathrm{d}^3\boldsymbol{k}}{(2\pi)^3}\frac{\mathrm{d}^3\boldsymbol{k'}}{(2\pi)^3} e^{i(\boldsymbol{r}.(\boldsymbol{k}+\boldsymbol{k'})-\omega\tau-\omega'\tau')} \langle \psi_\uparrow(\boldsymbol{k},\omega)\psi_\downarrow(\boldsymbol{k'},\omega')\rangle_{\mathrm{BCS}}. \tag{4.2.15}$$

We can now evaluate the correlator on the right hand side through partial derivatives of the partition function in momentum space,

$$\begin{aligned} \langle \psi_\uparrow(\boldsymbol{k},\omega)\psi_\downarrow(\boldsymbol{k'},\omega')\rangle_{\mathrm{BCS}} &= \lim_{h\to 0}\frac{1}{\mathcal{Z}}\frac{\partial}{\partial\bar{h}_\uparrow(\boldsymbol{k},\omega)}\frac{\partial}{\partial\bar{h}_\downarrow(\boldsymbol{k'},\omega')}\mathcal{Z} \\ &= \lim_{h\to 0}\frac{1}{\mathcal{Z}}\frac{\partial}{\partial\bar{h}_\uparrow(\boldsymbol{k},\omega)}\left(\frac{\Delta(-\boldsymbol{k'},-\omega')\bar{h}_\uparrow(-\boldsymbol{k'},-\omega') - (i\omega' - \xi_{-k})h_\downarrow(\boldsymbol{k'},\omega)}{\omega'^2 + \xi_{k'}^2 + |\Delta|^2}\mathcal{Z}\right), \\ &= \delta(\boldsymbol{k}+\boldsymbol{k'})\delta(\omega+\omega')\frac{\Delta}{\omega^2+\xi_k^2+|\Delta|^2}. \end{aligned} \tag{4.2.16}$$

With the delta functions we can integrate over a $\boldsymbol{k}$ and an ω, leaving us with:

$$\langle \psi_\uparrow(\boldsymbol{r},\tau)\psi_\downarrow(\boldsymbol{r},\tau')\rangle_{\mathrm{BCS}} = \int \frac{\mathrm{d}\omega}{2\pi}\frac{\mathrm{d}^3\boldsymbol{k}}{(2\pi)^3} e^{i\omega(\tau-\tau')}\frac{\Delta}{\omega^2+\xi_k^2+|\Delta|^2}. \tag{4.2.17}$$

This integral over $\boldsymbol{k}$ is a standard procedure, see Landau & Lifshitz [30]. We limit ourselves only to a narrow band around the Fermi surface, which gives the result:

$$\begin{aligned}\langle\psi_\uparrow(\boldsymbol{r},\tau)\psi_\downarrow(\boldsymbol{r},\tau')\rangle_{\mathrm{BCS}} &= \pi N(0)|\Delta|e^{i\Phi}\int_0^\infty \mathrm{d}\omega \frac{e^{i\omega(\tau-\tau')}}{\sqrt{\omega^2+|\Delta|^2}},\\ &= \pi N(0)|\Delta|e^{i\Phi}\mathrm{K}_0(|\Delta|(\tau-\tau')),\end{aligned} \tag{4.2.18}$$

where $N(0)$ the density of states at the Fermi level and the modified Bessel's function of the second kind[1] is defined as

$$\mathrm{K}_0(z) = \int_0^\infty \mathrm{d}t \frac{e^{itz}}{\sqrt{1+t^2}}.$$

For large argument, this function decays exponentially [32] thus suppressing the correlation function for times $\tau - \tau' \gg 1/|\Delta|$.

4.3 Luttinger Liquid Correlation Functions

The Luttinger liquid is another important physical model in this thesis, and the correlation functions of the fields are another example of using the tools of functional integration. We shall follow closely to Appendix C of Giamarchi [16] and calculate correlation functions of the phase field,

$$\left\langle[\varphi(r)-\varphi(0)]^2\right\rangle.$$

This is more readily calculated in Fourier space as,

$$\left\langle[\varphi(r_1)-\varphi(r_2)]^2\right\rangle = \frac{1}{(\beta\Omega)^2}\sum_{\boldsymbol{q}_1,\boldsymbol{q}_2}\langle\varphi(\boldsymbol{q}_1)\varphi(\boldsymbol{q}_2)\rangle\left(e^{i\boldsymbol{q}_1 r_1}-e^{i\boldsymbol{q}_1 r_2}\right)\left(e^{i\boldsymbol{q}_2 r_1}-e^{i\boldsymbol{q}_2 r_2}\right), \tag{4.3.1}$$

where $r=(x,c\tau)$, $\boldsymbol{q}=(k,\omega_n/c)$ and $e^{i\boldsymbol{q}r}=e^{i(kx-\omega_n\tau)}$. Expressed as a functional integral, the average we need to calculate is now:

$$\langle\varphi(\boldsymbol{q}_1)\varphi(\boldsymbol{q}_2)\rangle = \frac{1}{\mathcal{Z}}\int \mathrm{D}\varphi(x,\tau)\mathrm{D}\theta(x,\tau)\varphi(\boldsymbol{q}_1)\varphi(\boldsymbol{q}_2)e^{-S_{\mathrm{LL}}/\hbar} \tag{4.3.2}$$

[1] Also known as the Macdonald Function [31]

To calculate this we start by using the Hamiltonian Eq. 2.2.11 to create the imaginary time action ($\hbar = 1$),

$$-S_{\mathrm{LL}} = \int_0^\beta \mathrm{d}\tau \int \mathrm{d}x \left[i\frac{1}{\pi}(\partial_x\varphi)(\partial_\tau\theta) - \frac{1}{2\pi}\left(cK\left(\partial_x\varphi\right)^2 + \frac{c}{K}\left(\partial_x\theta\right)^2 \right) \right]. \tag{4.3.3}$$

This can be written in Fourier space as,

$$e^{-S_{\mathrm{LL}}} = e^{\frac{1}{\beta\Omega}\sum_{\boldsymbol{q}}\left[-\frac{ik\omega_n}{\pi}\theta(\boldsymbol{q})\varphi(-\boldsymbol{q}) - \frac{cK}{2\pi}k^2\varphi(\boldsymbol{q})\varphi(-\boldsymbol{q}) - \frac{c}{2\pi K}k^2\theta(\boldsymbol{q})\theta(-\boldsymbol{q})\right]}. \tag{4.3.4}$$

To make it more applicable to calculate correlation functions we shall write this in matrix form,

$$S_{\mathrm{LL}} = \frac{1}{2}\frac{1}{\beta\Omega}\sum_{\boldsymbol{q}}\left(\varphi^*_{\boldsymbol{q}}, \theta^*_{\boldsymbol{q}}\right) M^{-1} \begin{pmatrix} \varphi_{\boldsymbol{q}} \\ \theta_{\boldsymbol{q}} \end{pmatrix} = \frac{1}{2}\frac{1}{\beta\Omega}\sum_{\boldsymbol{q}}\left(\varphi^*_{\boldsymbol{q}}, \theta^*_{\boldsymbol{q}}\right) \begin{pmatrix} \frac{cK}{\pi}k^2 & \frac{ik\omega_n}{\pi} \\ \frac{ik\omega_n}{\pi} & \frac{c}{K\pi}k^2 \end{pmatrix} \begin{pmatrix} \varphi_{\boldsymbol{q}} \\ \theta_{\boldsymbol{q}} \end{pmatrix} \tag{4.3.5}$$

In this instance, the average we are computing has no dependence on the field θ, we can perform the integration over θ in (4.3.2). This is happily done as the action has no non-quadratic terms in θ. To do so, we complete the square in θ with the new variable $\widetilde{\theta}(\boldsymbol{q}) = \theta(\boldsymbol{q}) + \frac{i\omega_n K}{ck}\varphi(\boldsymbol{q})$ and then perform the Gaussian integration. This then cancels with the contribution coming from the partition function, leaving the correlator expressed as a functional integral over φ only:

$$\langle\varphi(\boldsymbol{q}_1)\varphi(\boldsymbol{q}_2)\rangle = \frac{1}{\mathcal{Z}_\varphi}\int \mathrm{D}\varphi(x,\tau)\varphi(\boldsymbol{q}_1)\varphi(\boldsymbol{q}_2)e^{-S_\varphi}. \tag{4.3.6}$$

Here we have defined the action,

$$\begin{aligned} S_\varphi &= \frac{1}{\beta\Omega}\sum_{\boldsymbol{q}}\frac{K}{2\pi c}\left[\omega_n^2 + c^2k^2\right]\varphi^*(\boldsymbol{q})\varphi(\boldsymbol{q}) \\ &= \frac{K}{2\pi c}\int \mathrm{d}x \int_0^\beta \mathrm{d}\tau\left[(\partial_\tau\varphi(r))^2 + c^2(\partial_x\varphi(r))^2\right]. \end{aligned} \tag{4.3.7}$$

Similarly we could have made an action in terms of θ only, which would be identical up to the transformation $K \to 1/K$,

$$S_\theta = \frac{1}{2\pi K c}\int \mathrm{d}x \int_0^\beta \mathrm{d}\tau \left[(\partial_\tau \theta(r))^2 + c^2(\partial_x \theta(r))^2\right]. \tag{4.3.8}$$

We can use the result from (4.1.14) to evaluate the correlation function,

$$\langle \varphi(\boldsymbol{q}_1)\varphi(\boldsymbol{q}_2)\rangle = \frac{\pi c}{K}\frac{\beta\Omega}{\omega_n^2 + c^2k^2}\delta_{\boldsymbol{q}_1,-\boldsymbol{q}_2}. \tag{4.3.9}$$

Alternatively this could also be seen from the action (4.3.5), for the term that couples φ^* and φ. With this substitution, the correlator (4.3.1) becomes,

$$\left\langle [\varphi(r) - \varphi(0)]^2 \right\rangle = \frac{1}{\beta}\sum_{\omega_n}\int \frac{\mathrm{d}k}{2\pi}\frac{2\pi c}{K}\frac{1}{\omega_n^2 + c^2k^2}\left[1 - \cos(kx + \omega_n\tau)\right]. \tag{4.3.10}$$

The evaluation of this summation over ω_n and integral over k can be carefully performed (see Mahan [33] for full details). In doing so we introduce a factor of $e^{-\xi|k|}$ in the integrand to ensure convergence, and mimic the finite bandwidth of a real system by limiting modes of $k > 1/\xi$ where ξ is the shortest length scale the Luttinger liquid can change at[1],

$$F_1(x,\tau) = \left\langle [\varphi(r) - \varphi(0)]^2 \right\rangle = \frac{1}{2K}\ln\left[\frac{\beta^2c^2}{\xi^2\pi^2}\left(\sin^2\left(\frac{\pi\tau}{\beta}\right) + \sinh^2\left(\frac{\pi x}{c\beta}\right)\right)\right]. \tag{4.3.11}$$

For correlations of the form, $\left\langle e^{i(\varphi(r)-\varphi(0))}\right\rangle$, they can be calculated by the identity:

$$\left\langle e^{i(\varphi(r)-\varphi(0))}\right\rangle = e^{-\frac{1}{2}\left\langle [\varphi(r)-\varphi(0)]^2\right\rangle} \tag{4.3.12}$$

$$= \left[\frac{\beta^2c^2}{\xi^2\pi^2}\left(\sin^2\left(\frac{\pi\tau}{\beta}\right) + \sinh^2\left(\frac{\pi x}{c\beta}\right)\right)\right]^{-\frac{1}{4K}} \tag{4.3.13}$$

It can be seen here that the decay of this correlation function is not exponential, but a power law that depends on the Luttinger parameter. These algebraic decays are a signature of strictly 1D behaviour and

[1] This is the healing length of the Gross-Pitaevskii equation (1.1.8) for a bosonic Luttinger liquid, or the coherence length from the Ginzburg-Landau equation (1.2.2) for a superconducting system.

will re-appear in many other calculations performed in this thesis.

Chapter 5

Renormalisation Group

This chapter will serve as an introduction to the Renormalisation Group (RG) as a theoretical technique, mainly following the Wilson's shell approach [34]. We shall also investigate two instances of using the RG on Luttinger liquid systems, those being a single impurity (Kane-Fisher) and a global Sine-Gordon type impurity.

5.1 How to perform RG

The Renormalization Group is a technique that assesses how certain parameters or couplings change as the lengths in the system are scaled, for example it can be used to find critical points in systems where phase transitions occur. It can be thought of as "integrating" out details of what happens at small length scales, or equivalently averaging the high momentum modes. If the procedure succeeds then we shall be left with a description of the low energy behaviour of the system, where the couplings have been scaled by some factor. A full description of RG can be found in [35]. A momentum space RG process follows three steps, coarse-graining, averaging and finally re-scaling. To start with we consider a system at low energies, with only frequencies below a certain ultraviolet cutoff Λ. The system is described by an action $S[\phi]$, where ϕ is the relevant field. This system has a partition function of:

$$Z = \int \prod_{|\omega|<\Lambda} \mathrm{d}\phi(\omega)\, e^{S(\phi(\omega))}, \tag{5.1.1}$$

The first step to a RG procedure is coarse graining, where an artificial separation between "fast" and "slow" modes is made. The fast modes are live in a shell around the cutoff frequency, defined by the scaling parameter $b \geq 1$:

$$\begin{aligned} \phi_< &= \phi(\omega), \qquad 0 < |\omega| < \frac{\Lambda}{b}, \\ \phi_> &= \phi(\omega), \qquad \frac{\Lambda}{b} < |\omega| < \Lambda. \end{aligned}$$

The next step is decimation, where we integrate over all the fast modes to attain an effective action. We hope that this action has the same form of the original action up to scalings because then that means the RG procedure can be iterated, i.e. the mapping is closed. To perform the integration we split the action into pieces containing only slow/fast modes and a term involving terms that mix the two:

$$S(\phi_<, \phi_>) = S_0(\phi_<) + S_0(\phi_>) + S_I(\phi_<, \phi_>). \tag{5.1.2}$$

This separation is done to make S_0 a quadratic function of it's argument. Substituting this into the partition function allows us to define what this effective action is:

$$\begin{aligned} Z &= \int \prod_{0<|k|<\frac{\Lambda}{b}} \mathrm{d}\phi(k) \int \prod_{\frac{\Lambda}{b}<|k|<\Lambda} \mathrm{d}\phi(k)\, e^{S_0(\phi_<)}\, e^{S_0(\phi_>)}\, e^{S_I(\phi_<,\phi_>)}, \\ &= \int [\mathrm{d}\phi_<]\, [\mathrm{d}\phi_>]\, e^{S_0(\phi_<)}\, e^{S_0(\phi_>)}\, e^{S_I(\phi_<,\phi_>)}, \\ &= \int [\mathrm{d}\phi_<]\, e^{S_0(\phi_<)} \int [\mathrm{d}\phi_>]\, e^{S_0(\phi_>)+S_I(\phi_<,\phi_>)}, \\ &= \int [\mathrm{d}\phi_<]\, e^{S'(\phi_<)}, \end{aligned} \tag{5.1.3}$$

where the effective, coarse grained, action is defined as:

$$\begin{aligned} e^{S'(\phi_<)} &= e^{S_0(\phi_<)} \int [\mathrm{d}\phi_>]\, e^{S_0(\phi_>)}\, e^{S_I(\phi_<,\phi_>)} \\ &= e^{S_0(\phi_<)}\, \frac{\int [\mathrm{d}\phi_>]\, e^{S_0(\phi_>)}\, e^{S_I(\phi_<,\phi_>)}}{\int [\mathrm{d}\phi_>]\, e^{S_0(\phi_>)}} \times \int [\mathrm{d}\phi_>]\, e^{S_0(\phi_>)} \\ &= e^{S_0(\phi_<)} \left\langle e^{S_I(\phi_<,\phi_>)} \right\rangle_{0>} Z_{0>}. \end{aligned} \tag{5.1.4}$$

The partition function $Z_{0>}$ is irrelevant as it is constant with respect to the slow variables and will be cancelled in the calculation of any correlation function.

The next stage is to rescale the momenta in the effective action, $k' = bk$, so that the cutoff momenta has the same numerical value in the effective action. Then the fields are rescaled, $\phi'(\omega') = \zeta^{-1}\phi_<\left(\frac{\omega'}{s}\right)$, and ζ is picked so that the quadratic part of the action has a fixed coefficient. With this definition of the RG transformation we obtain a mapping of Hamiltonians/Actions onto eachother. We can then examine how couplings within the action transform under successive RG steps, to see if their effects are amplified or suppressed by the coarse graining and averaging. We now turn to apply this technique to an impurity in a Luttinger Liquid.

5.2 Single Impurity in a Luttinger Liquid

We shall investigate the effect that a weak scattering impurity has on the Luttinger liquid. This was first done by Kane & Fisher [36] and is often known as a Kane-Fisher impurity. To model an impurity we add a perturbative term to the bare Luttinger action:

$$S_{\text{imp}} = \int \mathrm{d}\tau \mathrm{d}x\, V(x)\rho(x), \tag{5.2.1}$$

where $V(x)$ is the impurity potential and $\rho(x)$ is the density of the Luttinger Liquid. The density can also be expressed as a function of the density field (2.2.3):

$$\begin{aligned}\rho(x) &= \frac{1}{\pi}\partial_x\Theta(x)\sum_{n=-\infty}^{\infty}\delta\left(\Theta(x) - n\pi\right), \\ &= \left(\rho_0 - \partial_x\theta(x)\right)\sum_{n=-\infty}^{\infty} e^{2ni\theta(x)},\end{aligned} \tag{5.2.2}$$

which to leading order is:

$$\rho(x) = \left(\rho_0 - \partial_x\theta(x)\right)\left(1 + 2\cos(2\theta(x))\right) \tag{5.2.3}$$

For a point-like impurity at the origin, the potential is $V(x) = V_0\delta\left(x\right)$, where V_0 is the strength of

the impurity. We assume that that V_0 is small compared to other energies in the system, Fermi energy or bosonic equivalent, so that the bosonisation representation is still valid. This gives the impurity action, to leading order;

$$S_{\text{imp}} = V_0 \int \mathrm{d}\tau \left[\rho_0 - \frac{1}{\pi}\partial_x \theta(0) + 2\rho_0 \cos(2\theta(0)) \right]. \tag{5.2.4}$$

The first two terms are the forward scattering and can be removed using a gauge transformation, which when substituting into the total action (in terms of θ only) gives:

$$S = \frac{1}{2\pi K c} \int_0^\beta \mathrm{d}\tau \int \mathrm{d}x \left[(\partial_\tau \theta)^2 + c^2 (\partial_x \theta)^2 \right] + \tilde{V}_0 \int_0^\beta \mathrm{d}\tau \cos(2\theta(0)). \tag{5.2.5}$$

This action is Gaussian at all points apart from $x = 0$, where the impurity is. We can integrate over the field $\theta(x)$ at all points except the origin where $\theta(0) = \theta_0$. To impose this condition we introduce a Lagrange multiplier, $\lambda(\tau)$,

$$e^{-S_{\text{eff}}} = \int \mathrm{D}\theta \mathrm{D}\lambda \, e^{-S_{LL} + i \int \mathrm{d}\tau \lambda(\tau)[\theta_0 - \theta(x=0,\tau)]}. \tag{5.2.6}$$

We now substitute the Luttinger action into this expression and integrate over the bulk field θ. The integral over momentum q can now be performed, and finally the functional integral over the Lagrange multiplier λ,

$$\begin{aligned}
e^{-S_{\text{eff}}} &= \int \mathrm{D}\theta \mathrm{D}\lambda \, e^{\frac{1}{2\pi c K} \int \frac{\mathrm{d}\omega \mathrm{d}q}{4\pi^2} \left[(c^2 q^2 + \omega^2) |\theta(q,\omega)|^2 + i\lambda(-\omega)\theta(q,\omega) \right]} e^{i \int \frac{\mathrm{d}\omega}{2\pi} \lambda(-\omega)\theta_0(\omega)} \\
&= \int \mathrm{D}\lambda \, \exp\left\{ -\frac{1}{2} \int \frac{\mathrm{d}\omega \mathrm{d}q}{4\pi^2} \frac{\pi K c}{c^2 q^2 + \omega^2} |\lambda(\omega)|^2 + i \int \frac{\mathrm{d}\omega}{2\pi} \lambda(-\omega)\theta_0(\omega) \right\} \\
&= \int \mathrm{D}\lambda \exp\left\{ -\frac{1}{2} \int \frac{\mathrm{d}\omega}{2\pi} \left[\frac{K\pi}{2|\omega|} |\lambda(\omega)|^2 + i\lambda(-\omega)\theta_0(\omega) \right] \right\} \\
&= e^{-\frac{1}{2} \int \frac{\mathrm{d}\omega}{2\pi} \frac{2|\omega|}{K\pi} |\theta_0(\omega)|^2}.
\end{aligned} \tag{5.2.7}$$

This gives us an effective action in terms of fluctuations of the value of θ at the origin. Rescaling the

field, $2\theta_0 \to \theta_0$ then gives:

$$S_{\text{eff}} = \frac{1}{8\pi^2}\int_{|\omega|<\Lambda} \mathrm{d}\omega \frac{|\omega|}{K}|\theta(\omega)|^2 + \tilde{V_0}\int \mathrm{d}\tau\, \cos(\theta(\tau)). \tag{5.2.8}$$

With this action we can apply the RG procedure as outlined in section 5.1. We introduce the scaling parameter, $b \sim 1$, to separate the slow and fast modes by $\omega = \frac{\Lambda}{b}$. The first term in the action involved no mixing of the slow and fast terms so can be easily split into slow and fast actions, and then the cosine term can be investigated separately as it mixes terms. The integration over fast modes to generate the coarse grained action gives:

$$\begin{aligned} e^{-S_{\text{cg}}} &= \int \mathrm{D}\theta_> e^{-S_<(\theta_<)-S_>(\theta_>)-\tilde{V_0}\int \mathrm{d}\tau \cos(\theta_<(\tau)+\theta_>(\tau))} \\ &= e^{-S_<(\theta_<)}\int \mathrm{D}\theta_> e^{-S_>(\theta_>)}\left(1-\tilde{V_0}\int \mathrm{d}\tau \cos(\theta_<(\tau)+\theta_>(\tau))\right) \\ &= e^{-S_<(\theta_<)}\left\langle 1-\tilde{V_0}\int \mathrm{d}\tau \cos(\theta_<(\tau)+\theta_>(\tau))\right\rangle_> \\ &= e^{-S_<(\theta_<)-\tilde{V_0}\int \mathrm{d}\tau \langle\cos(\theta_<(\tau)+\theta_>(\tau))\rangle_>}. \end{aligned} \tag{5.2.9}$$

The average, $\langle\cos(\theta_<(\tau)+\theta_>(\tau))\rangle_>$, can be calculated by first expanding the cosine and employing the identity $\left\langle e^{iA}\right\rangle = e^{-\frac{1}{2}\left\langle A^2\right\rangle}$:

$$\langle\cos(\theta_<(\tau)+\theta_>(\tau))\rangle_> = \cos(\theta_<(\tau))\, e^{-\frac{1}{2}\left\langle\theta_>(\tau)^2\right\rangle}, \tag{5.2.10}$$

and then using the correlation Eq. 4.1.14, previously calculated to get:

$$\begin{aligned} \left\langle\theta_>(\tau)^2\right\rangle_> &= \left\langle\int \frac{\mathrm{d}\omega_1}{2\pi}\frac{\mathrm{d}\omega_2}{2\pi} e^{i\tau(\omega_1+\omega_2)}\theta_>(\omega_1)\theta_>(\omega_2)\right\rangle_> \\ &= \int_{\frac{\Lambda}{b}<|\omega|<\Lambda} \mathrm{d}\omega \frac{K}{|\omega|} \\ &= 2K\ln b. \end{aligned} \tag{5.2.11}$$

Putting this back into the coarse grained action eq. 5.2.9 gives:

$$S' = \frac{1}{8\pi^2}\int_{|\omega|<\frac{\Lambda}{b}} \mathrm{d}\omega \frac{|\omega|}{K}|\theta(\omega)|^2 + b^{-K}\tilde{V_0}\int \mathrm{d}\tau \cos(\theta(\tau)). \tag{5.2.12}$$

The final stage of performing the RG is to rescale the fields. To do so, we start by rescaling ω so that the UV cutoff remains the same numerical value. This rescaling is: $\omega' = b\omega$, so that $\tau' = \tau/b$. We also want the term inside the cosine to remain invariant under scaling $[\theta'(\tau') = \theta(\tau)]$. From the definition of the Fourier transform, $\theta(\tau) = \int \frac{\mathrm{d}\omega}{2\pi} e^{i\omega\tau}\theta(\omega)$, this means that the field $\theta(\omega)$ scales as: $\theta'(\omega') = \theta(\omega)/b$. With these rescalings, the action now looks like:

$$S' = \frac{1}{8\pi^2}\int_{|\omega|<\Lambda} \mathrm{d}\omega \frac{|\omega|}{K}|\theta(\omega)|^2 + b^{1-K}\tilde{V}_0 \int \mathrm{d}\tau \cos(\theta(\tau)). \tag{5.2.13}$$

The quadratic part of the action remains unchanged, and we can see that the coupling $\tilde{V}_0$ scales as:

$$\tilde{V_0}' = b^{1-K}\tilde{V}_0. \tag{5.2.14}$$

This results in an RG equation of:

$$\frac{\mathrm{d}\ln\tilde{V}_0}{\mathrm{d}\ln b} = 1 - K. \tag{5.2.15}$$

This tells us that for Luttinger parameters $K < 1$ the impurity strength will flow to larger values, meaning for any arbitrarily weak impurity in a fermionic Luttinger liquid it will have the effect of being an impassable barrier. The opposite is true for bosonic Luttinger liquids where $K > 1$. For an arbitrarily strong impurity, it's strength will be renormalised to zero, meaning the impurity can be ignored. It can also be seen if the weak barrier is replaced by a weak link, with a tunneling strength that gets renormalised instead of V_0. The same procedure is done except with the phase field ϕ instead of θ.

5.3 Sine-Gordon Impurity in a Luttinger Liquid

We have seen how a local impurity inside a Luttinger liquid behaves and how the physics is dominated by the value of the Luttinger parameter. In this section we shall investigate a global Sine-Gordon type impurity, one which is parasitic in spinful Luttinger liquids with $g_{1\perp}$ type scattering (see section 2.3 for details). The behaviour of this type of impurity is integral to the main result of this thesis, in chapter 7. This procedure will follow section 2.3.2 and Appendix E in Giamarchi [16], where we renormalise the

impurity through the functional integral we have seen before.

We start with the Hamiltonian, coming from Eq. 2.3.22. We use this Hamiltonian to make an action in the standard way, by integrating out the $\varphi_{\rho,\sigma}$ field

$$\begin{aligned} S_\sigma = \frac{1}{\pi v_\sigma K_\sigma} \int \mathrm{d}x\mathrm{d}\tau \left[(\partial_\tau \theta_\sigma)^2 + v_\sigma^2 (\partial_x \theta_\sigma)^2\right] \\ + 2g_{1\perp} \int \mathrm{d}x\mathrm{d}\tau \cos(4\theta_\sigma(x,\tau)). \end{aligned} \tag{5.3.1}$$

From here on we shall omit the subscript of σ on the fields and $\perp$ on the coupling as all the correlations we shall be seeking will only involve those in the spin sector, and there are no other couplings in the system. As we want to separate out fast and slow modes, we write the field θ in Fourier space:

$$\theta(x,\tau) = \frac{1}{\beta\Omega} \sum_{k,\omega_n} e^{i(kx-\omega_n\tau)} \theta(k,\omega_n). \tag{5.3.2}$$

This field can then be decomposed into the fast and slow with respect to the high frequency cut-off Λ (with $r = (x, v\tau)$, $\boldsymbol{q} = (k, \omega_n/v)$),

$$\begin{aligned} \theta^<(r) &= \frac{1}{\beta\Omega} \sum_{\|\boldsymbol{q}\|<\Lambda'} e^{i\boldsymbol{q}r} \theta(\boldsymbol{q}) \\ \theta^>(r) &= \frac{1}{\beta\Omega} \sum_{\Lambda'<\|\boldsymbol{q}\|<\Lambda} e^{i\boldsymbol{q}r} \theta(\boldsymbol{q}) \end{aligned} \tag{5.3.3}$$

with the notation of, $\boldsymbol{q}r = kx - \omega_n\tau$. The quadratic part of action Eq. (5.3.1) becomes:

$$S_0 = \frac{1}{\pi K} \frac{1}{\beta\Omega} \sum_{\boldsymbol{q}} \left[\omega_n^2/v + vk^2\right] \theta^*(\boldsymbol{q})\theta(\boldsymbol{q}). \tag{5.3.4}$$

This action does not mix fast and slow terms, so therefore can be written as: $S_0 = S_0^< + S_0^>$. The way to tackle the non-quadratic component of the action is through a perturbative expansion. The partition

function $\mathcal{Z} = \int \mathrm{D}\theta e^{-S}$ is expanded in a power series in g (where $\mathcal{Z}_0$ is the partition function for $g = 0$):

$$\frac{\mathcal{Z}}{\mathcal{Z}_0} = \frac{1}{\mathcal{Z}_0}\int \mathrm{D}\theta e^{-S_0^< - S_0^>}\left[1 - 2g\int \frac{\mathrm{d}^2 r}{v}\cos\big(4(\theta^<(r) + \theta^>(r))\big) + 2g^2\int\frac{\mathrm{d}^2 r_1}{v}\int\frac{\mathrm{d}^2 r_2}{v}\cos\big(4(\theta^<(r_1)+\theta^>(r_1))\big)\cos\big(4(\theta^<(r_2)+\theta^>(r_2))\big)\right]. \tag{5.3.5}$$

The fast fields can be isolated and then averaged over, giving:

$$\frac{\mathcal{Z}}{\mathcal{Z}_0} = \frac{1}{\mathcal{Z}_0^<}\int \mathrm{D}\theta e^{-S_0^<}\left[1 - 2g\int\frac{\mathrm{d}^2 r}{v}\cos\big(4\theta^<(r)\big)e^{-8\langle\theta^>(r)^2\rangle_>} + g^2\sum_{\epsilon=\pm1}\int\frac{\mathrm{d}^2 r_1}{v}\int\frac{\mathrm{d}^2 r_2}{v}\cos\big(4(\theta^<(r_1)+\epsilon\theta^<(r_2))\big)e^{-8\langle(\theta^>(r)+\epsilon\theta^>(r_2))^2\rangle_>}\right]. \tag{5.3.6}$$

This is then re-exponentiated to create an effective action, which gives:

$$\frac{\mathcal{Z}}{\mathcal{Z}_0} = \frac{1}{\mathcal{Z}_0^<}\int \mathrm{D}\theta \exp\left[-S_0^< - 2g\int\frac{\mathrm{d}^2 r}{v}\cos\big(4\theta^<(r)\big)e^{-8\langle\theta^>(r)^2\rangle_>}\right] \exp\left[g^2\int\frac{\mathrm{d}^2 r_1}{v}\int\frac{\mathrm{d}^2 r_2}{v}\left(\sum_{\epsilon=\pm}\cos\big(4(\theta^<(r_1)+\epsilon\theta^<(r_2))\big)e^{-8\langle(\theta^>(r_1)+\epsilon\theta^>(r_2))^2\rangle_>}\right)\right] \exp\left[-2g^2\int\frac{\mathrm{d}^2 r_1}{v}\int\frac{\mathrm{d}^2 r_2}{v}\cos\big(4\theta^<(r_1)\big)e^{-8\langle\theta^>(r_1)^2\rangle}\cos\big(4\theta^<(r_2)\big)e^{-8\langle\theta^>(r_2)^2\rangle}\right] \tag{5.3.7}$$

The first term in this action corresponds to the original SG impurity, but only over slow fields. The terms of order g^2 can be shown to be less relevant in the RG, as they will renormalise based on faster oscillating terms. For further details on what happens to these terms, refer to Giamarchi Appendix E [16] or Nozieres & Gallet [37]. Renormalising the order g cosine is sufficient to show which values of K makes this perturbation relevant. Since the fast modes have been integrated out, the fields shall be re-scaled to bring the cut-offs back to their original numerical value:

$$\mathrm{d}k = \frac{\Lambda'}{\Lambda}\mathrm{d}k'. \tag{5.3.8}$$

The same is done for ω_n and the accordingly for the real space variables:

$$\mathrm{d}x = \frac{\Lambda}{\Lambda'}\mathrm{d}x', \qquad \mathrm{d}\tau = \frac{\Lambda}{\Lambda'}\mathrm{d}\tau'. \tag{5.3.9}$$

With these re-scalings it can be seen from the first line in Eq. (5.3.7) that the coupling, g, will scale as:

$$g(\Lambda') = \left(\frac{\Lambda}{\Lambda'}\right)^2 g(\Lambda) e^{-8\left\langle \theta^{>}(r)^2 \right\rangle_{>}} = \left(\frac{\Lambda}{\Lambda'}\right)^2 g(\Lambda) e^{-\frac{4}{\beta\Omega}\sum_{\Lambda'<\|\boldsymbol{q}\|<\Lambda}\frac{\pi K v}{\omega_n^2+v^2k^2}}. \tag{5.3.10}$$

In the zero temperature and infinite length limit, $\beta, L \to \infty$, the sum inside the exponent can be converted to an integral:

$$g(\Lambda') = \left(\frac{\Lambda}{\Lambda'}\right)^2 g(\Lambda) e^{-2\int_{\Lambda'<\|\boldsymbol{q}\|<\Lambda} \mathrm{d}q \frac{K}{q}} \tag{5.3.11}$$

$$= \left(\frac{\Lambda}{\Lambda'}\right)^2 g(\Lambda) e^{-2K\ln\left(\Lambda/\Lambda'\right)}. \tag{5.3.12}$$

By parameterising the scaling by a scale factor $b > 1$, with $b\Lambda' = \Lambda$, the RG equation for g will then read:

$$\frac{\mathrm{d}\ln g}{\mathrm{d}\ln b} = 2 - 2K. \tag{5.3.13}$$

This has the critical point of $K^* = 1$, which corresponds to the the non-interacting spin sector back in the original model Eq. (2.3.22). For $K_\sigma > 1$ then the Sine-Gordon impurity term is RG irrelevant, and can be ignored in the low energy description of the system.

In the opposite limit, $K_\sigma < 1$, the sine-Gordon impurity is relevant and g flows to larger values under each RG step. This means that the spin sector is "massive", and the presence of the $g_{1\perp}$ term will cause the spectrum to be gapped. The $g_{1\perp}$ term will cause the field $\theta_\sigma(x,\tau)$ to be pinned at the value that minimises the cosine, $g_{1\perp}\cos(4\theta_\sigma)$. This can lead to two different situations depending on the sign of $g_{1\perp}$. For either case, the field θ_σ takes a definite, static, value which means that the dual field ϕ_σ disorders due to the uncertainty principle. This means that the spin sector, S_σ, will have no dynamics as the behaviour is entirely dominated by the sine-Gordon term.

In chapter 7 this result will be used as part of a 1D system of interacting fermions, to suppress dynamics of spin excitations.

Part III

Results

Chapter 6

The Bosonic System

In the following chapter I shall introduce the model for the key system of this thesis, a 1D wire/channel connected to two 3D reservoirs. The first case of interest is what happens when the constituent particles are bosonic, with the reservoirs containing BECs. This is the concern of [8], and is the foundation for the main result of this thesis in chapter 7. We shall start with introducing the model, discuss why perturbation theory fails and then proceed to solve the system with a non-perturbative mean field solution.

6.1 The Model

The system that we are investigating consists of three parts, as illustrated in Fig. 6.1. Firstly are the reservoirs, which we are modelling as a harmonically trapped BEC. These are described by an order parameter (see Eq. 1.1.9), $\Psi_{\mathrm{L,R}} = \sqrt{N_{\mathrm{L,R}}/V}e^{i\Phi_{\mathrm{L,R}}}$, and action;

$$\mathcal{S}_{s=\mathrm{L,R}} = \int_0^\beta \mathrm{d}\tau \left[\frac{1}{2}\dot{N}_s - \dot{\Phi}_s N_s + V_{\mathrm{ext}} N_s + \frac{g}{2}N_s^2\right] \tag{6.1.1}$$

For the system in question we are preparing the reservoirs at an equal chemical potential, which sets $N_{\mathrm{L}} = N_{\mathrm{R}}$. Without loss of generality we can set the phases in the right/left reservoirs as $\pm\Phi$. The total phase difference across the junction is 2Φ which will be used to drive the current through the system, much like a Josephson junction. The second part of the system is the 1D channel, of length L which contains N bosons. We centre the channel symmetrically about $x = 0$, so that the channel

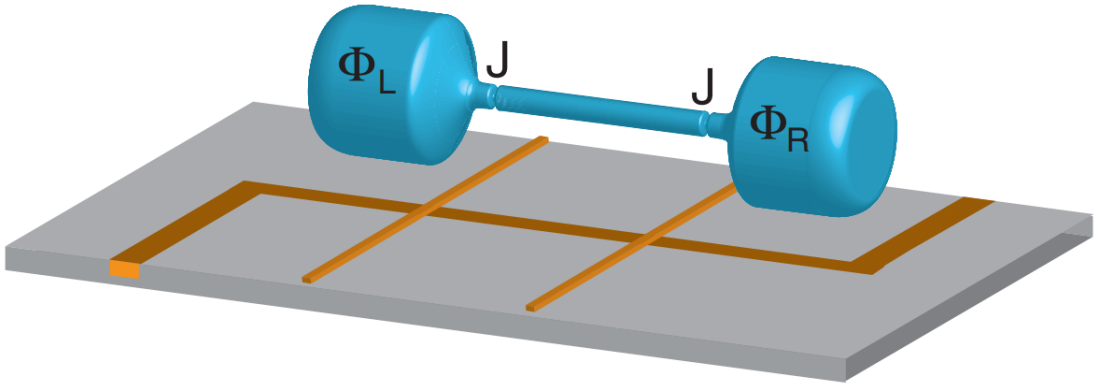

Figure 6.1: Schematic of the geometry of the bosonic system

meets the reservoirs at the points $x = \pm L/2$. The bosons in the channel form a quasi-condensate with order parameter $\psi_{\mathrm{LL}}(x,t) = \sqrt{\rho_0 - \frac{1}{\pi}\theta(x,t)}e^{i\varphi(x,,t)}$, where φ is the phase field and $\partial_x\theta$ is the density fluctuations about the mean density $\rho_0 = N/L$. We shall model the channel as a Luttinger liquid, with the imaginary time action ($\hbar = 1$):

$$S_{\mathrm{LL}} = \int_0^\beta \mathrm{d}\tau \int_{-L/2}^{L/2} \mathrm{d}x \left[-i\frac{1}{\pi}(\partial_x\varphi)(\partial_\tau\theta) + \frac{1}{2\pi}\left(cK\left(\partial_x\varphi\right)^2 + \frac{c}{K}\left(\partial_x\theta\right)^2 \right) \right]. \tag{6.1.2}$$

As the particles as bosons, $K >> 1$ and c is the Bogoliubov speed of sound described in section 1.1.2. The final piece of the system is a connection between the reservoirs and the channel. This comes in the form of a Josephson style tunnelling term, much like in section 1.2.3. The tunnelling Hamiltonian for such a process is:

$$H_{\mathrm{tun}} = -t\left[\Psi_{\mathrm{L}}^\dagger\, \psi(x = -L/2) + \Psi_{\mathrm{R}}^\dagger\, \psi(x = L/2) + \mathrm{h.c.} \right], \tag{6.1.3}$$

where t is the tunnelling amplitude. Much like in a Josephson junction, we can express the tunnelling in terms of the phase difference. In this case we have two phase differences, the difference between the phase in the left reservoir and the channel at $x = -L/2$ and similarly between the right reservoir and the

channel at $x = +L/2$. These phase differences are defined as:

$$\begin{aligned} \phi_{\mathrm{L}} &= \Phi - \varphi\left(-L/2\right) \\ \phi_{\mathrm{R}} &= \varphi\left(L/2\right) + \Phi. \end{aligned} \tag{6.1.4}$$

With these phase differences, the tunnelling action becomes:

$$S_{\mathrm{tun}} = -2J \int_0^\beta \mathrm{d}\tau \left[\cos\phi_{\mathrm{R}} + \cos\phi_{\mathrm{L}}\right]. \tag{6.1.5}$$

The tunnelling energy $J = t\sqrt{\rho_0 N/V}$ is a small parameter, since the tunnelling Hamiltonian Eq. 6.1.3 is valid only for small overlaps of wavefunctions. This gives the system a total action of:

$$\mathcal{S} = S_{\mathrm{res}} + S_{\mathrm{LL}} + S_{\mathrm{tun}}, \tag{6.1.6}$$

leading to a partition function of $\mathcal{Z} = \int \mathrm{D}\left[\Phi_{\mathrm{L}}, \Phi_{\mathrm{R}}\right] \mathrm{D}\left[\varphi, \theta\right] \exp(-\mathcal{S})$. Due to the absence of any non-quadratic terms in θ, we can integrate out θ in the Luttinger action Eq. 6.1.2, which leads to the action expressed in terms of φ alone:

$$S_{\mathrm{LL}} = \frac{K}{2\pi c} \int_0^\beta \mathrm{d}\tau \int_{-L/2}^{L/2} \mathrm{d}x \left[(\partial_\tau \varphi)^2 + c^2 (\partial_x \varphi)^2\right]. \tag{6.1.7}$$

This form is more convenient when investigating currents and their dependence on the applied phase difference driving them.

The geometry of this system is practically identical to similar systems considered in [6, 7], except for the particles that make up the system being fermions. The main difference that this brings is the value of the Luttinger parameter, K, in the channel. We shall see in the next subsection how this difference in K causes problems when attempting a perturbative solution to this bosonic system.

6.2 Perturbation Theory

The key property we are investigating in the system described above is the supercurrent, driven solely by the phase difference between the reservoirs. To calculate this current we first calculate the free energy, $F \propto \ln \mathcal{Z}$, and then take the derivative with respect to the phase difference[1], $I \propto \partial F/\partial \Delta\Phi$. The action is quadratic except for the tunnelling term S_{tun}, and so to evaluate the partition function we need to deal with it in some way. Since the tunnelling strength J is a small parameter, this incentivises us to try a perturbative expansion in S_{tun}:

$$\begin{aligned}\mathcal{Z} &= \int \mathrm{D}\left[\Phi_{\mathrm{L}}, \Phi_{\mathrm{R}}\right] \mathrm{D}\left[\varphi, \theta\right] e^{-S_{\text{res}} - S_{\text{LL}} - S_{\text{tun}}} \\ &= \int \mathrm{D}\left[\Phi_{\mathrm{L}}, \Phi_{\mathrm{R}}\right] e^{-S_{\text{res}}} \int \mathrm{D}\left[\varphi, \theta\right] e^{-S_{\text{LL}}} \left(1 - S_{\text{tun}} + \frac{1}{2} S_{\text{tun}}^2 + \dots\right) \\ &= \int \mathrm{D}\left[\Phi_{\mathrm{L}}, \Phi_{\mathrm{R}}\right] e^{-S_{\text{res}}} \left\langle 1 - S_{\text{tun}} + \frac{1}{2} S_{\text{tun}}^2 + \dots \right\rangle_{S_{\text{LL}}}.\end{aligned} \tag{6.2.1}$$

The lowest order term that would generate a dependence on the phase difference is at second order in S_{tun}, as we can have terms that couple the phases of the left and right reservoirs. These terms will correspond to a boson tunnelling from a reservoir and then tunnelling out of the channel into the opposite reservoir. This means that we can replace the tunnelling action with an effective action that contains only the relevant processes,

$$\begin{aligned}S_{\text{tun}}^{\text{eff}} &= -2J^2 \int \mathrm{d}\tau_1 \mathrm{d}\tau_2 \cos\left(\Phi_{\mathrm{L}}(\tau_1) - \varphi(-L/2, \tau_1)\right) \cos\left(\Phi_{\mathrm{R}}(\tau_2) - \varphi(L/2, \tau_2)\right) \qquad (6.2.2) \\ &= -J^2 \int \mathrm{d}\tau_1 \mathrm{d}\tau_2 \Big[\cos\left(\Phi_{\mathrm{L}}(\tau_1) + \Phi_{\mathrm{R}}(\tau_2) - \varphi(-L/2, \tau_1) - \varphi(L/2, \tau_2)\right) \\ &\qquad + \cos\left(\Phi_{\mathrm{L}}(\tau_1) - \Phi_{\mathrm{R}}(\tau_2) - \varphi(-L/2, \tau_1) + \varphi(L/2, \tau_2)\right)\Big]. \qquad (6.2.3)\end{aligned}$$

The average over the Luttinger action can be done using the results from chapter 4, namely eq. (4.3.11),

$$\left\langle S_{\text{tun}}^{\text{eff}} \right\rangle_{\text{LL}} = -2J^2 \int \mathrm{d}\tau_1 \mathrm{d}\tau_2 \cos\left(\Phi_{\mathrm{L}}(\tau_1) - \Phi_{\mathrm{R}}(\tau_2)\right) e^{-\frac{1}{4K} \ln\left[\frac{\beta^2 c^2}{\xi^2 \pi^2}\left(\sin^2\left(\frac{\pi(\tau_1 - \tau_2)}{\beta}\right) + \sinh^2\left(\frac{\pi L}{c\beta}\right)\right)\right]}. \tag{6.2.4}$$

[1] From a Hamiltonian mechanics perspective, number N and phase Φ are canonical conjugates and so the current, $\dot{N}$, can be calculated from the derivative of the Hamiltonian with respect to Φ.

Making the change into relative ($\Delta\tau = \tau_2 - \tau_1$) and collective ($\tau = (\tau_1 + \tau_2)/2$) time co-ordinates we can interrogate this integral,

$$\left\langle S_{\text{tun}}^{\text{eff}} \right\rangle_{\text{LL}} = -2J^2 \int \mathrm{d}\tau \cos\left(\Phi_{\text{L}} - \Phi_{\text{R}}\right) \int \mathrm{d}\Delta\tau e^{-\frac{1}{4K}\ln\left[\frac{\beta^2 c^2}{\xi^2 \pi^2}\left(\sin^2\left(\frac{\pi\Delta\tau}{\beta}\right)+\sinh^2\left(\frac{\pi L}{c\beta}\right)\right)\right]}. \tag{6.2.5}$$

This will give the leading order term in the free energy that is dependent on $\Phi_{\text{L}} - \Phi_{\text{R}}$:

$$F = -\frac{1}{\beta}\ln\mathcal{Z} = 2J^2\cos\left(\Phi_{\text{L}} - \Phi_{\text{R}}\right) \int \mathrm{d}\Delta\tau e^{-\frac{1}{4K}\ln\left[\frac{\beta^2 c^2}{\xi^2 \pi^2}\left(\sin^2\left(\frac{\pi\Delta\tau}{\beta}\right)+\sinh^2\left(\frac{\pi L}{c\beta}\right)\right)\right]}. \tag{6.2.6}$$

In the zero temperature limit, $\beta \to \infty$ the integral becomes more tractable;

$$F = 2J^2\cos\left(\Phi_{\text{L}} - \Phi_{\text{R}}\right) \int_{-\infty}^{\infty} \mathrm{d}\Delta\tau e^{-\frac{1}{4K}\ln\left[\frac{L^2}{\xi^2}\left(\frac{c^2\Delta\tau^2}{L^2}+1\right)\right]}. \tag{6.2.7}$$

Finally, we can de-dimensionalise the integral,

$$F = 2J^2\cos\left(\Phi_{\text{L}} - \Phi_{\text{R}}\right)\left(\frac{L}{\xi}\right)^{-\frac{1}{2K}}\frac{L}{c}\int_{-\infty}^{\infty}\mathrm{d}z\left(1+z^2\right)^{-\frac{1}{4K}} \tag{6.2.8}$$

$$= 2\frac{J^2}{\mu}\left(\frac{L}{\xi}\right)^{1-\frac{1}{2K}} I_0\cos\left(\Phi_{\text{L}} - \Phi_{\text{R}}\right) \tag{6.2.9}$$

where I_0 is defined to be the Beta function [31]

$$I_0 = \int_{-\infty}^{\infty}\mathrm{d}z\left(1+z^2\right)^{-\frac{1}{4K}} = \mathrm{B}\left(\frac{1}{2}, \frac{1}{4K} - \frac{1}{2}\right).$$

This integral is divergent for $K > 1/2$, which unfortunately is the limit of K that we are considering for this bosonic system ($K \gg 1$). It is clear that perturbation theory fails and a different approach is needed, which we shall develop in the next section.

6.3 Mean Field Solution

In this section we shall introduce and use the non-perturbative mean field solution developed by Simpson et. al. [8] to solve the system described above. We shall calculate the supercurrent as a function of phase

difference and then discuss the non-trivial behaviour and degeneracy that is present in the solution.

This mean field solution comes from considering the Luttinger liquid action, Eq. 6.1.7, and minimising it. For a stationary solution, $\varphi_0(x)$, this means that φ satisfies the 1D Laplace equation,

$$\frac{\mathrm{d}^2\varphi_0}{\mathrm{d}x^2} = 0. \tag{6.3.1}$$

Any linear function satisfies this equation, and the intercept and gradient are set by the boundary conditions. The tunnelling action gives boundary conditions on φ at each end of the channel:

$$\begin{aligned} \varphi\left(-L/2\right) &= \Phi - \phi_{\mathrm{L}} \\ \varphi\left(L/2\right) &= -\Phi + \phi_{\mathrm{R}}. \end{aligned} \tag{6.3.2}$$

This gives a mean field phase profile in the channel of:

$$\varphi_0(x) = -\phi_- - 2(\Phi - \phi_+)\frac{x}{L}, \tag{6.3.3}$$

where $\phi_\pm \equiv \frac{1}{2}(\phi_L \pm \phi_R)$ are the symmetric and asymmetric combinations of the phase drops at either end. Substituting this form of φ back into Eq. 6.1.7, we can perform the integration over x. This will leave us with an action expressed in terms of the edge fields, $\phi_\pm$, only. This combines with the tunnelling action, which is also solely a function of the edge fields, to give:

$$S_\varepsilon = \int_0^\beta \mathrm{d}\tau \left[2\frac{Kc}{\pi L}(\Phi - \phi_+)^2 - 4J\cos\phi_+\cos\phi_-\right]. \tag{6.3.4}$$

This action, with subscript ε, is equivalent to the mean field[1] energy of this system.The first term is the kinetic energy of the superfluid in the channel, which flows with velocity $v = -2(\Phi - \phi_+)/mL$. This results in a kinetic energy of $\frac{1}{2}mNv^2$, which gives us our first term. The second term is the Josephson energy from the tunnelling processes at either side. Minimising this action/energy to find $\phi_\pm$ as function

[1]It is a mean field solution because it does not have quantum fluctuations, only the semi-classical

of Φ will give us the final mean field solution. This minimisation gives us the simultaneous equations,

$$\Phi - \phi_+ = \alpha \sin\phi_+ \cos\phi_-, \tag{6.3.5a}$$

$$\cos\phi_+ \sin\phi_- = 0. \tag{6.3.5b}$$

Here the dimensionless tunnelling constant is defined as $\alpha \equiv J/J_c$, where $J_c \equiv Kc/\pi L \ll \pi\rho_0 c$ so that α can range from 0 to values $\gg 1$ while the tunnelling Hamiltonian Eq. 6.1.3 still remains valid.

The condition Eq. 6.3.5b, sets either $\cos\phi_+ = 0$ or $\sin\phi_- = 0$. To investigate the (classical) stability of these solutions we investigate the Hessian matrix of second derivatives of energy $\varepsilon = 2(\Phi - \phi_+)^2 - 4\alpha\cos\phi_+\cos\phi_-$, and its determinant:

$$H[\phi_+, \phi_-] = \begin{pmatrix} 4 + 4\alpha\cos\phi_+\cos\phi_- & -4\alpha\sin\phi_+\sin\phi_- \\ -4\alpha\sin\phi_+\sin\phi_- & 4\alpha\cos\phi_+\cos\phi_- \end{pmatrix}, \tag{6.3.6}$$

$$D[\phi_+, \phi_-] = 16\left[\alpha\cos\phi_+\cos\phi_- + \alpha^2(\cos\phi_+\cos\phi_-)^2 - \alpha^2(\sin\phi_+\sin\phi_-)^2\right]. \tag{6.3.7}$$

For values of ϕ_+ where $\cos\phi_+ = 0$, the determinant is always negative meaning that the solutions are always unstable (i.e. saddle points). This now restricts us to have $\sin\phi_- = 0$, which yields $\phi_- = 0, \pi$ as the only solutions on $\phi_- \in [0, 2\pi)$. As the energy is 2π periodic in ϕ_- no other values that ϕ_- can take will produce anything new. The choice of $\phi_- = 0$ corresponds to symmetric phase drops on both sides with $\phi_+ = \phi_{\mathrm{L}} = \phi_{\mathrm{R}}$ and the choice of $\phi_- = \pi$ corresponds to an asymmetric phase drop, where $\phi_{\mathrm{L}} = 2\pi + \phi_{\mathrm{R}}$. A sketch of what both of these phase profiles look like is given in figure 6.2. With these symmetric and asymmetric branches, the remaining condition eq. 6.3.5a is now:

$$\Phi - \phi_+ = \pm\alpha\sin\phi_+. \tag{6.3.8}$$

This equation is transcendental, and unable to be inverted to get ϕ_+ as a closed form function of Φ. There are a few concrete pieces of information we can glean analytically, one of which is the periodicity of the solutions that we will obtain by solving equation (6.3.8). For some ϕ_+ that satisfies Eq. 6.3.8, if $\Phi \to \Phi + 2\pi$ then $\phi_+ \to \phi_+ + 2\pi$ is going to be a solution as well that gives the same energy. This means

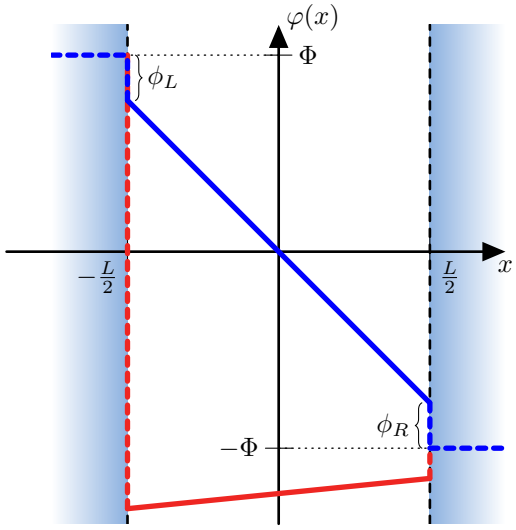

Figure 6.2: Phase profile along the channel. The blue lines show a symmetric solution where $\phi_L = \phi_R$. The red lines show an asymmetric solution where $\phi_L = 2\pi + \phi_R$.

that the energy on a given branch is 2π periodic in Φ and therefore 4π periodic in 2Φ, the total phase difference.

We can also assess the stability of solutions that it will admit. The stable solutions on either branch (local minima of the energy landscape) we require both of the eigenvalues of $H[\phi_+, \phi_-]$ to be positive. For $\sin\phi_- = 0$, the off diagonal terms in the Hessian are zero, giving the condition of

$$\pm\alpha\cos\phi_+(1 \pm \alpha\cos\phi_+) > 0, \tag{6.3.9}$$

to be satisfied for the symmetric/asymmetric branches respectively. For $\alpha < 1$ there are only stable solutions for $\pm\cos\phi_+ > 0$, which for the symmetric branch gives stable solutions in intervals about $\phi_+ = 2j\pi$ where $j \in \mathbb{Z}$. Solutions stable at $\phi_+ = 0$ remain stable in the interval $\phi_+ \in [-\pi/2, \pi/2]$. From Eq. 6.3.8 we can deduce that this symmetric branch solution remains stable for applied phases $\Phi \in [-(\pi/2+\alpha), \pi/2+\alpha]$. Similarly for the asymmetric branch, stable solutions exist around $\phi_+ = (2j+1)\pi$ where $j \in \mathbb{Z}$. The solution centred about $\phi_+ = \pi$ remains stable in the region $\phi_+ \in [\pi/2, 3\pi]$, leading to stability for the applied phases in the interval $\Phi \in [\pi/2 - \alpha, 3\pi + \alpha]$. This means that for all values of Φ, there exists at least one stable solution and about half integer multiples of π there is a region of width 2α where solutions from both branches are stable. This means that if we were to increase Φ from 0, we

would initially start on the symmetric branch and have the phase drops at both barriers to be the same, until switching to the asymmetric branch for $\Phi > \pi/2 + \alpha$ where the asymmetric branch is stable but the symmetric is not. These ranges of stability means that the energy and current will have the expected 2π periodicity in phase difference. Both branches are 4π periodic in the applied phase difference, but their regions of stability we would see an energy/current that is 2π periodic in phase difference if we were to increase Φ monotonically. The equation (6.3.8) can be solved numerically to find ϕ_+ as a function of Φ, and then the mean field energy found as a function of Φ. This is plotted in figure 6.3.

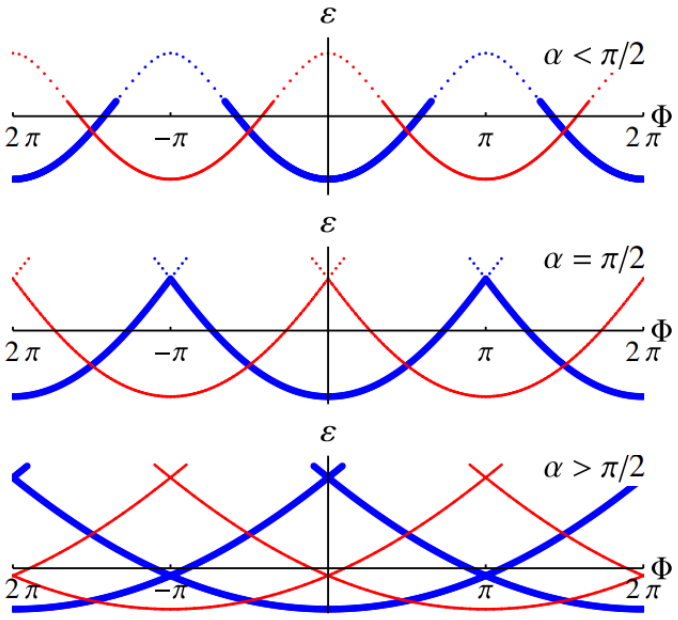

Figure 6.3: Plots of the mean field energy in channel for different values of α. Blue lines are solutions from the symmetric branch, red lines are from the asymmetric branch. [8].

The choice between branches can be thought of the balance between having most of the phase difference closed up by having a current in the channel (symmetric branch) or by accumulating most of the phase drop on one of the boundaries. For $|\Phi| < \pi/2$, the kinetic energy cost is small so the lower energy state is the symmetric branch. For $|\Phi| \sim \pi$, most of the phase difference can be made up through the phase drop when tunnelling on the asymmetric branch, thus giving it the lower energy. At $\Phi = \pi/2$ the branches are degenerate, and they are both simultaneously stable for any values of α. The existence of this degeneracy and mechanism that could lift it will be discussed later in subsections 6.4 and 6.4.2.

Extra solutions on both branches appear as α is increased. For $\alpha > 1$ extra solutions appear around

$\Phi = (2j+1)\pi$ for the symmetric branch and $\Phi = 2j\pi$ for the asymmetric branch. These remain metastable until $\Phi = \pi/2$ where they are stable for the whole interval $[0, \pi]$. This can be seen in figure 6.3 where the solid lines represent regions where the solution is stable. The current through the channel is the gradient

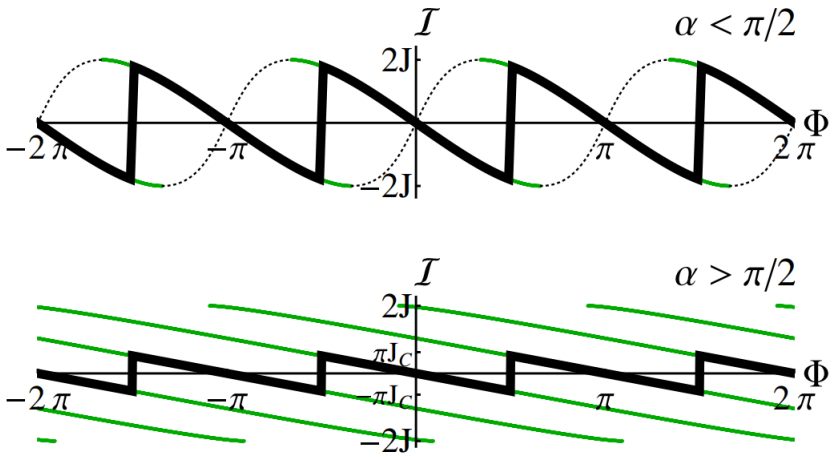

Figure 6.4: Dependence of the current on 2Φ. Black lines represent the lowest energy configuration and green represent metastable solutions. The dotted lines represent unstable solutions and are used to guide the eye [8].

of the phase given by Eq. 6.3.3, with the substitution of Eq. 6.3.8 giving:

$$\mathcal{I} = \mp 2J \sin \phi_+. \tag{6.3.10}$$

This is the same form as the standard Josephson current. The main differences to note is the fact that it is non-perturbative, it is of a lower order in J than perturbation theory would give us. Secondly, it differs from the Josephson formula due to the non-trivial (and non-linear) dependence of ϕ_+ on the phase difference 2Φ. The sign of the current comes from the $\cos \phi_-$ that defines the branches. As Φ is increased past $\pi/2$ the lowest energy solution becomes the solution on the asymmetric branch, hence the current corresponding to the lowest energy will discontinuously flip at $\Phi = \pi/2$. The profile will be piecewise sinusoidal due to the changing of the branches, as seen in figure 6.4. Experimentally this will be measurable as a hysteresis in the current, because the symmetric branch is still stable as Φ increases past $\pi/2$ but is no longer the solution corresponding to the lowest energy. We can see how this solution is non-perturbative, as the current is a lower power of J than would be obtained by the perturbative calculation. This behaviour is qualitatively different to that exhibited by an equivalent system of fermions

[6, 7, 3], where the current exhibits Ohmic dissipation even in the absence of impurities, very different to the non-perturbative behaviour of the current we've obtained.

6.4 Fluctuations

So far we have seen the classical stability of the solutions, however more analysis is needed to verify if this mean field solution is robust against phase fluctuations. This will be done by adding fluctuations on top of the mean field solution and generating an effective action that describes fluctuations. With this action, we shall investigate how the addition of fluctuations affects the non-quadratic part of the action. Through a renormalisation group process, as seen in chapter 5, we shall see that fluctuations don't erase the features of the mean field solution. It also implies that fluctuations won't provide a mechanism of lifting the degeneracy at $\Phi = \pi/2$, making it dynamically protected.

In this section we shall outline the key results, full details can be found in [8, 38]. We start with the action Eq. 6.1.7 where the Luttinger liquid is described in terms of φ alone[1] The fluctuations within the channel are defined as: $\varphi(x,\tau) = \varphi_0(x) + \widetilde{\varphi}(x,\tau)$, which are independent from the fluctuations on the boundary defined as: $\phi_{\mathrm{L,R}}(\tau) = \phi_{\mathrm{L,R}} + \widetilde{\phi}_{\mathrm{L,R}}(\tau)$. From Eq. 6.3.2 the fluctuating field have the boundary conditions:

$$\begin{aligned} \widetilde{\varphi}\left(-L/2,\tau\right) &= -\widetilde{\phi_{\mathrm{L}}}(\tau), \\ \widetilde{\varphi}\left(L/2,\tau\right) &= \widetilde{\phi_{\mathrm{R}}}(\tau). \end{aligned} \tag{6.4.1}$$

From integrating out the Gaussian fluctuations inside the channel, the action for the fluctuations on the edge is,

$$\begin{aligned} S_{\mathrm{fl}} &= \frac{K}{2\pi}\int \frac{\mathrm{d}\omega}{2\pi}|\omega| \left(\left|\widetilde{\phi}_{\mathrm{L}}(\omega)\right|^2 + \left|\widetilde{\phi}_{\mathrm{R}}(\omega)\right|^2\right) \\ &= \frac{K}{\pi}\int \frac{\mathrm{d}\omega}{2\pi}|\omega| \left(\left|\widetilde{\phi}_{+}(\omega)\right|^2 + \left|\widetilde{\phi}_{-}(\omega)\right|^2\right) \end{aligned} \tag{6.4.2}$$

Here the limit of $\omega \gg c/L$ has been taken, as we are interested in high frequency fluctuations far away from the minumum phononic frequency the channel can support (c/L). In the second line we define the

[1] A qualitatively identical approach starting with action Eq. 6.1.2 can be done, and full details can be found in section 7.4 of this thesis.

fluctuations of the symmetric/asymmetric phase drops $2\widetilde{\phi}_{\pm}(\tau) \equiv \widetilde{\phi}_L(\tau) \pm \widetilde{\phi}_R(\tau)$ The substitution of the fluctuating fields into the action Eq. 6.3.4 leads to:

$$S_\varepsilon = \frac{Kc}{\pi L}\int_0^\beta \mathrm{d}\tau \left[2(\Phi-\phi_+)^2 - 4(\Phi-\phi_+)\widetilde{\phi}_+(\tau) - 4\alpha\cos\Big(\phi_+ + \widetilde{\phi}_+(\tau)\Big)\cos\Big(\phi_- + \widetilde{\phi}_-(\tau)\Big)\right]. \tag{6.4.3}$$

In the next subsection we shall investigate the impact that high energy fluctuations have on this action, in particular the non-quadratic cosine term coming from the tunnelling at the barriers.

6.4.1 RG Analysis

We now embark on using the Renormalisation Group to assess the stability and validity of this mean field solution. With the action eq. (6.4.2) we shall use RG to integrate out the high energy fluctuations in the standard way to see how the couplings (namely the tunnelling α) scale. We proceed in the standard way (detailed in chapter 5) and identify "fast" and "slow" fields:

$$\begin{aligned}\widetilde{\phi}_{\pm}(\tau) &= \int\limits_{|\omega|<\frac{\Lambda}{b}} \mathrm{d}\omega e^{i\omega\tau}\widetilde{\phi}_{\pm}(\omega) + \int\limits_{\frac{\Lambda}{b}<|\omega|<\Lambda} \mathrm{d}\omega e^{i\omega\tau}\widetilde{\phi}_{\pm}(\omega) \\ &= \widetilde{\phi}^{<}_{\pm}(\tau) + \widetilde{\phi}^{>}_{\pm}(\tau)\end{aligned} \tag{6.4.4}$$

The action for fluctuations does not mix terms of different speeds, easily allowing for the identification of actions for slow, $S^{<}_{\mathrm{fl}}$, and fast, $S^{>}_{\mathrm{fl}}$, fluctuations. Integrating out the fast modes is equivalent to performing the average $\langle\ldots\rangle_{>} \equiv \int \mathrm{D}\phi^{>}(\ldots)e^{-S^{>}_{\mathrm{fl}}} / \int \mathrm{D}\phi^{>} e^{-S^{>}_{\mathrm{fl}}}$. Using the identity:

$$\left\langle \exp\left[\pm i\widetilde{\phi}^{>}_{\pm}\right]\right\rangle_{\pm,>} \equiv \exp\left[-\frac{1}{2}\left\langle\left(\widetilde{\phi}^{>}_{\pm}\right)^2\right\rangle_{\pm,>}\right], \tag{6.4.5}$$

we can renormalise the non-Gaussian cosine term:

$$\left\langle\cos\Big(\phi_\pm + \widetilde{\phi}^{<}_{\pm}(\tau) + \widetilde{\phi}^{>}_{\pm}(\tau)\Big)\right\rangle_{>,\pm} = \exp\left[-\frac{1}{2}\left\langle(\widetilde{\phi}^{>}_{\pm}(\tau))^2\right\rangle_{>,\pm}\right]\cos\Big(\phi_\pm + \widetilde{\phi}^{<}_{\pm}(\tau)\Big). \tag{6.4.6}$$

The average inside the exponential can be calculated more readily in Fourier space,

$$\left\langle (\widetilde{\phi}^{>}_{\pm}(\tau))^2 \right\rangle_{>,\pm} = \int_{>} \frac{\mathrm{d}\omega_1}{2\pi}\frac{\mathrm{d}\omega_2}{2\pi} e^{i\tau(\omega_1+\omega_2)} \left\langle \widetilde{\phi}_{\pm}(\omega_1)\widetilde{\phi}_{\pm}(\omega_2) \right\rangle_{>,\pm}. \tag{6.4.7}$$

From the action for fluctuations, Eq. (6.4.2) we can see that the the averages for both symmetric and asymmetric fluctuations will be identical, giving an average of;

$$\left\langle \widetilde{\phi}_{\pm}(\omega_1)\widetilde{\phi}_{\pm}(\omega_2) \right\rangle_{>,\pm} = \frac{\pi^2}{K|\omega_1|}\delta_{-\omega_1,\omega_2}. \tag{6.4.8}$$

Substituting this back into Eq. (6.4.7) gives:

$$\left\langle (\widetilde{\phi}^{>}_{\pm}(\tau))^2 \right\rangle_{>,\pm} = \frac{1}{4K}\int_{>} \mathrm{d}\omega \frac{1}{|\omega|} = \frac{1}{2K}\int_{\Lambda/b}^{\Lambda} \mathrm{d}\omega \frac{1}{\omega} = \frac{1}{2K}\ln b. \tag{6.4.9}$$

Now we can integrate out fast modes from both the symmetric and asymmetric fluctuations to renormalise the cosines:

$$\begin{aligned}
&\left\langle \cos\Big(\phi_+ + \widetilde{\phi}^{<}_{+}(\tau) + \widetilde{\phi}^{>}_{+}(\tau)\Big)\cos\Big(\phi_- + \widetilde{\phi}^{<}_{-}(\tau) + \widetilde{\phi}^{>}_{-}(\tau)\Big)\right\rangle_{>} \\
&= \exp\left[-\frac{1}{2}\left\langle (\widetilde{\phi}^{>}_{+}(\tau))^2 \right\rangle_{>,+} - \frac{1}{2}\left\langle (\widetilde{\phi}^{>}_{-}(\tau))^2 \right\rangle_{>,-}\right]\cos\Big(\phi_+ + \widetilde{\phi}^{<}_{+}(\tau)\Big)\cos\Big(\phi_- + \widetilde{\phi}^{<}_{-}(\tau)\Big) \\
&= \exp\left[-\frac{1}{2K}\ln b\right]\cos\Big(\phi_+ + \widetilde{\phi}^{<}_{+}(\tau)\Big)\cos\Big(\phi_- + \widetilde{\phi}^{<}_{-}(\tau)\Big)
\end{aligned} \tag{6.4.10}$$

The final stage of the RG procedure is the rescaling of the fields $\widetilde{\phi}_{\pm}$ and frequencies ω, similar to the procedure in chapter 5. The result of this scaling is the coefficient of the tunnelling term, α, gets renormalised by a factor of $b^{1-1/2K}$ after each RG step. This gives an RG flow equation for α of:

$$\frac{\mathrm{d}\ln\alpha}{\mathrm{d}\ln b} = 1 - \frac{1}{2K}. \tag{6.4.11}$$

To get what the renormalised dimensionless tunnelling energy is at low energies, we integrate Eq. (6.4.11) from our high energy cut-off, down to the low energy cut-off. The infra-red cut-off is $\omega_{\min} \sim \max(T, c/L)$ and the UV cut-off is related to the chemical potential, $\Lambda \sim c/\xi = \mu$. Therefore at low energies the

dimensionless tunnelling energy is given by: $\alpha(\omega_{\min}) = \alpha_0(\Lambda/\omega_{\min})^{1-\frac{1}{2K}}$. Here the base value of the tunnelling energy is what it was defined as earlier, $\alpha_0 = J/J_c$.

From Eq. (6.4.11) we can see that $K = 1/2$ is a critical value in the RG flow. For $K < 1/2$, α will flow towards smaller values, meaning it is an RG irrelevant parameter. What this means is that fluctuations dominate the low energy behaviour and destroy the structure of the mean field solution. Conversely for $K > 1/2$, α flows towards larger values, strengthening the mean field solution. This is the case for a bosonic Luttinger liquid which will have $K \gg 1$.

6.4.2 Degeneracy & Discussion

At an applied phase of $\Phi = \pi/2$, both branches will have the same energy, and there is no mechanism in the mean field theory that lifts this degeneracy. With the inclusion of fluctuations we have seen that in the case of a bosonic Luttinger liquid the fluctuations only strengthen the mean field solution. This means that fluctuations aren't capable of connecting the two branches as they are power-law suppressed.

This dynamically protected degeneracy, along with the 4π periodicity of the individual branches, echoes the same predicted behaviour of the systems claimed to host Majorana Fermions [9, 10]. This raises a few questions, how closely linked our the Majorana systems to our system? Can we describe our degeneracy as some topological edge excitation? Are there other systems that exhibit the same behaviour as the bosonic system that are closer to the Majorana systems? It is this last question that we shall investigate in the following chapter, by looking at if we can recreate the physics of the bosonic system where we use fermions as our constituent particles.

Chapter 7

The Fermionic System

In this chapter we shall discuss the main results of this thesis, and demonstrate how the same physics of the bosonic system considered in chapter 6 can be achieved in a system consisting of fermions. These results are to be published as a pre-print. We shall begin with the motivation for investigating such a system, and then discuss the ingredients needed to construct a model that will allow us to recreate the physics of the bosonic system.

This model consists of BCS superconducting reservoirs, connected with weak tunnelling links, to a Luttinger liquid of attractive fermions, we shall create an effective tunnelling action for particle pairs and see that for channels that have attractive fermionic interactions will reproduce the same action as seen for bosons in section 6.1. The final step is to apply a mean field solution plus fluctuations, and see that high energy fluctuations do not destroy the structure of it.

7.1 Motivation

The bosonic system considered in chapter 6 is novel due to the non-perturbative mean field solution that exhibits similar qualities of the semiconductor-superconductor nanowire systems proposed to exhibit Majorana zero modes [9, 10], as described in chapter 3. The bosonic system has 4π periodicity in the current as a function of applied phase, which is a signature of MZMs in the semiconductor-superconductor nanowires.

Both systems also have a protected degeneracy; the nanowires have a topologically protected degeneracy due to the MZMs, whereas the bosonic system has a protection against fluctuations that is not fully understood. It is possible that there is a description of this degeneracy in terms of topological edge modes. The next step to better understand this degeneracy is to try to recreate it without using bosons.

The system that we choose to investigate has the same geometry as the bosonic system; two reservoirs of particles that connect to two ends of a 1D wire with weak tunnelling links. The difference is that the particles we shall fill the geometry with will be fermions, with the reservoirs forming a BCS superconductor and the wire forming a Luttinger Liquid with attractive interactions between the fermions. It will be the phase difference between the BCS order parameters of the two superconductors that will drive the current. A possible realisation of this system would be in cold atoms, by using an atom chip. These are electronic devices that are fabricated in a way, so that the currents through the chip produce finely tuned magnetic fields for the purpose of trapping cold atoms. The fields produced by atom chips can generate trapping potentials that produce the geometry of the reservoirs, 1D channel and the tunnelling barrier between them (as demonstrated in the supplementary material of [8]). Another advantage of cold atoms is that interactions between atoms are tunable through Feshbach resonances. This will allow for the behaviour explored in this chapter to be investigated, where the interactions are required to be attractive, and easily compared to systems that have repulsive interactions [6].

The key to the behaviour of the bosonic system in chapter 6 was the value of the Luttinger parameter, $K > 1$. This is satisfied for bosons with any repulsive interactions. To recreate this with fermions this corresponds to attractive interactions (see section 2.3 for details on which interactions we can include to guarantee this). This system of superconducting reservoirs connected by a Luttinger liquid has already been considered by Fazio et. al. [6]. For them a perturbative solution to 4th order in the tunnelling parameter suffices, however it breaks down for $K > 1$. I shall show that for the fermionic system with $K > 1$, we can use a non-perturbative mean field solution to calculate the current as a function of phase difference, akin to Simpson et. al. [8] for a bosonic system.

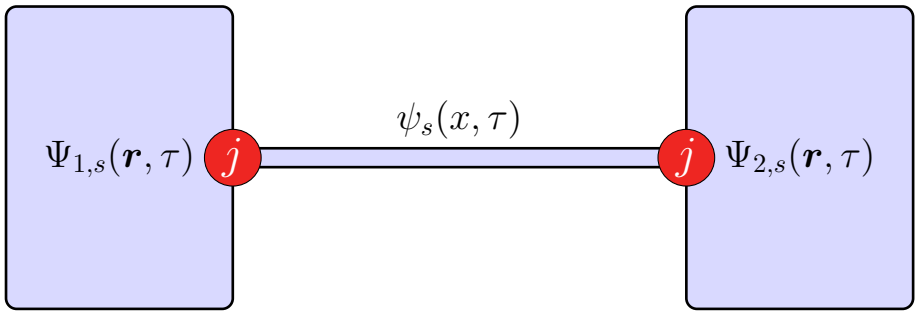

Figure 7.1: A cartoon of the system

7.2 The Model

We consider a system consisting of two bulk reservoirs, containing BCS superconductors, that couple to the ends of a 1D channel of fermions that we model as a Luttinger Liquid (LL). The imaginary time action for the full system is the sum of the actions describing the reservoirs, channel and a tunnelling action, $S_{\rm tun}$, coupling them together: $\mathcal{S} = S_{\rm res} + S_{\rm LL} + S_{\rm tun}$. In the left and right hand side reservoirs we have BCS superconductors described by actions, $S_1 + S_2 = S_{\rm res}$, which are the standard BCS actions (as described in Eq. (4.2.6))

$$-S_\ell[\overline{\Psi}_{\ell,s},\Psi_{\ell,s}] = \int_0^\beta \mathrm{d}\tau \int \mathrm{d}^3 r \left(\overline{\Psi}_{\ell,\uparrow}(\boldsymbol{r},\tau), \Psi_{\ell,\downarrow}(\boldsymbol{r},\tau)\right) \begin{pmatrix} -\partial_\tau + \frac{1}{2m}\nabla^2 + \mu & \Delta_\ell \\ \Delta_\ell^* & -\partial_\tau - \frac{1}{2m}\nabla^2 - \mu \end{pmatrix} \begin{pmatrix} \Psi_{\ell,\uparrow}(\boldsymbol{r},\tau) \\ \overline{\Psi}_{\ell,\downarrow}(\boldsymbol{r},\tau) \end{pmatrix} \tag{7.2.1}$$

Here the index $\ell = 1, 2$ denotes which reservoir the fields are from and the index $s =\uparrow,\downarrow= \pm$ is the spin. We are working in the mean field limit for Δ, where fluctuations of the superconducting order parameter, $\Delta_\ell = |\Delta|e^{i\Phi_\ell}$ are small. They are related to the fermionic fields inside the reservoirs in the standard way (see Eq. (4.2.18)):

$$\begin{aligned} \langle \Psi_{\ell,\uparrow}(\tau)\Psi_{\ell,\downarrow}(\tau')\rangle_{S_\ell} &= \pi N_0 e^{i\Phi_\ell} \int \frac{\mathrm{d}\omega}{2\pi} \frac{|\Delta| e^{i\omega(\tau-\tau')}}{\sqrt{\omega^2 + |\Delta|^2}} \\ &= \pi N_0 |\Delta| e^{i\Phi_\ell} \mathrm{K}_0\left(|\Delta|(\tau-\tau')\right). \end{aligned} \tag{7.2.2}$$

As before in section 4.2, N_0 is the density of states at the Fermi surface and K_0 is the modified Bessel's function of the second kind. The Bessel's function is exponentially small for $|\tau - \tau'| \gg \frac{1}{|\Delta|}$, which suppresses $\tau \neq \tau'$. Without loss of generality we choose $\Phi_1 = -\Phi_2 \equiv \Phi$. We assume that the two reservoirs have been equilibrated to the same chemical potential and the same density of particles. This ensures that the current through the channel is entirely driven by the phase difference, 2Φ.

We model the coupling between the reservoirs and channel by a tunnelling action that involves the reservoir fields $\Psi_{\ell,s}(\tau)$ and channel fields $\psi_s(x,\tau)$,

$$S_{\mathrm{tun}}\left[\overline{\Psi}_{m,s}, \Psi_{m,s}, \overline{\psi}_s, \psi_s\right] = j\int_0^\beta \mathrm{d}\tau \sum_{s=\uparrow,\downarrow} \left[\overline{\Psi}_{1,s}\psi_s(x=-L/2) + \overline{\Psi}_{2,s}\psi_s(x=L/2) + (\mathrm{H.c.})\right]. \tag{7.2.3}$$

The tunnelling matrix elements, j, are taken to be constant and equal on the left and right barriers. Inside the channel we choose to bosonise the fermionic fields and describe the channel as a Luttinger Liquid. We use the bosonisation identity with phase (φ) and conjugate density (ϑ) fields:

$$\psi_s(x,\tau) = \sqrt{\varrho_0}\sum_{\eta=\pm 1} e^{i(\eta k_F - \pi/L)x} e^{-i(\eta\vartheta_\rho - \varphi_\rho)} e^{-is(\eta\vartheta_\sigma - \varphi_\sigma)}, \tag{7.2.4}$$

where the index η denotes right/left moving fermions and ϱ_0 is the density of particles in the channel (assuming equal densities of spin species). This defines the charge (ρ) and spin (σ) degrees of freedom identically to Eq. (2.3.14). The Luttinger liquid action in terms of these fields is:

$$S_{\mathrm{LL}}[\varphi_\nu, \vartheta_\nu] = \frac{1}{\pi}\int_0^\beta \mathrm{d}\tau \int_{-L/2}^{L/2} \mathrm{d}x \left\{ \sum_{\nu=\rho,\sigma} \Big(-2i\partial_x\varphi_\nu\partial_\tau\vartheta_\nu + v_\nu K_\nu(\partial_x\varphi_\nu)^2 + \frac{v_\nu}{K_\nu}(\partial_x\vartheta_\nu)^2 \Big) + g_{1\perp}\cos(4\vartheta_\sigma) \right\} \tag{7.2.5}$$

where v_ν and K_ν are the sound velocity and Luttinger parameter in the charge and spin sectors respectively. There are two points to note about this Luttinger liquid action. First is the inclusion of the global Sine-Gordon impurity term in the spin sector, arising from the spin flip ($g_{1\perp}$) interactions. This is included to cause the spin sector to be gapped, pinning the field ϑ_σ to the minimum of the cosine. This suppresses the dynamics of the spin sector, leaving the charge sector to be the platform where the physics of the bosonic system is recreated. To enable this, we want $K_\sigma < 1$ to ensure that the sine-Gordon

impurity is a relevant perturbation (see section 5.3 for details). The second point about this Luttinger liquid action is that we have not integrated out one of the fields, to be left with an action in only one of them. This is because the tunnelling term is non-quadratic in both fields currently and needs to be dealt with carefully. The full partition function for the system is:

$$\mathcal{Z} = \int \mathrm{D}\left[\overline{\Psi}, \Psi\right]_{\mathrm{res}} \mathrm{D}\left[\overline{\psi}, \psi\right]_{\mathrm{LL}} \exp\bigl(-S_{\mathrm{res}}[\overline{\Psi}, \Psi] - S_{\mathrm{LL}}[\overline{\psi}, \psi] - S_{\mathrm{tun}}[\overline{\Psi}, \Psi, \overline{\psi}, \psi]\bigr). \tag{7.2.6}$$

In the next section we shall look more closely at the tunnelling term, and find a way to couple the phase of the superconductors to the channel fields.

7.3 Generating Effective Tunnelling

To replicate the physics of the bosonic system, we need to replicate the tunnelling action Eq. (6.1.5). In the bosonic system, this term couples the phase of the reservoirs with the phase of the Luttinger liquid at the boundaries. For the fermionic system, with tunnelling action Eq. (7.2.3), things aren't as simple. The phase of the reservoirs comes into play at second order in Ψ when calculating anomalous correlation functions, $\langle \Psi_\uparrow \Psi_\downarrow \rangle_{\mathrm{res}}$, such as Eq. (4.2.18). We will need to produce these sorts of correlations if we are to recreate the same tunnelling action as for bosons. The way to generate these correlation functions that depend on the phases of the reservoirs is through a perturbative expansion. The partition function is expanded in a power series in the tunnelling parameter j:

$$\begin{aligned}
\mathcal{Z} &= \int \mathrm{D}\vartheta_{\rho,\sigma}\mathrm{D}\varphi_{\rho,\sigma}\mathrm{D}\Psi_{1,2}\, e^{-S_{\mathrm{res}}-S_{\mathrm{LL}}-S_{\mathrm{tun}}} \\
&\simeq \int \mathrm{D}\vartheta_{\rho,\sigma}\mathrm{D}\varphi_{\rho,\sigma}\mathrm{D}\Psi_{1,2}\, e^{-S_{\mathrm{LL}}-S_{\mathrm{res}}} \left[1 + \tfrac{1}{2}S_{\mathrm{tun}}^2 + \tfrac{1}{4!}S_{\mathrm{tun}}^4 + \dots\right] \\
&\simeq \left\langle 1 + \tfrac{1}{2}S_{\mathrm{tun}}^2 + \tfrac{1}{4!}S_{\mathrm{tun}}^4 \right\rangle_{\mathrm{res,LL}}
\end{aligned} \tag{7.3.1}$$

The current through the channel is proportional to, $I \propto \frac{\partial \ln \mathcal{Z}}{\partial \Delta\Phi}$, where $\Delta\Phi$ is the phase difference between the two reservoirs. In this solely perturbative approach, the lowest order term that contains dependence

on $\Delta\Phi$ is at 4th order. The terms that would have dependence on $\Delta\Phi$ look like[1]:

$$\overline{\Psi}_{1,s}(\tau_1)\overline{\Psi}_{1,\bar{s}}(\tau_2)\psi_s(-L/2,\tau_1)\psi_{\bar{s}}(-L/2,\tau_2)\overline{\psi}_s(L/2,\tau_3)\overline{\psi}_{\bar{s}}(L/2,\tau_4)\Psi_{2,s}(\tau_3)\Psi_{2,\bar{s}}(\tau_4)$$

A term like this corresponds to a (singlet) pair of fermions tunnelling into the channel from the right (subscript 2) reservoir, propagating through the channel and then tunnelling into the left (subscript 1) reservoir. Upon averaging with respect to their respective reservoir actions, the $\overline{\Psi}_{1,s}(\tau_1)\overline{\Psi}_{1,\bar{s}}(\tau_2)$ and $\Psi_{2,s}(\tau_3)\Psi_{2,\bar{s}}(\tau_4)$ parts together become proportional to $e^{i(\Phi_2-\Phi_1)} = e^{-i\Delta\Phi}$. It is then the quartic Luttinger liquid correlators that need to be calculated to fully evaluate the current through the channel. Fazio et. al. [6] performed these functional integrals, which are divergent as $T \to 0$ for $K_\rho > 1$. This is the equivalent analysis as shown in section 6.2 for the bosonic system. The purely perturbative approach fails, and a different method is needed. What we shall do is the equivalent to the bosonic case, where a non-perturbative mean field solution is applied to the action. The issue with doing this with the fermionic system is that the tunnelling action does not couple the phases of the reservoirs, and needs to include the averages $\langle\Psi_\uparrow\Psi_\downarrow\rangle$ for the phases to enter.

To get these averages, we start our analysis by taking the second order term in the perturbative expansion Eq. (7.3.1), and average over the reservoir actions only. We are only interested in terms that will generate the anomalous correlators, as they will be the ones that generate dependencies on the phases of the reservoirs[2]. With this averaging done we re-exponentiate to get an effective action for tunnelling, involving the phases of the reservoirs and the un-averaged fields of the 1D channel,

$$\begin{aligned}
\mathcal{Z} &= \int \mathrm{D}\vartheta_{\rho,\sigma}\mathrm{D}\varphi_{\rho,\sigma}\mathrm{D}\Psi_{1,2}e^{-S_{\mathrm{res}}-S_{\mathrm{LL}}-S_{\mathrm{tun}}} \\
&\simeq \int \mathrm{D}\vartheta_{\rho,\sigma}\mathrm{D}\varphi_{\rho,\sigma}e^{-S_{\mathrm{LL}}}\int \mathrm{D}\Psi_{1,2}e^{-S_{\mathrm{res}}}\left(1+\tfrac{1}{2}S_{\mathrm{tun}}^2+\dots\right) \\
&\simeq \int \mathrm{D}\vartheta_{\rho,\sigma}\mathrm{D}\varphi_{\rho,\sigma}e^{-S_{\mathrm{LL}}}\left\langle 1+\tfrac{1}{2}S_{\mathrm{tun}}^2+\dots\right\rangle_{\mathrm{res}} \\
&\simeq \int \mathrm{D}\vartheta_{\rho,\sigma}\mathrm{D}\varphi_{\rho,\sigma}e^{-S_{\mathrm{LL}}+\frac{1}{2}\left\langle S_{\mathrm{tun}}^2\right\rangle_{\mathrm{res}}}
\end{aligned} \tag{7.3.2}$$

[1] Up to Hermitian conjugation and permutation of τ's

[2] We also omit terms that would form correlators mixing different reservoirs, $\langle\Psi_{1,s}\Psi_{2,s'}\rangle$. These correlations would be exponentially suppressed by their spatial separation.

With the rules for selecting terms we consider in the expansion, the terms that are pertinent are:

$$\begin{aligned}\left\langle S^2_{\text{tun}}\right\rangle_{\text{res}} = -j^2\int_0^\beta \mathrm{d}\tau\mathrm{d}\tau' \sum_s \Big[&\left\langle \overline{\Psi}_{1,s}(\tau)\overline{\Psi}_{1,\bar{s}}(\tau')\right\rangle \psi_s(-L/2,\tau)\psi_{s'}(-L/2,\tau') \\ &+ \overline{\psi}_s(-L/2,\tau)\overline{\psi}_{\bar{s}}(-L/2,\tau')\left\langle \Psi_{1,s}(\tau)\Psi_{1,\bar{s}}(\tau')\right\rangle \\ &+ \left\langle \overline{\Psi}_{2,s}(\tau)\overline{\Psi}_{2,\bar{s}}(\tau')\right\rangle \psi_s(L/2,\tau)\psi_{\bar{s}}(L/2,\tau') \\ &+ \overline{\psi}_s(L/2,\tau)\overline{\psi}_{\bar{s}}(L/2,\tau')\left\langle \Psi_{2,s}(\tau)\Psi_{2,\bar{s}}(\tau')\right\rangle \Big] + \text{other terms}\end{aligned} \tag{7.3.3}$$

Using Eq. (4.2.18), we can substitute the value the anomalous correlations take (restoring the L/R index on the reservoir phases for clarity), and perform the sum over spin indices. Dropping the other terms, this gives us what our effective tunnelling will be:

$$\begin{aligned}S^{\text{eff}}_{\text{tun}} = -\frac{1}{2}j^2\pi N_0|\Delta|\int_0^\beta \mathrm{d}\tau\mathrm{d}\tau' \mathrm{K}_0\big(|\Delta|(\tau-\tau')\big)\Big\{ &e^{-i\Phi_{\mathrm{L}}}\Big(\psi_\uparrow(-\tfrac{L}{2},\tau)\psi_\downarrow(-\tfrac{L}{2},\tau') + \psi_\uparrow(-\tfrac{L}{2},\tau')\psi_\downarrow(-\tfrac{L}{2},\tau)\Big) \\ &+ e^{i\Phi_{\mathrm{L}}}\Big(\overline{\psi}_\uparrow(-\tfrac{L}{2},\tau)\overline{\psi}_\downarrow(-\tfrac{L}{2},\tau') + \overline{\psi}_\uparrow(-\tfrac{L}{2},\tau')\overline{\psi}_\downarrow(-\tfrac{L}{2},\tau)\Big) \\ &+ e^{-i\Phi_{\mathrm{R}}}\Big(\psi_\uparrow(\tfrac{L}{2},\tau)\psi_\downarrow(\tfrac{L}{2},\tau') + \psi_\uparrow(\tfrac{L}{2},\tau')\psi_\downarrow(\tfrac{L}{2},\tau)\Big) \\ &+ e^{i\Phi_{\mathrm{R}}}\Big(\overline{\psi}_\uparrow(\tfrac{L}{2},\tau)\overline{\psi}_\downarrow(\tfrac{L}{2},\tau') + \overline{\psi}_\uparrow(\tfrac{L}{2},\tau')\overline{\psi}_\downarrow(\tfrac{L}{2},\tau)\Big)\Big\}\end{aligned} \tag{7.3.4}$$

We have ordered all the pairs of terms the same way, with $\uparrow$ spins on the left of $\downarrow$ spins. This is to respect the symmetry of the singlet, prior to bosonisation where we omit anti-commuting Klein factors.

The effective tunnelling action Eq. (7.3.4) can be readily seen as the sum of two tunnelling terms, one at the left side of the channel and one at the right side. Focusing on the term on the left hand side, we can bosonise using the identity Eq. (7.2.4),

$$\psi_\uparrow(-\tfrac{L}{2},\tau)\psi_\downarrow(-\tfrac{L}{2},\tau') = \varrho_0 \sum_{\eta,\chi=\pm1} e^{-i\left((\eta+\chi)\frac{k_{\mathrm{F}}L}{2}-\pi\right)} e^{-i(\eta\vartheta_\rho(\tau)+\chi\vartheta_\rho(\tau')-\varphi_\rho(\tau)-\varphi_\rho(\tau'))} e^{-i(\eta\vartheta_\sigma(\tau)-\chi\vartheta_\sigma(\tau'))}. \tag{7.3.5}$$

Here the chirality indices, $\eta,\chi = \pm1$ denote right and left movers respectively, and the fields ϑ and φ are implicitly evaluated at $x = -L/2$. As mentioned previously, due to the Bessel's function K_0 being

dependent on the difference in times $(\tau - \tau')$, and exponentially small for $(\tau - \tau') > 1/|\Delta|$, we can ignore any time differences bigger than $1/|\Delta|$. We assume that $|\Delta|$ is one of the largest energy scales in our system, thus making $1/|\Delta|$ a timescale at which the fields cannot fluctuate faster than. Therefore we can happily perform an integral over a relative time coordinate to be left with one integral over a collective time coordinate. This gives us

$$\psi_\uparrow(-\tfrac{L}{2},\tau)\psi_\downarrow(-\tfrac{L}{2},\tau) = \varrho_0 \sum_{\eta,\chi=\pm 1} e^{-i\left((\eta+\chi)\frac{k_\mathrm{F}L}{2}-\pi\right)} e^{-i((\eta+\chi)\vartheta_\rho - 2\varphi_\rho)} e^{-i((\eta-\chi)\vartheta_\sigma)}. \tag{7.3.6}$$

We can see that there will be two types of terms arising from the different combinations of chiralities. If the chiralities are different, $\eta + \chi = 0$, then that would physically correspond to a singlet pair that tunnels with net momentum of zero. The pair is created at each Fermi-point, meaning that it is a 1D analogue of a Cooper pair. Terms that have this combination of chiralities will from now be referred to as "Cooper" terms. Alternatively, the terms with the same chirality, $\eta - \chi = 0$, would physically correspond to Andreev reflection. This is a phenomenon in which a single fermion (electron in the solid state, fermionic atom in cold atoms) tunnels into a superconductor below the energy gap. It does so by tunnelling into the superconductor as a Cooper pair, and reflects a hole back into the normal metal. Performing the sum over chiralities, this term becomes:

$$\psi_\uparrow(-\tfrac{L}{2},\tau)\psi_\downarrow(-\tfrac{L}{2},\tau) = -2\varrho_0 e^{2i\varphi_\rho}\Big[\cos(2\vartheta_\sigma) + \cos(2\vartheta_\rho + k_\mathrm{F}L)\Big]. \tag{7.3.7}$$

Inside the brackets, the first term corresponds to the Cooper tunnelling, with the second corresponding to Andreev tunnelling. A key point to note is that the Andreev term has a non-quadratic dependence on ϑ_ρ, which prevents us from integrating out ϑ_ρ from our Luttinger liquid action Eq. (7.2.5). Including the conjugated term, the total tunnelling action on the left side is given to be:

$$\begin{aligned} S_\mathrm{L}^\mathrm{eff} &= -j^2\pi N_0 \int_{-\frac{\beta|\Delta|}{2}}^{-\frac{\beta|\Delta|}{2}} \mathrm{d}z\, \mathrm{K}_0(z) \int_0^\beta \mathrm{d}\tau \left\{ e^{-i\Phi_\mathrm{L}} \psi_\uparrow(-\tfrac{L}{2},\tau)\psi_\downarrow(-\tfrac{L}{2},\tau) + e^{i\Phi_\mathrm{L}} \overline{\psi}_\uparrow(-\tfrac{L}{2},\tau)\overline{\psi}_\downarrow(-\tfrac{L}{2},\tau) \right\} \\ &= 4j^2\pi^2 N_0 \varrho_0 \int_0^\beta \mathrm{d}\tau \cos\big(\Phi_\mathrm{L} - 2\varphi_\rho(-\tfrac{L}{2},\tau)\big)\Big[\cos\big(2\vartheta_\sigma(-\tfrac{L}{2},\tau)\big) + \cos\big(2\vartheta_\rho(-\tfrac{L}{2},\tau) + k_\mathrm{F}L\big)\Big]. \end{aligned} \tag{7.3.8}$$

We can define an effective tunnelling constant, $J = 2j^2\pi^2 N(0)\varrho_0$ which then reduces the term into one which looks more similar to the bosonic tunnelling action Eq. (6.1.5). Doing the same on the right side, we can collect a total effective tunnelling action of:

$$\begin{aligned} S_{\text{tun}}^{\text{eff}} = -2J \int_0^\beta \mathrm{d}\tau \Big\{ &\cos\big(\Phi_{\text{L}} - 2\varphi_\rho(-\tfrac{L}{2},\tau)\big)\Big[\cos\big(2\vartheta_\sigma(-\tfrac{L}{2},\tau)\big) + \cos\big(2\vartheta_\rho(-\tfrac{L}{2},\tau) + k_{\text{F}}L\big)\Big] \\ &+ \cos\big(\Phi_{\text{R}} - 2\varphi_\rho(\tfrac{L}{2},\tau)\big)\Big[\cos\big(2\vartheta_\sigma(\tfrac{L}{2},\tau)\big) + \cos\big(2\vartheta_\rho(\tfrac{L}{2},\tau) - k_{\text{F}}L\big)\Big]\Big\}. \end{aligned} \tag{7.3.9}$$

This combines with the full Luttinger action, Eq. (7.2.5), to be the effective action for the system. The spin sector is gapped due to the presence of the $g_{1\perp}$ term, which will be a relevant parameter due to $K_\sigma < 1$. This means that $4\vartheta_\sigma$ takes the value which minimises the cosine, which then depends on what sign $g_{1\perp}$ has. For $g_{1\perp} > 0$, repulsive spin interactions, $4\vartheta_\sigma = \pi$. This then will mean that the Cooper terms in Eq. (7.3.9) will vanish as they contain a factor of $\cos 2\vartheta_\sigma$. This would only leave the Andreev terms, which we shall see in section 7.4 are suppressed by fluctuations. This means that we require $g_{1\perp} < 0$, thus pinning $4\vartheta_\sigma = 0$. Physically this makes sense, as we are encouraging the formation of singlets in the Luttinger liquid with attractive interactions between opposite spin species.

We also define the phase drops similarly to what was done in the bosonic system:

$$\begin{aligned} \phi_{\text{L}} &= \tfrac{\Phi_{\text{L}}}{2} - \varphi_\rho(\tfrac{-L}{2}), & \phi_{\text{R}} &= \varphi_\rho(\tfrac{L}{2}) - \tfrac{\Phi_{\text{R}}}{2}, \\ \theta_{\text{L}} &= \vartheta_\rho(\tfrac{-L}{2}) + \tfrac{k_F L}{2}, & \theta_{\text{R}} &= \vartheta_\rho(\tfrac{L}{2}) - \tfrac{k_F L}{2}. \end{aligned} \tag{7.3.10}$$

This then leaves the effective tunnelling action as only a function of charge sector variables:

$$S_{\text{tun}}^{\text{eff}} = -2J \int_0^\beta \mathrm{d}\tau \Big\{ \cos 2\phi_{\text{L}}\Big[1 + \cos 2\theta_{\text{L}}\Big] + \cos 2\phi_{\text{R}}\Big[1 + \cos 2\theta_{\text{R}}\Big]\Big\}. \tag{7.3.11}$$

We expect (and shall show that) the Andreev terms are suppressed, because correlation functions of Andreev terms include an oscillating factor on top of the power law decay we expect from 1-D correlations. This means that they decay much faster than correlations that involve Cooper terms. We can see some hint that this will be true for our effective tunnelling. As ϑ and φ are conjugate variables if one gets

pinned to a fixed value (by a mean field solution stable to fluctuations or otherwise) then the other will be free to disorder. If one orders, the other disorders. So if we order φ with a mean field solution like in the bosonic system, that will mean that the fluctuations of ϑ won't be suppressed. Therefore, the Andreev terms that contain cosines of ϑ will oscillate wildly and average to zero. This then leaves the Cooper pair tunnelling as the only term left in the effective tunnelling, thus making an exact mapping onto the bosonic system.

To investigate this we shall now apply a mean field solution plus fluctuations, as seen in section 6.4 for the bosonic system, and then perform RG analysis to assess the low energy behaviour of the solution found.

7.4 Fluctuational Solution

In this section we shall develop a mean field solution for the system of fermions described above. We shall apply a mean field solution in φ and ϑ with fluctuations and investigate the low energy behaviour through RG analysis. In the low energy limit we shall see that the mean field solution is identical to the mean field solution for the bosonic problem covered in chapter 6, up to trivial scalings of fields and tunnelling parameters.

The mean field solution, $\vartheta_{0,\rho}(x), \varphi_{0,\rho}(x)$, comes from minimising the Luttinger liquid action Eq. (7.2.5) with respect to ϑ_ρ and φ_ρ. This means that $\vartheta_{0,\rho}$ and $\varphi_{0,\rho}$ both solve the 1D Laplace equation,

$$\frac{\mathrm{d}^2\vartheta_{0,\rho}}{\mathrm{d}x^2} = 0, \qquad \frac{\mathrm{d}^2\varphi_{0,\rho}}{\mathrm{d}x^2} = 0. \tag{7.4.1}$$

These makes both $\vartheta_{0,\rho}$, and $\varphi_{0,\rho}$ linear functions of x, with gradients and intercepts related to the boundary conditions Eq. (7.3.10). By defining the symmetric and asymmetric combinations of $\phi_{\mathrm{L,R}}$ and $\theta_{\mathrm{L,R}}$,

$$\phi_\pm \equiv \frac{1}{2}(\phi_\mathrm{L} \pm \phi_\mathrm{R}), \qquad \theta_\pm \equiv \frac{1}{2}(\theta_\mathrm{L} \pm \theta_\mathrm{R}), \tag{7.4.2}$$

the mean field phase and density profiles are:

$$\varphi_{0,\rho}(x) = -\phi_- - \frac{2x}{L}\left(\tfrac{\Phi}{2} - \phi_+\right), \tag{7.4.3}$$

$$\vartheta_{0,\rho}(x) = \theta_+ - \frac{2x}{L}\theta_-. \tag{7.4.4}$$

On top of this mean field solution we shall add fluctuations:

$$\varphi_\rho(x,\tau) = \varphi_{0,\rho}(x) + \widetilde{\varphi}_\rho(x,\tau), \qquad \vartheta_\rho(x,\tau) = \vartheta_{0,\rho}(x) + \widetilde{\vartheta}_\rho(x,\tau). \tag{7.4.5}$$

The fluctuations can be separated into two types, fluctuations of the boundary fields $\phi_\pm, \theta_\pm$ and then fluctuations that respect Dirichlet boundary conditions (vanishing on the boundary). For the phase field we have that the fluctuations take the form of:

$$\widetilde{\varphi}_\rho(x,\tau) = -\widetilde{\phi}_-(\tau) + \frac{2x}{L}\widetilde{\phi}_+(\tau) + \sum_{n=1}^{\infty}\left[\phi_n^e(\tau)\cos\frac{(2n-1)\pi x}{L} + \phi_n^o(\tau)\sin\frac{2n\pi x}{L}\right]. \tag{7.4.6}$$

The fluctuations of the density field are defined in a similar way:

$$\widetilde{\vartheta}_\rho(x,\tau) = -\widetilde{\theta}_+(\tau) - \frac{2x}{L}\widetilde{\theta}_-(\tau) + \sum_{n=1}^{\infty}\left[\theta_n^e(\tau)\cos\frac{(2n-1)\pi x}{L} + \theta_n^o(\tau)\sin\frac{2n\pi x}{L}\right]. \tag{7.4.7}$$

One can then put these into the quadratic terms of the full Luttinger Liquid action Eq. (7.2.5) and evaluate the spatial integrals:

$$\partial_x\varphi_\rho(x,\tau) = -\frac{2}{L}(\tfrac{\Phi}{2} - \phi_+(\tau)) + \sum_{n=1}^{\infty}\left[-\frac{(2n-1)\pi}{L}\phi_n^e(\tau)\sin\frac{(2n-1)\pi x}{L} + \frac{2n\pi}{L}\phi_n^o(\tau)\cos\frac{2n\pi x}{L}\right], \tag{7.4.8}$$

$$\int_{-L/2}^{L/2}\mathrm{d}x\,(\partial_x\varphi_\rho(x,\tau))^2 = \frac{4}{L}(\tfrac{\Phi}{2} - \phi_+ - \widetilde{\phi}_+(\tau))^2 + \sum_{n=1}^{\infty}\left[\frac{(2n-1)^2\pi^2}{2L}\phi_n^e(\tau)^2 + \frac{2n^2\pi^2}{L}\phi_n^o(\tau)^2\right]. \tag{7.4.9}$$

$$\partial_x \vartheta_\rho(x,\tau) = -\frac{2}{L}\theta_-(\tau) + \sum_{n=1}^{\infty}\left[-\frac{(2n-1)\pi}{L}\theta_n^e(\tau)\sin\frac{(2n-1)\pi x}{L} + \frac{2n\pi}{L}\theta_t n^o(\tau)\cos\frac{2n\pi x}{L}\right], \tag{7.4.10}$$

$$\int_{-L/2}^{L/2}\mathrm{d}x\left(\partial_x\vartheta_\rho(x,\tau)\right)^2 = \frac{4}{L}(\theta_- + \widetilde{\theta}_-(\tau))^2 + \sum_{n=1}^{\infty}\left[\frac{(2n-1)^2\pi^2}{2L}\theta_n^e(\tau)^2 + \frac{2n^2\pi^2}{L}\theta_n^o(\tau)^2\right]. \tag{7.4.11}$$

For the term in the action Eq. (7.2.5) with the time derivative, we have:

$$\partial_\tau\theta_\rho(x,\tau) = -\partial_\tau\widetilde{\theta}_+(\tau) - \frac{2x}{L}\partial_\tau\widetilde{\theta}_-(\tau) + \sum_{n=1}^{\infty}\left[\partial_\tau\theta_n^e(\tau)\cos\frac{(2n-1)\pi x}{L} + \partial_\tau\theta_n^o(\tau)\sin\frac{2n\pi x}{L}\right]. \tag{7.4.12}$$

Combining this with for the term: $(\partial_x\phi_\rho)(\partial_\tau\theta_\rho)$, gives a lot of terms. Many of these disappear when integrating over x, but the ones that survive are:

$$\begin{aligned}\int_{-L/2}^{L/2}\mathrm{d}x(\partial_x\phi_\rho(x,\tau))(\partial_\tau\theta_\rho(x,\tau)) = \int_{-L/2}^{L/2}\mathrm{d}x\Bigg[&-\frac{2}{L}(\tfrac{\Phi}{2}-\phi_+(\tau))\partial_\tau\widetilde{\theta}_+(\tau)\\ &+\sum_{n=1}^{\infty}\Bigg\{-\frac{2}{L}(\tfrac{\Phi}{2}-\phi_+(\tau))\partial_\tau\widetilde{\theta}_n^e(\tau)\cos\frac{(2n-1)\pi x}{L} + \frac{2(2n-1)\pi}{L^2}\phi_n^e(\tau)\partial_\tau\widetilde{\theta}_-(\tau)x\sin\frac{(2n-1)\pi x}{L}\\ &+\sum_{m=1}^{\infty}\Bigg(-\frac{(2n-1)\pi}{L}\phi_n^e(\tau)\partial_\tau\theta_m^o(\tau)\sin\frac{(2n-1)\pi x}{L}\sin\frac{2m\pi x}{L}\\ &-\frac{2n\pi}{L}\phi_n^o(\tau)\partial_\tau\theta_m^o(\tau)\cos\frac{2n\pi x}{L}\cos\frac{(2m-1)\pi x}{L}\Bigg)\Bigg\}\Bigg].\end{aligned} \tag{7.4.13}$$

These terms can then be integrated over space, with the results of the integrals being:

$$\int_{-L/2}^{L/2}\mathrm{d}x x\sin\frac{(2n-1)\pi x}{L} = -\frac{2L^2}{(2n-1)^2\pi^2}(-1)^n, \tag{7.4.14}$$

$$\int_{-L/2}^{L/2}\mathrm{d}x\cos\frac{(2n-1)\pi x}{L} = -\frac{2L}{(2n-1)\pi}(-1)^n, \tag{7.4.15}$$

$$\int_{-L/2}^{L/2}\mathrm{d}x x\cos\frac{2n\pi x}{L} = 0, \tag{7.4.16}$$

$$\int_{-L/2}^{L/2}\mathrm{d}x x\sin\frac{(2n-1)\pi x}{L}\sin\frac{2m\pi x}{L} = -\frac{2L}{\pi}(-1)^{n+m}\frac{2m}{(2n-1)^2-(2m)^2}, \tag{7.4.17}$$

$$\int_{-L/2}^{L/2}\mathrm{d}x x\cos\frac{2n\pi x}{L}\cos\frac{(2m-1)\pi x}{L} = \frac{2L}{\pi}(-1)^{n+m}\frac{2m-1}{(2n)^2-(2m-1)^2}. \tag{7.4.18}$$

Substituting these integrals into Eq. (7.4.13) gives the full form for the mixed term:

$$\begin{aligned}\int_{-L/2}^{L/2}\mathrm{d}x(\partial_x\phi_\rho(x,\tau))(\partial_\tau\theta_\rho(x,\tau)) &= -2(\tfrac{\Phi}{2}-\phi_+(\tau))\partial_\tau\widetilde{\theta}_+(\tau)\\ &+\sum_{n=1}^{\infty}\Bigg[\frac{4(-1)^n}{(2n-1)\pi}(\tfrac{\Phi}{2}-\phi_+(\tau))\partial_\tau\theta_n^e(\tau)-\frac{4(-1)^n}{(2n-1)\pi}\phi_n^e(\tau)\partial_\tau\widetilde{\theta}_-(\tau)\\ &+2\sum_{m=1}^{\infty}\Big\{(-1)^{n+m}\frac{2m(2n-1)}{(2n-1)^2-(2m)^2}\phi_n^e(\tau)\partial_\tau\theta_m^o(\tau)\\ &+(-1)^{n+m}\frac{2n(2m-1)}{(2n)^2-(2m-1)^2}\phi_n^o(\tau)\partial_\tau\theta_m^e(\tau)\Big\}\Bigg]\end{aligned} \tag{7.4.19}$$

With equations, (7.4.9), (7.4.11) and (7.4.19) the action can be written as $\mathcal{S}=S_\varepsilon+S_0+S_\mathrm{o}+S_\mathrm{e}+S_\mathrm{m}$ where ε denotes the mean field energy component of the action, 0 is the quadratic fluctuations of the boundary fields and o,e,m denotes the odd, even & mixed fluctuations within the channel. The first action identified is:

$$S_\varepsilon=\frac{4}{\pi}\int\mathrm{d}\tau\left[\frac{v_\rho K_\rho}{L}\Big\{(\Phi-\phi_+)^2-2(\Phi-\phi_+)\widetilde{\phi}_+(\tau)\Big\}+\frac{v_\rho}{LK_\rho}(\theta_-^2+2\theta_-\widetilde{\theta}_-(\tau))\right]+S_\mathrm{tun}^\mathrm{eff}, \tag{7.4.20}$$

which contains all the terms that give the mean field energy of the system. The minimisation of this action will give us the mean field equations for $\phi_\pm$ to solve. The next action, S_0 contains only fluctuations of the boundary fields,

$$S_0=\int\frac{\mathrm{d}\omega}{2\pi}\left[\frac{4v_\rho K_\rho}{\pi L}\left|\widetilde{\phi}_+(\omega)\right|^2+\frac{4v_\rho}{\pi LK_\rho}\left|\widetilde{\theta}_-(\omega)\right|^2+\frac{2\omega}{\pi}\widetilde{\phi}_+(-\omega)\widetilde{\theta}_+(\omega)\right], \tag{7.4.21}$$

which can be simplified with the shift:

$$\widetilde{\phi}_+(\omega)\to\widetilde{\phi}_+(\omega)-\frac{\omega L}{4v_\rho K_\rho}\widetilde{\theta}_+(\omega), \tag{7.4.22}$$

to make the action Eq. (7.4.21) quadratic in all fields:

$$S_0=\int\frac{\mathrm{d}\omega}{2\pi}\left[\frac{4v_\rho K_\rho}{\pi L}\left|\widetilde{\phi}_+(\omega)\right|^2+\frac{4v_\rho}{\pi LK_\rho}\left|\widetilde{\theta}_-(\omega)\right|^2+\omega^2\frac{L}{4\pi v_\rho K_\rho}\left|\widetilde{\theta}_+(\omega)\right|^2\right]. \tag{7.4.23}$$

The next two terms in the full action are of the fluctuations inside the channel, only containing odd &

even fluctuations respectively:

$$S_{\rm o} = \int \frac{{\rm d}\omega}{2\pi} \sum_{n=1}^{\infty} \left[\frac{2v_\rho K_\rho \pi n^2}{L} |\phi_n^o(\omega)|^2 + \frac{2v_\rho \pi n^2}{K_\rho L} |\theta_n^o(\omega)|^2 \right], \tag{7.4.24}$$

$$\begin{aligned} S_{\rm e} = \int \frac{{\rm d}\omega}{2\pi} \sum_{n=1}^{\infty} \Bigg[& \frac{v_\rho K_\rho \pi (2n-1)^2}{2L} |\phi_n^e(\omega)|^2 + \frac{v_\rho \pi (2n-1)^2}{2K_\rho L} |\theta_n^e(\omega)|^2 + \\ & - \frac{4(-1)^n}{\pi^2(2n-1)} \omega \phi_n^e(-\omega) \widetilde{\theta}_-(\omega) + \frac{4(-1)^n}{\pi^2(2n-1)} \omega (\Phi - \phi_+(-\omega)) \theta_n^e(\omega) \Bigg]. \end{aligned} \tag{7.4.25}$$

The final term contains terms that mix odd and even fluctuations;

$$\begin{aligned} S_{\rm m} = \int \frac{{\rm d}\omega}{2\pi} \sum_{n,m=1}^{\infty} \frac{2}{\pi} \Bigg[& (-1)^{n+m} \frac{2m(2n-1)}{(2n-1)^2 - (2m)^2} \omega \phi_n^e(-\omega) \theta_m^o(\omega) \\ & + (-1)^{n+m} \frac{2n(2m-1)}{(2n)^2 - (2m-1)^2} \omega \phi_n^o(-\omega) \theta_m^e(\omega) \Bigg]. \end{aligned} \tag{7.4.26}$$

Note how odd and even fluctuations are only mixed between ϕ and θ terms. They only ever come into the action quadratically as well, meaning that the fluctuations can be integrated out. We begin by integrating out the odd fields:

$$\begin{aligned} & \int {\rm D}\phi_n^o \exp\left(- \int \frac{{\rm d}\omega}{2\pi} \sum_{n=1}^{\infty} \left[\frac{2v_\rho K_\rho \pi n^2}{L} |\phi_n^o(\omega)|^2 + \frac{4n}{\pi} (-1)^n \omega \phi_n^o(-\omega) \sum_{m=1}^{\infty} \frac{(-1)^m (2m-1)}{(2n)^2 - (2m-1)^2} \theta_m^e(\omega) \right] \right) \\ & = \exp\left(\int \frac{{\rm d}\omega}{2\pi} \left[\frac{L}{v_\rho K_\rho \pi} \sum_{n=1}^{\infty} \frac{2}{\pi^2} \omega^2 \sum_{m,m'=1}^{\infty} \frac{(-1)^{m+m'} (2m-1)(2m'-1)}{[(2n)^2 - (2m-1)^2][(2n)^2 - (2m'-1)^2]} \theta_m^e(-\omega) \theta_{m'}^e(\omega) \right] \right). \end{aligned} \tag{7.4.27}$$

Similarly we can integrate out the odd θ fields:

$$\begin{aligned} & \int {\rm D}\theta_n^o \exp\left(- \int \frac{{\rm d}\omega}{2\pi} \sum_{n=1}^{\infty} \left[\frac{2v_\rho \pi n^2}{K_\rho L} |\theta_n^o(\omega)|^2 - \frac{4n}{\pi} (-1)^n \omega \theta_n^o(-\omega) \sum_{m=1}^{\infty} \frac{(-1)^m (2m-1)}{(2n)^2 - (2m-1)^2} \phi_m^e(-\omega) \right] \right) \\ & = \exp\left(\int \frac{{\rm d}\omega}{2\pi} \left[\frac{K_\rho L}{v_\rho \pi} \sum_{n=1}^{\infty} \frac{2}{\pi^2} \omega^2 \sum_{m,m'=1}^{\infty} \frac{(-1)^{m+m'} (2m-1)(2m'-1)}{[(2n)^2 - (2m-1)^2][(2n)^2 - (2m'-1)^2]} \phi_m^e(-\omega) \phi_{m'}^e(\omega) \right] \right). \end{aligned} \tag{7.4.28}$$

With these terms (Eq. (7.4.27) & 7.4.28) the sum over n can be evaluated using the result (see appendix

A.1 for details):

$$\sum_{n=1}^{\infty} \frac{1}{n^2 - a^2} = \frac{1}{2a^2} - \frac{\pi}{2a} \cot(\pi a). \tag{7.4.29}$$

This then will allow us to perform the sum over n present in Eq. (7.4.28),

$$\sum_{n=1}^{\infty} \frac{ab}{(n^2 - a^2)(n^2 - b^2)} = -\frac{1}{2ab} + \frac{\pi}{2} \frac{a \cot(\pi b) - b \cot(\pi a)}{a^2 - b^2}. \tag{7.4.30}$$

Here $a = m - 1/2$ and $b = m' - 1/2$. For $a = b$, the diagonal terms when $m = m'$, the limit of the second term in Eq. (7.4.30) needs to be taken carefully, which gives:

$$\sum_{n=1}^{\infty} \frac{a^2}{(n^2 - a^2)^2} = -\frac{1}{2a^2} + \frac{\pi}{4a} \cot(\pi a) + \frac{\pi^2}{4} \csc^2(\pi a). \tag{7.4.31}$$

As a and b are always half integers, the cotangent term in Eq. (7.4.31) is eliminated and the cosec squared term is always unity. In full, the action for the even ϕ fluctuations in the channel is:

$$\begin{aligned} S_{\phi^e} = \int \frac{\mathrm{d}\omega}{2\pi} \Bigg\{ \sum_{n,m=1}^{\infty} \Bigg[\phi^e_m(-\omega) \Bigg(& - \frac{K_\rho L \omega^2}{4 v_\rho \pi^3} \frac{(-1)^{m+n}}{(m - \frac{1}{2})(n - \frac{1}{2})} \\ & + \frac{K_\rho}{2\pi} \frac{16 v_\rho^2 \pi^2 (n - \frac{1}{2})^2 + L^2 \omega^2}{4 L v_\rho} \delta_{m,n} \Bigg) \phi^e_n(\omega) \Bigg] \\ & - \sum_{n=1}^{\infty} \frac{2(-1)^n}{\pi^2 (n - \frac{1}{2})} \omega \phi^e_n(-\omega) \widetilde{\theta}_-(\omega) \Bigg\}. \end{aligned} \tag{7.4.32}$$

This action is now in a form in which it can be integrated with the standard functional integration result of:

$$\prod_n \int \frac{\mathrm{d}\phi_n^* \mathrm{d}\phi_n}{2\pi i} \, e^{-\sum_{ij} \phi_i^* M_{ij} \phi_j + \sum_i h_i^* \phi_i + \phi_i^* h_i} = \frac{e^{\sum_{ij} h_i^* (M^{-1})_{ij} h_j}}{\det(M)}.$$

In this case the inversion of the matrix M seems like a daunting task due to the infinite size and non-sparseness of it, however it can be done reasonably simply. The details of inverting the matrix can be found in appendix A.2. With the inverted matrix, the functional integral over the even fluctuations of ϕ

is:

$$\int \mathrm{D}\phi_n^e e^{-S_{\phi_n^e}} = \exp\left[\frac{L}{2\pi K_\rho v_\rho}\int \frac{\mathrm{d}\omega}{2\pi}\frac{\omega^2}{\pi^4}\left|\widetilde{\theta}_-(\omega)\right|^2\left\{\sum_{n=1}^{\infty}\frac{1}{\left(n-\frac{1}{2}\right)^2\left((n-\frac{1}{2})^2+\left(\frac{L\omega}{4\pi v_\rho}\right)^2\right)}+\right.\right.$$
$$\left.\left.+\frac{2}{\pi}\left(\frac{L\omega}{4\pi v_\rho}\right)^3\coth\left(\frac{L\omega}{4v_\rho}\right)\left(\sum_{n=1}^{\infty}\frac{1}{\left(n-\frac{1}{2}\right)^2\left((n-\frac{1}{2})^2+\left(\frac{L\omega}{4\pi v_\rho}\right)^2\right)}\right)^2\right\}\right]. \tag{7.4.33}$$

Evaluating these sums and collecting like terms simplifies down to:

$$\int \mathrm{D}\phi_n^e e^{-S_{\phi_n^e}} = \exp\left[\frac{1}{\pi K_\rho}\int \frac{\mathrm{d}\omega}{2\pi}\left|\widetilde{\theta}_-(\omega)\right|^2\left(\omega\coth\left(\frac{L\omega}{4v_\rho}\right)-\frac{4v_\rho}{L}\right)\right]. \tag{7.4.34}$$

When combined with the other $\left|\widetilde{\theta}_-(\omega)\right|^2$ term in Eq. (7.4.21), the constant terms vanish and we are left with the coth term. An identical procedure can be done to the other field, in equation 7.4.27. The only difference is that $K_\rho \to 1/K_\rho$, leading to an effective action for (Ohmic) fluctuations as:

$$\begin{aligned} S_{\mathrm{Ohm}} &= \int \frac{\mathrm{d}\omega}{2\pi}\omega\coth\left(\frac{L\omega}{4v_\rho}\right)\left[\frac{K_\rho}{\pi}\left|\widetilde{\phi}_+(\omega)\right|^2+\frac{1}{\pi K_\rho}\left|\widetilde{\theta}_-(\omega)\right|^2\right], \\ &= \int \frac{\mathrm{d}\omega}{2\pi}|\omega|\left[\frac{K_\rho}{\pi}\left|\widetilde{\phi}_+(\omega)\right|^2+\frac{1}{\pi K_\rho}\left|\widetilde{\theta}_-(\omega)\right|^2\right]. \end{aligned} \tag{7.4.35}$$

The simplification to $|\omega|$ can be made because we are concerned with the high frequency limit of this action, where we don't care about frequencies lower than the smallest phononic frequency supported by the channel, $\pi v_\rho/L \ll \omega$. Added with the remaining term from Eq. (7.4.23) gives the full action of fluctuations on the boundary:

$$S_{\mathrm{fl}} = \int \frac{\mathrm{d}\omega}{2\pi}\left[\frac{K_\rho}{\pi}|\omega|\left|\widetilde{\phi}_+(\omega)\right|^2+\frac{1}{\pi K_\rho}|\omega|\left|\widetilde{\theta}_-(\omega)\right|^2+\omega^2\frac{L}{4\pi v_\rho K_\rho}\left|\widetilde{\theta}_+(\omega)\right|^2\right]. \tag{7.4.36}$$

This is of the same form as the action for bosonic fluctuations, with the addition of an ω^2 dependent term that will be exponentially suppressed in the RG.

7.4.1 Renormalisation Group Analysis

With the mean field energy action Eq. (7.4.20) we can identify two different parts, one which contains only $\phi_\pm$ terms which will come from the kinetic energy of the superfluid and Cooper tunnelling terms:

$$S_{\varepsilon,\phi} = \frac{v_\rho K_\rho}{2\pi L}\int \mathrm{d}\tau \left[2\left(\Phi - 2\phi_+\right)^2 - 4\left(\Phi - 2\phi_+\right)\left(2\widetilde{\phi}_+(\tau)\right) - 4\alpha_C \cos(2\phi_+(\tau))\cos(2\phi_-(\tau))\right]. \quad (7.4.37)$$

Here the dimensionless tunnelling constant for Cooper tunnelling is defined as, $\alpha_C = J/J_c$ where the critical current is defined as $J_c \equiv v_\rho K_\rho/2\pi L$. The other term that we consider involves the dual fields $\theta_\pm$, and is the energy from density fluctuations and Andreev tunnelling processes:

$$S_{\varepsilon,\theta} = \frac{v_\rho}{2\pi L K_\rho}\int \mathrm{d}\tau \Bigg[(2\theta_-)^2 + 4\theta_-\widetilde{\theta}_-(\tau) - 4\alpha_A \cos(2\phi_+(\tau))\cos(2\phi_-(\tau))\cos(2\theta_+(\tau))\cos(2\theta_-(\tau)) \\ - 4\alpha_A \sin(2\phi_+(\tau))\sin(2\phi_-(\tau))\sin(2\theta_+(\tau))\sin(2\theta_-(\tau))\Bigg]. \quad (7.4.38)$$

The dimensionless tunnelling constant for Andreev tunnelling is $\alpha_A = J/(\frac{v_\rho}{2\pi L K_\rho}) = K_\rho^2\alpha_C$. This term has no analogue in the bosonic system, and we shall show in this section that it is RG irrelevant.

To investigate the low energy behaviour of these mean field actions, we proceed in the standard way, as illustrated in chapter 5. The aim here is to see what terms remain relevant after the averaging over the fast fluctuations. We shall see that the terms that remain are identically the ones present in the action that describes the bosonic system, allowing us to use the mean field solution outlined in chapter 6 up to trivial rescalings.

We define "fast" and "slow" fields being of frequency $\Lambda/b < |\omega| < \Lambda$ and $0 < |\omega| < \Lambda/b$ respectively:

$$\begin{aligned}\widetilde{\phi}_+(\tau) &= \int\limits_{|\omega|<\frac{\Lambda}{b}} \mathrm{d}\omega e^{i\omega\tau}\widetilde{\phi}_+(\omega) + \int\limits_{\frac{\Lambda}{b}<|\omega|<\Lambda} \mathrm{d}\omega e^{i\omega\tau}\widetilde{\phi}_+(\omega) \\ &= \widetilde{\phi}_+^{<}(\tau) + \widetilde{\phi}_+^{>}(\tau).\end{aligned} \quad (7.4.39)$$

The same can be done for the $\widetilde{\theta}_\pm$, with the same UV cutoff. As the fluctuations of ϕ_+, θ_- and θ_+ are not mixed in action Eq. (7.4.36) we can do these calculations independently. Integrating over

the fast modes is equivalent to performing an average over the fast oscillating fluctuations, $\langle \ldots \rangle_{>} = \int \mathrm{D}\phi^{>}\mathrm{D}\theta^{>}(\ldots)e^{-S_{\mathrm{fl}}^{>}} / \int \mathrm{D}\phi^{>}\mathrm{D}\theta^{>}e^{-S_{\mathrm{fl}}^{>}}$. The only part of the mean field action Eq. (7.4.37) that mixes fast and slow terms is the cosine. With the identity,

$$\left\langle \exp\left[\pm i\widetilde{\phi}_{+}^{>}\right]\right\rangle_{+,>} \equiv \exp\left[-\frac{1}{2}\left\langle\left(\widetilde{\phi}_{+}^{>}\right)^{2}\right\rangle_{+,>}\right],$$

the cosine term from the Cooper tunnelling can be renormalised as:

$$\left\langle \cos\Big(2\phi_{+} + 2\widetilde{\phi}_{+}^{<}(\tau) + 2\widetilde{\phi}_{+}^{>}(\tau)\Big)\right\rangle_{>,+} = e^{-2\left\langle(\widetilde{\phi}_{+}^{<}(\tau))^{2}\right\rangle_{>,+}} \cos\Big(2\phi_{+} + 2\widetilde{\phi}_{+}^{<}(\tau)\Big). \tag{7.4.40}$$

To compute this average, first we Fourier transform:

$$\left\langle(\widetilde{\phi}_{+}^{<}(\tau))^{2}\right\rangle_{>,+} = \int_{>}\frac{\mathrm{d}\omega_1}{2\pi}\frac{\mathrm{d}\omega_2}{2\pi}e^{i\tau(\omega_1+\omega_2)}\left\langle\widetilde{\phi}_{+}(\omega_1)\widetilde{\phi}_{+}(\omega_2)\right\rangle_{>,+}. \tag{7.4.41}$$

This average can be calculated from the action Eq. (7.4.36), which gives:

$$\left\langle\widetilde{\phi}_{+}(\omega_1)\widetilde{\phi}_{+}(\omega_2)\right\rangle_{>,+} = \frac{\pi^2}{K_\rho|\omega_1|}\delta_{-\omega_1,\omega_2}, \tag{7.4.42}$$

thus giving the correlator to be:

$$\begin{aligned}\left\langle(\widetilde{\phi}_{+}^{<}(\tau))^{2}\right\rangle_{>,+} &= \int_{>}\frac{\mathrm{d}\omega_1}{2\pi}\frac{\mathrm{d}\omega_2}{2\pi}e^{i\tau(\omega_1+\omega_2)}\frac{\pi^2}{K_\rho|\omega_1|}\delta_{-\omega_1,\omega_2}\\ &= \frac{1}{4K_\rho}\int_{>}\mathrm{d}\omega\frac{1}{|\omega|},\\ &= \frac{1}{2K_\rho}\int_{\Lambda/b}^{\Lambda}\mathrm{d}\omega\frac{1}{|\omega|},\\ &= \frac{1}{2K_\rho}\ln(b).\end{aligned} \tag{7.4.43}$$

The final step is to rescale the other fields and then identify what the total scaling of α_C will be. The

frequencies, ω, times, τ, and fields, $\phi_+(\omega)$ are scaled like they are in section 5.2:

$$\begin{aligned} \omega' &= b\omega \\ \tau' &= \frac{\tau}{b} \\ \phi'_+(\omega') &= \frac{1}{b}\phi_+(\omega) \end{aligned} \tag{7.4.44}$$

This then lets us see that the Cooper tunnelling term is renormalised as:

$$\alpha_C \int \mathrm{d}\tau \cos\Big(2\phi_+ + 2\widetilde{\phi}_+(\tau)\Big) = \alpha_C b^{1-\frac{1}{K_\rho}} \int \mathrm{d}\tau' \cos\Big(2\phi_+ + 2\widetilde{\phi}_+(\tau')\Big), \tag{7.4.45}$$

resulting in an RG equation of:

$$\frac{\mathrm{d}\ln\alpha_C}{\mathrm{d}\ln b} = 1 - \frac{1}{K_\rho} \tag{7.4.46}$$

As expected, the Cooper pair term is relevant when $K_\rho > 1$. For this system of fermions with attraction, this is solidly achieved.

The other non-quadratic terms in the mean field energy action are in the θ part, Eq. (7.4.38). The cosines in this term can be renormalised as before. As the action for fluctuations does not mix the terms involving ϕ_+ and $\theta_\pm$ the renormalisations of each of the cosine factors can be done independently. The averages are calculated in the standard way:

$$\begin{aligned} \Big\langle (\widetilde{\theta}^<_-(\tau))^2 \Big\rangle_{>,-} &= \int_> \frac{\mathrm{d}\omega_1}{2\pi}\frac{\mathrm{d}\omega_2}{2\pi} e^{i\tau(\omega_1+\omega_2)} \Big\langle \widetilde{\theta}^<_-(\omega_1)\widetilde{\theta}^<_-(\omega_2)\Big\rangle \\ &= \int_> \frac{\mathrm{d}\omega_1}{2\pi}\frac{\mathrm{d}\omega_2}{2\pi} e^{i\tau(\omega_1+\omega_2)} \frac{K_\rho \pi^2}{|\omega_1|}\delta_{-\omega_1,\omega_2} \\ &= \frac{K_\rho}{4}\int_> \mathrm{d}\omega \frac{1}{|\omega|}, \\ &= \frac{K_\rho}{2}\int_{\Lambda/b}^{\Lambda} \mathrm{d}\omega \frac{1}{|\omega|}, \\ &= \frac{K_\rho}{2}\ln(b). \end{aligned} \tag{7.4.47}$$

The $\widetilde{\theta}_+$ correlator behaves slightly different due to its fluctuational action:

$$\left\langle \widetilde{\theta}_+(\omega_1)\widetilde{\theta}_+(\omega_2)\right\rangle_{>,+} = \frac{4K_\rho v_\rho \pi^2}{L}\frac{1}{\omega_1^2}\delta_{-\omega_1,\omega_2}. \tag{7.4.48}$$

This makes the correlator:

$$\begin{aligned}\left\langle (\widetilde{\theta}^<_+(\tau))^2\right\rangle_{>,+} &= \frac{K_\rho v_\rho}{L}\int_{\Lambda/b}^{\Lambda} \mathrm{d}\omega \frac{1}{\omega^2}, \\ &= \frac{K_\rho v_\rho}{L}\frac{(b-1)}{\Lambda}.\end{aligned} \tag{7.4.49}$$

All together, along with the field re-scalings the frequencies and times, the Cooper terms are renormalised as:

$$\alpha_A \int \mathrm{d}\tau \cos(2\phi_+(\tau))\cos(2\theta_+(\tau))\cos(2\theta_-(\tau)) = \alpha_A b^{1-K_\rho-\frac{1}{K_\rho}} e^{\frac{-2v_\rho K_\rho(b-1)}{L\Lambda}} \int \mathrm{d}\tau' \cos(2\phi_+(\tau'))\cos(2\theta_+(\tau'))\cos(2\theta_-(\tau')). \tag{7.4.50}$$

This results in the RG equation for α_A:

$$\frac{\mathrm{d}\ln\alpha_A}{\mathrm{d}\ln b} = 1 - \frac{1}{K_\rho} - K_\rho - \frac{2v_\rho K_\rho}{L\Lambda}. \tag{7.4.51}$$

For all values of K_ρ the right hand side always negative, allowing us to conclude that α_A is an irrelevant parameter. This is to be expected, as we have "fixed" a value of φ, which would cause ϑ to disorder because they are dual fields. This means that the cosine terms that involve ϑ will be oscillating wildly and average to zero. This then leaves us with only the Cooper tunnelling terms in our initial action $S^{\text{eff}}_{\text{tun}}$.

7.5 Mean Field Solution & Discussion

With the justification that the Andreev terms are irrelevant, there is nothing prohibiting us from integrating out ϑ_ρ and having an action in terms of φ_ρ alone. This then leads to the action $S_{\varepsilon,\phi}$ (Eq. (7.4.37))

giving the dimensionless mean field energy of the system:

$$\varepsilon = 2(\Phi - 2\phi_+)^2 - 4\alpha_C \cos 2\phi_+ \cos 2\phi_- \tag{7.5.1}$$

This is minimised with respect to ϕ_+ and ϕ_- to give the same equations that the phase drops $\phi_\pm$ in the bosonic system satisfy (Eqs. 6.3.5):

$$\Phi - 2\phi_+ = \alpha_C \sin 2\phi_+ \cos 2\phi_-, \tag{7.5.2a}$$

$$\cos 2\phi_+ \sin 2\phi_- = 0. \tag{7.5.2b}$$

These conditions are identical to the mean field equations for the bosonic system up to a scaling of $\phi_+ \to 2\phi_+$. This is due to the bosons in our channel being composed of two particles each contributing their phases. All the analysis presented in section 6.3 is applicable here.

As energy is 2π periodic in $2\phi_-$, we can restrict ourselves to the two solutions of , corresponding to symmetric phase drops, $2\phi_- = 0$ and asymmetric phase drops, $2\phi_- = \pi$. The solutions corresponding to $\cos 2\phi_+ = 0$ are always unstable (saddle points). The symmetric/asymmetric branch Eq. 7.5.2a is reduced to

$$\Phi - 2\phi_+ = \pm\alpha_C \sin 2\phi_+. \tag{7.5.3}$$

As seen before, this equation cannot be solved analytically for ϕ_+ as a function of Φ and for $\alpha_C > 1$ ϕ_+ becomes multivalued. We can however analyse the classical stability of the solutions that Eq. 7.5.3 admits.

7.5.1 Classical Stability of Solution

The Hessian matrix of mixed partial derivatives of energy Eq. (7.5.1) is identical to that of the bosonic system, Eqs. (6.3.6, 6.3.7) (up to a global factor of 4 which does not impact the regions of stability):

$$D[\phi_+, \phi_-] = 256\left[\alpha_C \cos 2\phi_+ \cos 2\phi_- + \alpha_C^2(\cos 2\phi_+ \cos 2\phi_-)^2 - \alpha_C^2(\sin 2\phi_+ \sin 2\phi_-)^2\right]. \tag{7.5.4}$$

As before, we can rule out solutions where $\cos 2\phi_+ = 0$ due to them being unstable saddle points of the energy landscape ($D[\phi_+, \phi_-] < 0$). This means that for $\alpha_C < 1$ there are only stable solutions for $\pm\cos 2\phi_+ > 0$. which for the symmetric branch gives stable solutions in intervals about $2\phi_+ = 2j\pi$ where $j \in \mathbb{Z}$. Solutions stable at $2\phi_+ = 0$ remain stable in the interval $\phi_+ \in [-\pi/2, \pi/2]$. From Eq. 7.5.3 we can deduce that this symmetric branch solution remains stable for applied phases $\Phi \in [-(\pi/2+\alpha_C), \pi/2+\alpha_C]$.

The same analysis from the bosonic system holds for the asymmetric branch. Stable solutions exist around $2\phi_+ = (2j+1)\pi$ where $j \in \mathbb{Z}$. The solution centred about $2\phi_+ = \pi$ remains stable in the region $2\phi_+ \in [\pi/2, 3\pi]$, leading to stability for the applied phases in the interval $\Phi \in [\pi/2 - \alpha_C, 3\pi + \alpha_C]$. This means that for all values of Φ, there exists at least one stable solution and about half integer multiples of π there is a region of width $2\alpha_C$ where solutions from both branches are stable. This means that if we were to increase Φ from 0, we would initially start on the symmetric branch and have the phase drops at both barriers to be the same, until switching to the asymmetric branch for $\Phi > \pi/2 + \alpha_C$ where the asymmetric branch is stable but the symmetric is not.

Each branch is 4π periodic in the applied phase difference 2Φ, but their regions of stability we would see an energy and current that is 2π periodic in phase difference. The scaling of the phases in the channel, $\phi_\pm \to 2\phi_\pm$, does not impact the periodicity of the mean field solution. The equations ((7.5.2b), (7.5.2a)) still give an energy that is 4π periodic in the applied phase difference 2Φ.

7.5.2 Current

The current of fermion pairs through the channel is the gradient of the phase given by Eq. 7.4.3, with the substitution of Eq. 7.5.3 giving:

$$\mathcal{I} = \mp 2J \sin 2\phi_+, \tag{7.5.5}$$

where the sign of the current comes from the factor of $\cos 2\phi_-$. This is the same form as the standard Josephson current, except for the non-linear dependence of $2\phi_+$ on the phase difference 2Φ. Another fact to note is that the current is non-perturbative, in the sense that it depends on a lower power of tunnelling, j, than the perturbative approach would give us. Fazio et. al. [6] calculated the critical current to be proportional to, $I_c \propto \frac{1}{Lv_\mathrm{F}} N(0)^2 |j|^4$, where L is the length of the 1D channel, v_F is the Fermi velocity in

the superconducting reservoirs, $N(0)$ is the density of states at the Fermi level and j is the tunnelling amplitude from the tunnelling action Eq. (7.2.3). The current in the system considered in this section is calculated to be proportional to $J \propto j^2 N(0)/\sqrt{L}$, which is two orders of j lower than the perturbative solution. This mirrors what was found in chapter 6, where the critical current for the bosonic system was found to depend on a lower order in the tunnelling parameter than what perturbation theory would give.

A key, qualitative, signature of this non-perturbative solution would be a hysteresis in the current. If the system was initialised with $\Phi = 0$, then we expect that the tunnelling on either end of the system will be symmetric, $\phi_{\mathrm{L}} = \phi_{\mathrm{R}}$, thus being on the symmetric branch of the mean field theory. As Φ is increased up to $\pi/2$ the symmetric tunnelling remains the lowest energy option for the system, and the current smoothly decreases from 0 to $-2J\sin\big(2\phi_+(\Phi = \frac{\pi}{2})\big)$. As Φ is increased past $\pi/2$ the lowest energy solution becomes the solution on the asymmetric branch, hence the current corresponding to the lowest energy will discontinuously flip at $\Phi = \pi/2$. This wouldn't be observed in practice though, because at $\Phi = \pi/2$ both branches are stable and the discontinuous flip will only happen once Φ is increased past $\pi/2 + \alpha_C$ and the symmetric branch becomes unstable. Similarly if Φ were decreasing from $\Phi > \pi/2 + \alpha_C$ the system would be tunnelling asymmetrically with, $2\phi_{\mathrm{L}} = 2\phi_{\mathrm{R}} + \pi$ until Φ decreased past $\Phi = \pi/2 - \alpha_C$. It is this overlapping region of stability for both branches of the mean field solution (symmetric and asymmetric tunnelling) that causes this hysteresis.

7.5.3 Degeneracy

At $\Phi = \pi/2$ (and other half integers of π) the two branches are degenerate. From the RG analysis performed in section 7.4 we can also conclude that this degeneracy is robust against dynamic fluctuations, i.e. fluctuations do not provide a mechanism to remove this degeneracy. This protection of this degeneracy is not known, but we can speculate that it could be linked to Majorana Zero Modes as predicted in systems of a similar geometry [39, 9, 10]. In these systems a 4π periodicity in the Andreev spectrum is a signature of Majorana zero modes appearing at the system edges and resulting in a degenerate ground state. To provide further connection to these systems the fermionic parity of the channel on each branch could be investigated, akin to Fidkowski et. al. [39]. Another aspect of investigation would be how these results relate to the BEC-BCS crossover [40] and whether the profile of the current could be smoothly

interpolated between our BEC limit and the BCS limit considered in [6, 41].

Chapter 8

Conclusions

This thesis is the result of my own work, the results of which are to be published as a preprint on arXiv. I began with an overview of concepts in physics and mathematical techniques that I learnt during my PhD study, which are relevant for understanding the results obtained.

I explained the prior results on the bosonic system, obtained by Simpson et. al. The system considered two reservoirs of Bose-Einstein condensate, connected to a 1D channel by weak tunnelling links. The current through the channel is driven entirely by the phase difference between the two reservoirs, 2Φ. I explained the non-perturbative solution required to calculate the current and how this solution has two separate branches, each of which are 4π periodic in applied phase difference. The branches are also degenerate at an applied phase difference of $2\Phi = \pi$ and I showed that fluctuations alone cannot lift the degeneracy. With these two qualities, I drew links to systems of semiconductor-superconductor nanowires that are predicted to host Majorana fermions as edge excitations. With this motivation I set out to reconstruct the physics of the bosonic system, with fermions as the constituent particles instead. This would allow for a closer comparison to the systems suspected to host Majorana fermions.

I theoretically investigated a system consisting of BCS superconducting reservoirs, connected via weak tunnelling links to a 1D channel of fermions with attractive interactions. I described the fermions in the channel as a Luttinger liquid with a gapped spin excitation spectrum. I performed a second order expansion in the tunnelling Hamiltonian and averaged over the reservoir fields to create an effective action of tunnelling pairs of fermions. I then applied a mean field solution that consisted of a static part plus

fluctuations. I integrated out these fluctuations and used the renormalisation group to analyse the low energy description of this model. From this low energy theory, I made an exact mapping of the fermionic system onto the bosonic system and was able to express the current as a function of phase difference. As with the bosonic system, the solution to the attractive fermionic system consists of two branches that are individually 4π periodic and degenerate at $2\Phi = \pi$. The exact nature of the degeneracy and what is protecting it is still an open question. Future work on this topic could be done to investigate the degeneracy in the fermionic system, and see if it can be described by some topological invariant such as fermion parity. Other systems could be investigated to try and explore richer behaviour, such as multi-channel Luttinger liquids that involve more than one species of boson/fermion [42].

It would be interesting for these theoretical predictions to be tested experimentally by creating the system with ultracold fermionic atoms. With tunable interactions between fermions both the attractive regime that I investigated and the repulsive/non-interacting regimes considered by Fazio et. al. could be explored. The hysteresis of the current in the attractive fermionic system could serve as an signature of the BEC-BCS crossover in the Fermi gas. The attractive fermionic system I considered will be strictly in the BEC regime, due to the fermionic pairs I considered behaving almost identically to a system of bosons.

Part IV

Appendix

Appendix A

Mathematical Smörgåsbord

A.1 Sums

I have used the result:

$$\sum_{n=1}^{\infty} \frac{1}{n^2 - a^2} = \frac{1}{2a^2} - \frac{\pi}{2a} \cot(\pi a). \tag{A.1.1}$$

This can be shown by considering the sinc function, as expressed as an infinite product of its roots:

$$\frac{\sin(\pi x)}{\pi x} = \left(1 - x\right)\left(1 + x\right)\left(1 - \frac{x}{2}\right)\left(1 + \frac{x}{2}\right)\left(1 - \frac{x}{3}\right)\left(1 + \frac{x}{3}\right)\ldots, \tag{A.1.2}$$

$$= \left(1 - x^2\right)\left(1 - \frac{x^2}{4}\right)\left(1 - \frac{x^2}{9}\right)\ldots, \tag{A.1.3}$$

$$= \prod_{n=1}^{\infty}\left(1 - \frac{x^2}{n^2}\right). \tag{A.1.4}$$

On the right hand side we can have some hint on how to create the sum in e.q. A.1.1. If we take the logarithm of the product, that can then be expressed as the sum of logarithms of the same argument. Differentiating this expression will then create the sum we desire:

$$\frac{d}{dx}\ln\left(\prod_{n=1}^{\infty}\left(1-\frac{x^2}{n^2}\right)\right)=\frac{d}{dx}\sum_{n=1}^{\infty}\ln\left(1-\frac{x^2}{n^2}\right), \tag{A.1.5}$$

$$=\sum_{n=1}^{\infty}\frac{-2x}{n^2-x^2}. \tag{A.1.6}$$

Performing the same procedure on the LHS of A.1.2 and re-arranging gives the result.

A.2 Sherman Morrison Formula

In eq. 7.4.32 we have a matrix which we wish to invert. The matrix's components are given by:

$$M_{mn}=\frac{K_\rho}{2\pi}\left[-\frac{L\omega^2}{2\pi^2 v_\rho}\frac{(-1)^{m+n}}{(m-\frac{1}{2})(n-\frac{1}{2})}+\left(\frac{16v_\rho^2\pi^2(n-\frac{1}{2})^2+L^2\omega^2}{4Lv_\rho}\right)\delta_{m,n}\right]. \tag{A.2.1}$$

It may seem daunting to invert because the matrix is of infinite size and it isn't sparse. However due to the form that it takes we can use a nifty formula to invert it. By employing the Sherman-Morrison formula [43], if a matrix that can be decomposed into the sum of an invertible matrix (A) and the outer product of two vectors ($uv^\intercal$), the inverse can be found easily:

$$(A+uv^\intercal)^{-1}=A^{-1}-\frac{A^{-1}uv^\intercal A^{-1}}{1+v^\intercal A^{-1}u}. \tag{A.2.2}$$

In our case the matrices we have are:

$$A_{m,n}=\frac{K_\rho}{2\pi}\left[\frac{16v_\rho^2\pi^2(n-\frac{1}{2})^2+L^2\omega^2}{4Lv_\rho}\delta_{m,n}\right], \tag{A.2.3}$$

which is trivially inverted to:

$$A^{-1}_{m,n}=\frac{2\pi}{K_\rho}\frac{L}{4v_\rho\pi^2}\frac{1}{(n-\frac{1}{2})^2+\left(\frac{L\omega}{4\pi v_\rho}\right)^2}\delta_{m,n}. \tag{A.2.4}$$

The vectors, who's outer product form the rest of matrix are easy to see as well:

$$u_m = \frac{K_\rho}{2\pi}\left(-\frac{L\omega^2}{2v_\rho\pi^2}\frac{(-1)^m}{(m-\frac{1}{2})}\right), \tag{A.2.5}$$

$$v_n^\intercal = \frac{(-1)^n}{n-\frac{1}{2}}. \tag{A.2.6}$$

In the Sherman-Morrison formula the denominator in the second term involves the scalar quantity:

$$v^\intercal A^{-1}u = -\frac{2}{\pi^2}\left(\frac{L\omega}{4\pi v_\rho}\right)^2\sum_{n=1}^{\infty}\frac{1}{\left(n-\frac{1}{2}\right)^2\left((n-\frac{1}{2})^2+\left(\frac{L\omega}{4\pi v_\rho}\right)^2\right)}. \tag{A.2.7}$$

This sum can be evaluated using the result:

$$\sum_{n=1}^{\infty}\frac{1}{\left(n-\frac{1}{2}\right)^2\left((n-\frac{1}{2})^2+a^2\right)} = \frac{\pi^2}{2a^2}-\frac{\pi\tanh(\pi a)}{2a^3}, \tag{A.2.8}$$

with $a = L\omega/4\pi v_\rho$, which gives:

$$1+v^\intercal A^{-1}u = \frac{4v_\rho}{L\omega}\tanh\left(\frac{L\omega}{4v_\rho}\right). \tag{A.2.9}$$

The numerator of the second term in the Sherman-Morrison formula will be:

$$\left[A^{-1}uv^\intercal A^{-1}\right]_{m,n} = -\frac{L}{K_\rho v_\rho\pi^4}\left(\frac{L\omega}{4\pi v_\rho}\right)^2\frac{(-1)^m}{(m-\frac{1}{2})\left((m-\frac{1}{2})^2+\left(\frac{L\omega}{4\pi v_\rho}\right)^2\right)}\frac{(-1)^n}{(n-\frac{1}{2})\left((n-\frac{1}{2})^2+\left(\frac{L\omega}{4\pi v_\rho}\right)^2\right)}. \tag{A.2.10}$$

All combined, this gives the inverse of matrix, M in eq. 7.4.32

$$\begin{aligned}[M^{-1}]_{mn} =& \frac{L}{2K_\rho v_\rho\pi}\left[\frac{1}{\left(n-\frac{1}{2}\right)^2\left((n-\frac{1}{2})^2+\left(\frac{L\omega}{4\pi v_\rho}\right)^2\right)}\delta_{m,n}\right.\\ &\left.+\frac{2}{\pi}\left(\frac{L\omega}{4\pi v_\rho}\right)^3\coth\left(\frac{L\omega}{4\pi v_\rho}\right)\frac{(-1)^m}{(m-\frac{1}{2})\left((m-\frac{1}{2})^2+\left(\frac{L\omega}{4\pi v_\rho}\right)^2\right)}\frac{(-1)^n}{(n-\frac{1}{2})\left((n-\frac{1}{2})^2+\left(\frac{L\omega}{4\pi v_\rho}\right)^2\right)}\right].\end{aligned} \tag{A.2.11}$$

Bibliography

[1] Immanuel Bloch, Jean Dalibard, and Wilhelm Zwerger. Many-body physics with ultracold gases. *Rev. Mod. Phys.*, 80:885–964, Jul 2008.

[2] Immanuel Bloch, Jean Dalibard, and Sylvain Nascimbene. Quantum simulations with ultracold quantum gases. *NATURE PHYSICS*, 8(4):267–276, APR 2012.

[3] Jean-Philippe Brantut, Jakob Meineke, David Stadler, Sebastian Krinner, and Tilman Esslinger. Conduction of ultracold fermions through a mesoscopic channel. *Science*, 337(6098):1069–1071, 2012.

[4] Sebastian Krinner, Tilman Esslinger, and Jean-Philippe Brantut. Two-terminal transport measurements with cold atoms. *Journal of Physics: Condensed Matter*, 29(34):343003, jul 2017.

[5] Gregor Jotzu, Michael Messer, Remi Desbuquois, Martin Lebrat, Thomas Uehlinger, Daniel Greif, and Tilman Esslinger. Experimental realization of the topological Haldane model with ultracold fermions. *NATURE*, 515(7526):237–U191, NOV 13 2014.

[6] Rosario Fazio, F. W. J. Hekking, and A. A. Odintsov. dc and ac Josephson effect in a superconductor - Luttinger-liquid - superconductor system. *prb*, 53(10):6653–6664, March 1996.

[7] Dmitrii L. Maslov, Michael Stone, Paul M. Goldbart, and Daniel Loss. Josephson current and proximity effect in luttinger liquids. *Phys. Rev. B*, 53:1548–1557, Jan 1996.

[8] D. P. Simpson, D. M. Gangardt, I. V. Lerner, and P. Krüger. One-Dimensional transport of bosons between weakly linked reservoirs. *Physical Review Letters*, 112(10):1–8, 2014.

[9] Roman M. Lutchyn, Jay D. Sau, and S. Das Sarma. Majorana fermions and a topological phase transition in semiconductor-superconductor heterostructures. *Phys. Rev. Lett.*, 105:077001, Aug 2010.

[10] Yuval Oreg, Gil Refael, and Felix von Oppen. Helical liquids and majorana bound states in quantum wires. *Phys. Rev. Lett.*, 105:177002, Oct 2010.

[11] M. Tinkham. *Introduction to Superconductivity*. Dover Books on Physics Series. Dover Publications, 2004.

[12] Christopher Pethick and Henrik Smith. *Bose-Einstein Condensation in Dilute Gases*. Cambridge University Press, Cambridge, United Kingdom, second edition, 2008.

[13] Mike H Anderson, Jason R Ensher, Michael R Matthews, Carl E Wieman, and Eric A Cornell. Observation of bose-einstein condensation in a dilute atomic vapor. *science*, 269(5221):198–201, 1995.

[14] M Albiez, R Gati, J Folling, S Hunsmann, M Cristiani, and MK Oberthaler. Direct observation of tunneling and nonlinear self-trapping in a single bosonic Josephson junction. *PHYSICAL REVIEW LETTERS*, 95(1), JUL 1 2005.

[15] W. J. Kwon, G. Del Pace, R. Panza, M. Inguscio, W. Zwerger, M. Zaccanti, F. Scazza, and G. Roati. Strongly correlated superfluid order parameters from dc josephson supercurrents. *Science*, 369(6499):84–88, 2020.

[16] Thierry Giamarchi. *Quantum physics in one dimension*. Internat. Ser. Mono. Phys. Clarendon Press, Oxford, 2004.

[17] M A Cazalilla. Bosonizing one-dimensional cold atomic gases. *Journal of Physics B: Atomic, Molecular and Optical Physics*, 37(7):S1–S47, mar 2004.

[18] Igor V. Lerner. One-dimensional transport of ultracold bosons, 2019.

[19] Alex Grishin, Igor V. Yurkevich, and Igor V. Lerner. Functional integral bosonization for an impurity in a luttinger liquid. *Phys. Rev. B*, 69:165108, Apr 2004.

[20] A. Baha Balantekin, André de Gouvêa, and Boris Kayser. Addressing the majorana vs. dirac question with neutrino decays. *Physics Letters B*, 789:488–495, 2019.

[21] Ettore Majorana and Luciano Maiani. *A symmetric theory of electrons and positrons*, pages 201–233. Springer Berlin Heidelberg, Berlin, Heidelberg, 2006.

[22] A Yu Kitaev. Unpaired majorana fermions in quantum wires. *Physics-Uspekhi*, 44(10S):131–136, oct 2001.

[23] Topology in condensed matter. https://topocondmat.org. Accessed: 2021-07-29.

[24] Liang Fu and C. L. Kane. Superconducting proximity effect and majorana fermions at the surface of a topological insulator. *Phys. Rev. Lett.*, 100:096407, Mar 2008.

[25] Jason Alicea. New directions in the pursuit of majorana fermions in solid state systems. *Reports on Progress in Physics*, 75(7):076501, jun 2012.

[26] C.W.J. Beenakker. Search for majorana fermions in superconductors. *Annual Review of Condensed Matter Physics*, 4(1):113–136, 2013.

[27] Lukasz Fidkowski, Roman M. Lutchyn, Chetan Nayak, and Matthew P. A. Fisher. Majorana zero modes in one-dimensional quantum wires without long-ranged superconducting order. *Phys. Rev. B*, 84:195436, Nov 2011.

[28] Alexander Altland and Ben Simons. *Condensed Matter Field Theory*. Cambridge University Press, Cambridge, United Kingdom, 2006.

[29] N. Nagaosa and S. Heusler. *Quantum Field Theory in Condensed Matter Physics*. Texts and monographs in physics. Springer, 1999.

[30] L.D. Landau, E.M. Lifšic, E.M. Lifshitz, L. P, L.P. Pitaevskii, J.B. Sykes, and M.J. Kearsley. *Statistical Physics: Theory of the Condensed State*. Course of theoretical physics. Elsevier Science, 1980.

[31] Milton Abramowitz and Irene A. Stegun. *Handbook of Mathematical Functions with Formulas, Graphs, and Mathematical Tables*. Dover, New York, ninth dover printing, tenth gpo printing edition, 1964.

[32] *NIST Digital Library of Mathematical Functions*. http://dlmf.nist.gov/, Release 1.1.1 of 2021-03-15. F. W. J. Olver, A. B. Olde Daalhuis, D. W. Lozier, B. I. Schneider, R. F. Boisvert, C. W. Clark, B. R. Miller, B. V. Saunders, H. S. Cohl, and M. A. McClain, eds.

[33] G.D. Mahan. *Many-Particle Physics*. Physics of Solids and Liquids. Springer US, 2013.

[34] Kenneth G. Wilson. The renormalization group: Critical phenomena and the kondo problem. *Rev. Mod. Phys.*, 47:773–840, Oct 1975.

[35] R. Shankar. Renormalization-group approach to interacting fermions. *Rev. Mod. Phys.*, 66:129–192, Jan 1994.

[36] C. L. Kane and Matthew P. A. Fisher. Transmission through barriers and resonant tunneling in an interacting one-dimensional electron gas. *Phys. Rev. B*, 46:15233–15262, Dec 1992.

[37] P NOZIERES, F GALLET, P Nozières, and F Gallet. The roughening transition of crystal surfaces. i. static and dynamic renormalization theory, crystal shape and facet growth. *Journal de physique.*, 48(3):353–367, 1987.

[38] David Simpson. *One Dimensional Transport of Ultracold Bosons*. PhD thesis, University of Birmingham, 2014.

[39] Lukasz Fidkowski, Roman M. Lutchyn, Chetan Nayak, and Matthew P. A. Fisher. Majorana zero modes in one-dimensional quantum wires without long-ranged superconducting order. *Phys. Rev. B*, 84:195436, Nov 2011.

[40] W. Zwerger. *The BCS-BEC Crossover and the Unitary Fermi Gas*. Lecture Notes in Physics. Springer Berlin Heidelberg, 2011.

[41] Dmitrii L. Maslov, Michael Stone, Paul M. Goldbart, and Daniel Loss. Josephson current and proximity effect in luttinger liquids. *Phys. Rev. B*, 53:1548–1557, Jan 1996.

[42] V. Kagalovsky, I. V. Lerner, and I. V. Yurkevich. Local impurity in a multichannel luttinger liquid. *Phys. Rev. B*, 95:205122, May 2017.

[43] Jack Sherman and Winifred J. Morrison. Adjustment of an Inverse Matrix Corresponding to a Change in One Element of a Given Matrix. *The Annals of Mathematical Statistics*, 21(1):124 – 127, 1950.